Ana Cristina Maia Fernandes

The impact of the embryonic molecular clock in early chick embryo elongation

UNIVERSIDADE DO ALGARVE

Departamento de Ciências Biomédicas e Medicina

2017

Ana Cristina Maia Fernandes

The impact of the embryonic molecular clock in early chick embryo elongation

Mestrado em:

Oncobiologia – Mecanismos Moleculares do Cancro

Trabalho efetuado sob a orientação de:

Professora Doutora Raquel P. Andrade

Professora Doutora Isabel Palmeirim

UNIVERSIDADE DO ALGARVE

Departamento de Ciências Biomédicas e Medicina

2017

Título do trabalho:

"The impact of the embryonic molecular clock in early chick embryo elongation"

Declaração de autoria do trabalho:

Declaro ser autora deste trabalho, que é original e inédito. Autores e trabalhos consultados estão devidamente citados no texto e constam na listagem de referências incluída.

Acknowledgements

As all journeys in our life, the work presented in this thesis was performed with the contribution of several people. To them all, I want to thank for being part of this journey.

First of all, I would like to thank my supervisor, Professor Raquel Andrade. For always being available, for all the support, guidance and patience. I'm very thankful for the opportunity to be a part of her group and to have the opportunity of learning as much as I learned during this year.

I would also like to thank my co-supervisor Professor Isabel Palmeirim for all the help, and for all the medical support.

To Professor Ana Marreiros I want to thank the help with the statistical analysis realized during this work, and for all incentive.

To the managers of the microscopy facilities, from the CBMR, doctor Claúdia Florindo and from Linbon, Doctor Gabriel Martins for the help and advice on the imaging. I would also like to additionally thank Gabriel Martins that kindly provided the Vital Dyes tested during this work.

To all professors of the Master in Oncobiology, I would like to thank for all the teachings.

To all the present and past members of the Chronobiology and the Temporal Control of Cell Differentiation Laboratories: Tomás, Gil, Patrícia, Rita, Isabel, Ramiro and Ana I would like to thank all the help and contributions to this work. Especially to Gil and Tomás that helped with the optimizations for the Light-sheet microscopy, the incubation chamber and for always being available to help. To Ana e Patrícia for all the help with the immunofluorescence and electroporation. To the "citocromos" Ramiro and Isabel for always making me look to unexpected perspectives and help. To Rita for all the helpful brainstorms and scientific conversations.

To all my friends in Faro and my special one, I would like to thank for all the patient, support and good moments lived. Specially to Tomás for always being there.

I want also to thank to all my friends of Cerveira: Pedro, Liliana, Hugo, Catarina, and to all members of my bracarence family: Carla, Patricia, Liliana, Angela, Augusto, Daniela, Diana and Bruno. Because even when they are away from my sight, they are always close to my heart.

Last, but not the least, to my parents and family a special thanks, because without them, this experience and thesis would be impossible. Thanks for all the support and help during these years.

This work was funded by my parents and by the Fundation for Science and Technology (Fundação para a Ciência e Tecnologia, Portugal (FCT)) project reference PTDC/BEX-BID/5410/2014 and project reference UID/BIM/04773/2013 CBMR

Abstract

Embryo development is strictly regulated in time and space. One of the mechanisms by which cells have temporal information is the somitogenesis clock. During somitogenesis, somites are formed periodically from the pre-somitic mesoderm (PSM) along the antero-posterior axis. The periodicity of somitogenesis is regulated by an oscillatory gene network that operates within PSM with the same period as somite formation. A member of this network in chick is *hairy1*, a member of the Hairy and Enhancer of Split (HES) family of transcription factors. The role of Hes proteins in biological contexts is broad, namely in development and more recently in cancer. Previous work from our lab showed that Hairy1 overexpression in PSM precursors in gastrulation stages delays embryo development.

To understand this phenotype, we started by evaluating the expression pattern of *hairy1* mRNA in gastrulating embryos. *hairy* is dynamically expressed along the antero-posterior and medial-lateral axes of the primitive streak. To evaluate embryo elongation, we performed live-imaging of embryos cultured in two different techniques: Chapman and New. The embryo elongates continuously over time with an average rate of 159 ± 55 uum/h independently of the culture system. The PSM and segmented region contribute the most for total embryo elongation. To understand the impact of Hairy1 overexpression we electroporated the PSM precursors in gastrulation stages and evaluated embryo elongation over time. The preliminary data obtained suggests that Hairy1 overexpression delays embryo elongation.

Our work provides a novel quantitative framework for embryo elongation which can be used for comparative studies of chick embryo development in different conditions. Also, it gives new insights on the role of Hairy1 during embryo development which could be important to better understand development and diseases, such as Cancer.

Key words: Chick embryo | Elongation | Live-imaging | Embryonic clock | Hairy1

Resumo

O desenvolvimento embrionário é um processo altamente regulado no tempo e espaço no qual uma única célula dá origem a um organismo completamente funcional e organizado. Todos os processos que ocorrem durante o desenvolvimento embrionário têm de desenrolar-se numa determinada ordem e no tempo e espaço corretos. Um dos principais eventos durante os primeiros estadios do desenvolvimento é a gastrulação (Gilbert, 2014). A gastrulação é um processo complexo e extremamente importante que envolve vários eventos, como a transição epitelial-mesenquimal, migração de células, entre outros (Gilbert, 2014). Este acontecimento é crucial dado que é nesta fase que se formam as três camadas germinativas: a mesoderme, a endoderme, a ectoderme. As três camadas germinativas irão mais tarde dar origem a toda a variedade de células e tecidos que povoam o organismo e que são necessárias para uma correta morfogénese (Gilbert, 2014). Nos estadios que antecedem a gastrulação, o embrião é composto por duas camadas de células: o epiblasto e o hipoblasto. As duas camadas têm diferentes funções sendo que as células do epiblasto irão dar origem às diferentes camadas embrionárias e o hipoblasto contribui para os tecidos extraembrionários e é importante para a sinalização molecular que regula a migração das células do epiblasto (Gilbert, 2014). À medida que a gastrulação ocorre no embrião, este alonga ao longo do eixo ântero-posterior. Os processos que regulam a elongação do embrião ainda não são totalmente compreendidos, no entanto assentam em reorganização de células dentro de tecidos, migração de células e divisão celular (revisto em Benazeraf and Pourquie, 2013). Após o inicio da gastrulação, e à medida que o embrião elonga, inicia-se a formação dos sómitos a partir da mesoderme pré-somítica (MPS) num evento chamado de somitogénese. Os sómitos são estruturas transientes que mais tarde se diferenciam em vertebras, músculo, entre outros tecidos. A somitogénese não só é a primeira evidência de segmentação do eixo ântero-posterior dos vertebrados mas também é um processo periódico e como tal é altamente regulado tanto no tempo como no espaço (revisto em Bailey, 2015). A primeira evidência experimental de como as células num embrião são capazes de "contar" tempo foi descoberta no contexto deste processo (Palmeirim et al., 1997). Palmeirim e os seus colaboradores mostraram que o mRNA de *hairy1*, oscillava na MPS com o mesmo periodo da formação dos sómitos na galinha. Hairy1 faz assim parte do relógio, sendo que este é um componente

do modelo mais aceite atualmente para explicar o processo de somitogénese: o modelo do relógio e frente de diferenciação ("clock and wavefront"). Este modelo divide-se em dois componentes: a frente de diferenciação que dá informação espacial às células e é composta por gradientes opostos de sinalização FGF/Wnt e de ácido retinóico; o relógio que dá informação temporal às células, que é composto por uma rede regulatória de genes que são expressos de forma cíclica com o mesmo período da formação dos sómitos na MPS (revisto em Bailey, 2015). Um dos membros deste relógio no embrião de galinha é Hairy1 (Palmeirim et al., 1997). Hairy1 pertence à família dos Hairy-enhancer-of-split (Hes) conhecidos por serem repressores de transcrição (revisto em Kageyama et al., 2007). Os Hes têm importantes funções durante o desenvolvimento embrionário regulando vários processos celulares, nomeadamente a diferenciação celular (reviewed in Kageyama et al., 2007). Hes1, homólogo humano de *hairy1*, foi também associado a vários processos no desenvolvimento e progressão do Cancro, nomeadamente a metástases e resistência a drogas (revisto em Liu et al., 2005). Alguns membros da família Hes apresentam expressão oscilatórias nas células. Os tempos de meia-vida curtos tanto do mRNA como da proteína e a sua regulação via ciclos de *feedback* negativo, permitem-lhes manter a expressão oscilatória ao longo do tempo (revisto em Uriu, 2016). A expressão dinâmica de genes e de proteínas tem importantes funções na determinação de respostas biológicas diferenciais, existindo assim uma correlação entre dinâmica de expressão/atividade e resposta celular. A dinâmica da expressão de Hes tem um papel crucial nas respostas diferenciais das células a estímulos e em diferentes processos do desenvolvimento, como por exemplo na neurogénese, onde expressão oscilatória de Hes1 leva a proliferação celular de células estaminais neurais enquanto que a expressão a níveis constantes leva à diferenciação das mesma células em astrócitos (revisto em Kageyama 200). Dado que a oscilação dos genes Hes é importante para as respostas celulares, alteração na dinâmica de expressão destes genes pode ter um impacto no desenvolvimento embrionário.

Trabalhos previamente realizados no laboratório mostraram que quando Hairy1 é sobre-expresso em células precursoras da MPS durante estádios de gastrulação, o tronco do embrião fica atrasado no desenvolvimento relativamente à cabeça. O fenótipo é visível morfologicamente mas também com recurso a marcadores moleculares, sendo que o fenótipo observado é transiente (Andrade et al., em revisão). A forma como Hairy1 tem um impacto no desenvolvimento e como o embrião recupera são ainda desconhecidos. Algumas das

hipóteses que poderão explicar o impacto da sobre-expressão de Hairy1 no desenvolvimento são: 1) Hairy1 afeta a divisão celular; 2) Hairy1 afeta a migração das células; 3) Hairy1 afeta a diferenciação das células.

De forma a tentar perceber o fenótipo descrito começou-se por caracterizar a expressão do mRNA de *hairy1* em embriões em estadios de gastrulação por in hibridação *in situ*. Observou-se que *hairy1* é dinâmicamente expresso ao longo dos eixos antero-posterior e medio-lateral da linha primitiva. Não foi possível avaliar a expressão proteica apesar de várias optmizações. De forma a compreender a elongação do embrião de galinha foi avaliado por imagiologia em tempo real, a taxa de elongação do embrião e de diferentes tecidos cultivados em dois sistemas de cultura diferentes: Chapman (Chapman et al., 2001) e New (New, 1959). Foi possível mostrar que o elongamento de embriões em estadios iniciais é independente do sistema de cultura usado. Observou-se que o embrião alonga continuamente ao longo do tempo com uma taxa de 159 ± 55 IUUUUm/h e que os estadios HH5/6 apresentam as taxas mais altas. A MPS e a zona segmentada são as porções que contribuem mais para a alongamento total do embrião. Para compreender o impacto da sobreexpressão de Hairy1 no desenvolvimento do embrião sobreexpressou-se Hairy1 nos precursores da MPS em estadios de gastrulação (HH4) e avaliou-se o alongamento dos embriões. Apesar do reduzido número de réplicas biológicas, os dados sugerem que a sobreexpressão de Hairy1 nos precursores da PSM atrasa o alongamento do embrião. Obtiveram-se resultados preliminares da aplicação de light-sheet microscopy mostrando que poderá ser usada no futuro para avaliar a divisão e migração de células em embriões de galinha.

Assim, no decurso deste trabalho obteve-se uma análise quantitativa de comprimentos ao longo do tempo do embrião e diferentes porções do mesmo. Esta análise constitui uma ferramenta muito útil no estudo do desenvolvimento de embriões de galinha e em diferentes condições experimentais. Durante o projeto mostrámos ainda que a sobrexpressão de Hairy1 em precursores da PSM provoca um atraso na alongamento do embrião. Compreender o papel de Hairy1 no desenvolvimento pode fornecer importantes dados para a compreensão do impacto dos seus homólogos, como Hes1, no Cancro.

Palavras chave: Embrião de galinha | Relógio embrionário | Elongamento | Imagiologia em tempo real | Hairy1

Contents

Figure index

Abbreviations

APC - Adenomatous polyposis

Ascl1 - *achaete-scute* homolog 1

BCIP - Bromo-5-4-Chloro-3-Indolyl-Phosphate

BBR - Boehringer's Blocking Reagent

BL - Blocking reagent

BMP - Bone morphogenic protein

CSC - Cancer stem cell

DTT - Ditiotreitol

EC - Early chick

ECM - Extracellular matrix

EDTA - Ethylenediamine tetraacetic acid

EGTA - Ethylene tetraacetic acid

EMT - Epithelial-to-mesenchymal

Erk - Extracellular Regulated Kinase

ES - embryonic stem

EtOH - Ethanol

FBS - Fetal bovine serum

FGF - Fibroblast Growth Factor

FN - Fibronectin

HDAC - Histone deacetylase

H1 - Hairy1

HCHO - Formaldehyde

ID - Triton X-100, BSA in PBS1x

MABT - Maleic acid, sodium chloride, Tween-20

MAPK - Mitogen-activated protein kinase

MeOH - Methanol

MPS - Mesoderme pré-somitica

NBT - 4-nitro blue tetrozolum chloride

NTMT - Tris-HCl with magnesium chloride and tween-20

o/n - Over night

PBS - Phosphate buffered saline

PBT - PBS 1% with Tween-20

PFA - Paraformaldehyde

PSM - Pré-somitic mesoderm

RA – Retinoic acid

RALDH2 - Retinaldehyde dehydrogenase 2

RNAsin - RNase inhibitor

RT – Room temperature

T - Brachyury

TAE - Tris-acetate-EDTA

TE - Tris-HCl with EDTA•Na_2

TGF-β - transforming growth factor beta

TLE - Transducin-like Enhancer of split

WT - Wild-type

1 - Introduction

Ever since the first Man, humankind is dazzled with the wonders of Nature and is in search for knowledge to understand it. One of the sources of fascination is how a single cell gives rise to a fully organized and functional organism - how embryo development occurs. During development, many processes need to occur in a strictly coordinated fashion. Developmental Biology studies strive to understand how cells divide, differentiate, and organize into structures, and how we can modulate them, for example, to regenerate tissues or delay/revert cancer progression.

1.1 - Developmental Biology and Oncogenesis

According to the World Health Organization (WHO) cancer was the second leading cause of death globally in 2015. The most common explanation of how a cancer develops focusses on the idea of a normal cell that suffers DNA mutations that allows the cell to gain capacities such as increased cell division, migration, among others, leading to uncontrolled growth, in a multistep process (Hanahan and Weinberg, 2000). Eventually tumor growth begins to affect the surrounding tissues and organs, or cells metastasize to other places. Without any treatment, the uncontrolled growth of cancer cells will compromise organ function and lead to host death (Hanahan and Weinberg, 2000).

Cancer can be seen as a disease of development, where cells have defects in cell-cell communication, paracrine pathways and are in an inappropriate environment (Gilbert, 2014). Supporting this idea are tumors that derive from cells with a normal genome, such as teratocarcinomas. Teratocarcinomas are malignant tumors that arise from germ cells or stem cells (Illmensee and Mintz, 1976; Stewart and Mintz, 1981). If cells of this tumor are placed in the inner cell mass of a mouse blastocyst, cells lose the malignant properties and divide normally, showing that the environment can play a crucial role in carcinogenesis. This also shows that embryo development has some parallelisms with carcinogenesis. Moreover, there are cases where tumor cells (derived from somatic cells), when placed in embryos behave as

normal cells during development (reviewed in Hendrix et al., 2007; Kasemeier-Kulesa et al., 2008; Postovit et al., 2008). Some of the most important signalling pathways in development, such as Hedgehog, Notch, Wnt and BMP/TGF-b/activin also have an important role, and are commonly deregulated, in carcinogenesis. This explains the existence of drugs that are teratogens, due to their action in developmental pathways, which can be very useful to treat cancer, such as cyclopamine (reviewed in Lee et al., 2014; Ma et al., 2010).

Considering the parallels between development and cancer, the knowledge that we can acquire from understanding the fundamental processes of cell differentiation and organogenesis during embryo development may give important contributions to understanding cancer and contribute to the development of new therapeutics.

1.2 - Key events in early embryo development

1.2.1 - Gastrulation

Gastrulation is one of the most important events during development. As Lewis Wolpert once said “It is not birth, marriage or death, but gastrulation which is truly the most important time in your life.” (Wolpert, 2008) This process occurs in early stages of development and is very dynamic, involving several events such as epithelial-to-mesenchymal transition (EMT) and cell motility.

Before gastrulation the avian embryo only has two cell layers, the epiblast and the hypoblast. The three embryonic germ layers come entirely from the epiblast (Rosenquist, 1966; Rosenquist, 1972). In amniotes (like the chick and human embryos) the germ layer identity is established before gastrulation starts, however the specification of cell type is controlled by inductive influences during and after the migration through the primitive streak (Rosenquist et al., 1996; Schoenwolf et al., 1992). The hypoblast contributes to form parts of the extraembryonic membranes and participates in the chemical signaling pathways that regulate the migration of the epiblast cells (Gilbert, 2014). Avian gastrulation shares many features with human gastrulation (Gilbert, 2014). Avian, reptilian and mammalian gastrulation occur through the primitive streak which appears to arise from Koller’s sickle

and the epiblast above it. (Gilbert, 2014; Bachvarova et al., 1998; Lawson and Schoenwolf, 2001a; Lawson and Schoenwolf, 2001b; Voiculescu et al., 2007). The primitive streak defines the major body axes of the chick embryo: anterior-posterior since it extends in a posterior-anterior direction; Dorsal-ventral since cells enter its dorsal part and move towards its ventral side; right-left since it divides the embryo in half along the midline (Gilbert, 2014). The avian organizer, also called the Hensen's node, forms at the anterior end of the primitive streak by a regional thickening of cells. In the center of the Hensen's node a depression is present through which cell can migrate.

The movements of cells in the epiblast, during streak formation, are called polonaise movements (Graper, 1926) (Figure 1.1) since they are similar to the dance with the same name. The cellular movements underlying the "cellular dance" were latter described in more detail: the cells come down in the sides of the epiblast and undergo immediately a directed intercalation in the posterior margin of the streak that is forming (Voiculescu et al., 2007). The movement of the cells towards the center of the embryo is mediated by the activation of the Wnt planar cell polarity pathway in the epiblast at the posterior edge of the embryo (Voiculescu et al., 2007). This pathway is important in directing the cells to the center of the embryo: if it is blocked both mesoderm and endoderm are formed peripherally instead of centrally. Fibroblast growth Factor (FGF) signaling from the hypoblast seems to be activating Wnt planar cell polarity activity. Ectopic expression of FGF signaling ectopically activates Wnt signaling leading to a change of the orientation of the primitive streak (reviewed in (Benazeraf and Pourquie, 2013). The rearrangements of cells that allow the characteristic polonaise movements in the epiblast (which is an epithelial tissue) are majorly driven by cell division (Figure 1.1). Intercalations mediated by cell division are necessary for the spatial patterning of the movements. When cell division is impaired, the spatial patterning is lost and cells tend to migrate towards the primitive streak (Firmino et al., 2016). The primitive streak elongates toward the anterior end until it reaches the head region at 60-75% of the length of the *area pellucida*. The extension of the streak seems to be achieved through convergent extension (Voiculescu et al., 2007). Cell division also contributes for the streak elongation, however it is not required for its formation (Wei and Mikawa, 2000). Importantly, inhibiting cell cycle progression blocks streak elongation, but not streak formation (Cui et al., 2005).

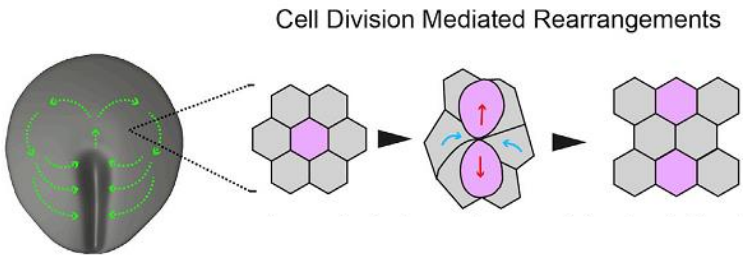

Figure 1.1 – **Cellular movements during chick primitive streak elongation – polonaise movements;**

Representation of a chicken embryo at stage HH3+ according to Hamburger and Hamilton (Hamburger and Hamilton, 1951). The green arrows show the direction of cell movements during – polonaise movements. The spatial patterning of the polonaise movements are driven by cell division. Figure was adapted from (Firmino et al., 2016)

In the chick embryo gastrulation, cells migrating from the anterior end of the Hensen's node to the deeper layers, will later form the notochord and the prechordal plate and the anterior somites. It was shown that the paraxial mesoderm, that gives rise to the somites, originates in two different places. The medial portion of the somite derives from a stem cell population located in the anterior part of the primitive streak. This population is continuously regenerating itself. The lateral portion of somites derive from continuous ingression of epiblast cells through the streak (Iimura et al., 2007; Psychoyos and Stern, 1996). The cells that give rise to the rest of the somites and to the heart and kidneys migrate through more median regions of the streak. Cells migrating from the most posterior part of the streak give rise to the lateral plate and the extraembryonic mesoderm (Figure 1.2) (Psychoyos and Stern, 1996), (Schoenwolf et al., 1992).

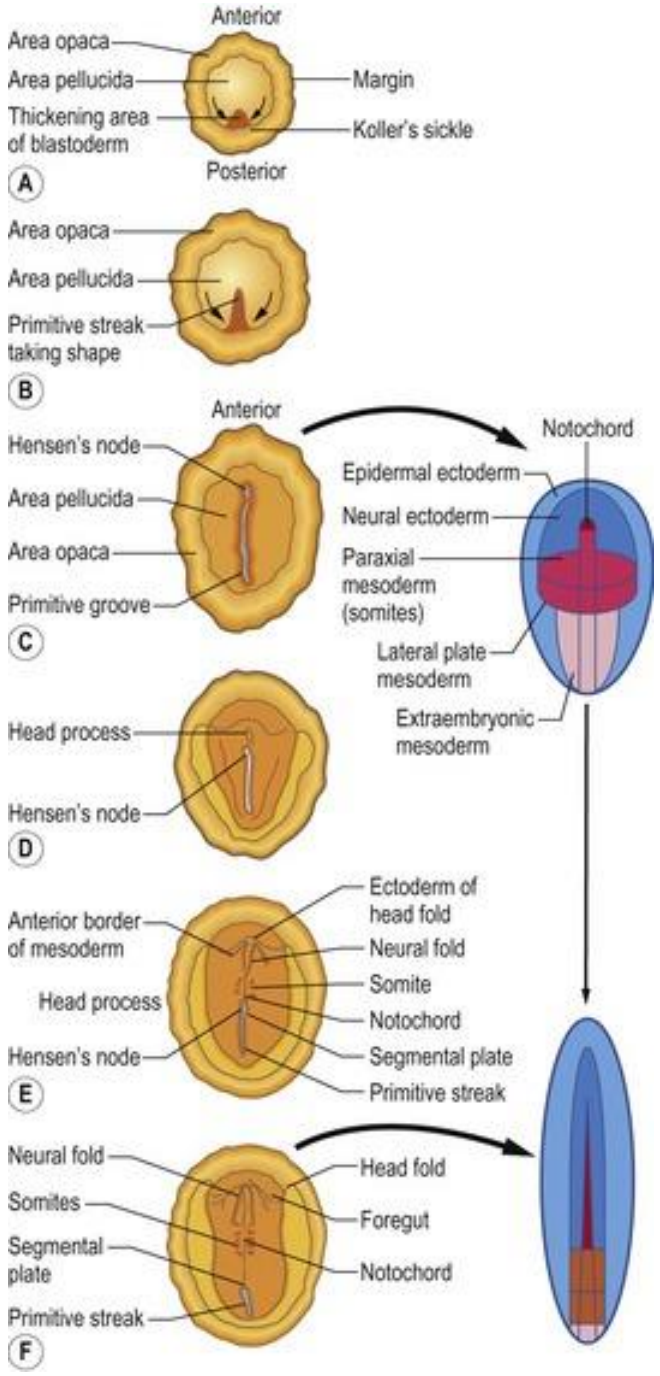

Figure 1.2 – **Early chicken embryo and gastrulation fate map;**

Representation of the structures of the early chicken embryo. A – HH2; B – HH3; C – HH4; D – HH5; E – HH7+; F – HH8; In stage HH2-HH3 is represented the formation of the primitive streak. In stage HH4 the primitive streak reaches its maximum length. After stage HH4, other structures begin to appear along the antero-to-posterior axis: the head process, notochord and somites. The fate maps of the epiblast are shown for stage HH4 and HH8. Figure from (Gilbert, 2014)

During gastrulation, cells from the epiblast need to undergo an EMT transition. As cells enter the primitive streak, the basal lamina beneath them breaks down allowing them to migrate through the embryo layers (DeLuca et al., 1999; Stern et al., 1990). As gastrulation proceeds and cells migrate through the primitive streak and enter the deeper layers of the embryo, the cells are specified into three layers. The deeper layer migrates toward the hypoblast and displaces the hypoblast cells to the side. The cells that reach the deeper layer give rise to the endoderm. The second layer of cells migrating spreads and form a layer of cells between the endoderm and the epiblast. This layer will give rise to the mesodermal parts of the embryonic tissues (Figure 1.3) (Gilbert, 2014).

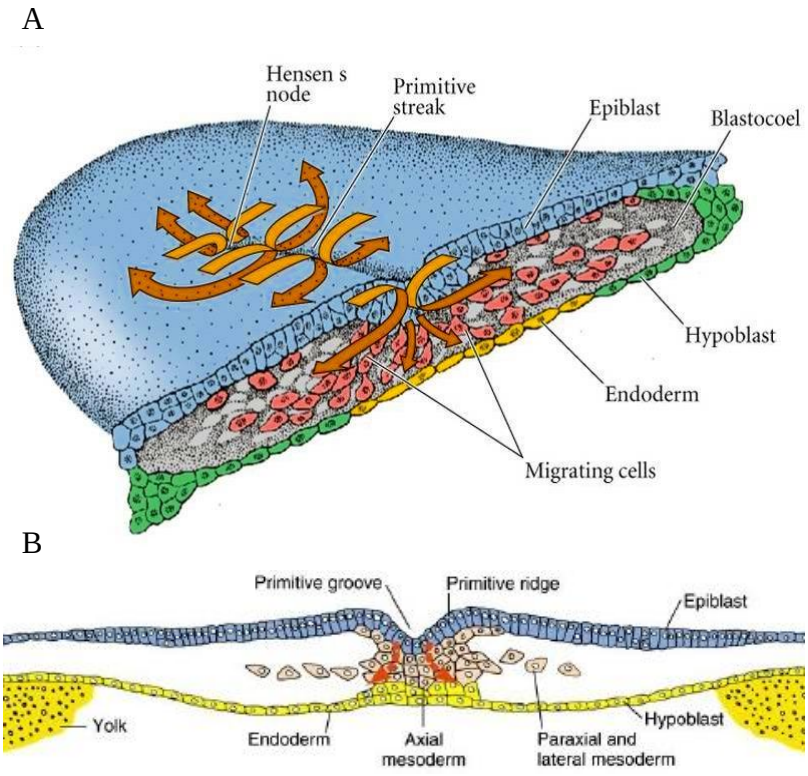

Figure 1.3 – **Migration of the epiblast cells through the primitive streak;**

A – Representation of a chicken embryo during gastrulation with the epiblast cellular movements represented. When cells reach the midline of the embryo, they ingress and migrate through the primitive streak. Cells migrating from the Hensen's node migrate anteriorly. Cells in the most anterior part of the primitive streak are going to migrate more laterally to form the paraxial mesoderm. Cells in more posterior regions are going to give rise to the intermediate mesoderm and lateral mesoderm. B – Representation of a transversal section of a chicken embryo. Epiblast cells are organized in an epithelial sheet and suffer an EMT in order to ingress through the streak. Adapted from (Gilbert, 2014)

FGF and Wnt signaling participate in the control of migration of mesodermal cells. FGF8 expressed in the posterior primitive streak repeals migrating cells away from the primitive streak, while FGF4 in the anterior streak attracts cells. Concordantly, beads releasing FGF8 or FGF4 alter the trajectory of migrating cells (Yang et al., 2002). Wnt signaling is important once cells are away from the streak, regulating the movements of the mesodermal precursors. Wnt5a directs cells to migrate broadly, and in the most posterior regions, leads cells to become lateral plate mesoderm. In most anterior regions Wnt3a is expressed and opposes Wnt5a, inhibiting migration and cells are specified as paraxial mesoderm (Sweetman et al., 2008).

1.2.2 - Embryo elongation

As development proceeds the embryo and different tissues elongate along the anterior-posterior axis. The mechanisms that drive embryo elongation are not completely understood, namely in later stages. It was already shown that the continuous ingression and proliferation of cells in the tail bud is necessary for axis extension (reviewed in Benazeraf and Pourquie, 2013). It was proposed that the elongation of the embryo could be driven by one or more specific tissues, that could force the other tissues to elongate (Benazeraf et al., 2010; Schoenwolf, 1978). One of the candidates was the notochord. Notochord plays an important role in providing signalling for cell-fate decisions to neighboring tissues and is a flexible tissue, which could be an important characteristic for the tissue driving elongation (Resende et al., 2010; Stemple, 2005). This would be an important characteristic since a flexible structure would be able to endure higher tensions without breaking, while forcing the adjacent tissues to elongate. Notochord elongation is regulated mainly by three different processes: the addition of cells from the Hensen's node (Sausedo and Schoenwolf, 1993); antero-posterior oriented cell division (Keller et al., 2003) and convergent extension or cell rearrangements (Glickman et al., 2003). In chick embryo, it was proposed that the rearrangements of cells as they leave the Hensen's node and enter the notochord are the main driver of notochord extension (Sausedo and Schoenwolf, 1993). Trying to address this same question, Bénazéraf and collaborators (2010), deleted caudal structures from the chicken embryo in order to address which would affect more embryo elongation. From all tissues

ablated (which didn't include the notochord), the caudal part of the paraxial mesoderm, or pre-somitic mesoderm (PSM), lead to an abrupt slowing down of embryo elongation (Benazeraf et al., 2010). In the posterior region of the PSM, cell movements are random and mainly caused by the continuous ingression of cells from the tailbud. FGF signaling is important for the cell movements in PSM (Benazeraf et al., 2010). The PSM is also rich in Extracellular matrix (ECM) proteins which would endure the forces needed for embryo elongation (Czirok et al., 2004; Duband et al., 1987; Martins et al., 2009; Rifes et al., 2007; Rifes and Thorsteinsdottir, 2012). Mutant mouse embryos for fibronectin or its receptor integrin α5 present posterior truncations (George et al., 1993; Georges-Labouesse et al., 1996; Yang et al., 1999; Yang et al., 1993). Also, mouse mutants in a motif of fibronectin that affect its binding to integrin show truncation and PSM patterning and migration defects (Giros et al., 2011), showing that the EMC is crucial for embryo elongation. Those evidences highlight a potential role of the PSM in chicken embryo elongation. The potential link between embryo elongation and the PSM is also supported by the events that occur upon embryo elongation termination. Embryo elongation termination coincides with the somitogenesis end and with PSM shrinkage. As elongation proceeds, somite formation is relatively constant, although the last somites are formed at a slower rate (Tam, 1981; Tenin et al., 2010). As the last somites are formed, PSM progressively shrinks leading to a closer proximity of the last somite and the tail bud. Somites produce retinoic acid (RA) which leads to axis truncation. In these stages, the protein that catabolizes retinoic acid (Cyp26) is downregulated and an enzyme responsible for RA production (Raldh2) is expressed in chick tail bud in those later stages (Iulianella et al., 1999; Kessel and Gruss, 1991; Tenin et al., 2010). Cultured tail bud exposed to RA also present higher levels of apoptosis (Shum et al., 1999; Tenin et al., 2010). Also, embryo elongation is regulated by FGF and WNT signaling. Mutations in those pathways leads to posterior axis truncations (Kondoh and Takemoto, 2012). Inhibiting cell division in chick embryos between stage HH10-11 does not affect embryo elongation (Benazeraf et al., 2010) showing that cell proliferation is not the main driver of axis elongation. Recently, it was shown that a gradient of glycolytic activity within the PSM is important during amniote elongation and that it seems to be coordinating FGF and Wnt signaling (Oginuma et al., 2017). This interesting observation raises the possible function of metabolism in PSM as a producer of metabolites for other pathways since it seems

that energy production is not the predominant role of glycolysis in the PSM (Naganathan and Oates, 2017). Also when glycolysis is blocked, embryo elongation and cell motility within PSM are affected (Oginuma et al., 2017). The link of cell motility and elongation was already exposed since cell movement inhibitors lead to slower elongation rate in chick embryos (Benazeraf et al., 2010). Furthermore, it was suggested that the PSM is the tissue that contributes the most to quail embryo elongation, which is concordant with the experiments of tissue ablation in the chick embryo (Benazeraf et al., 2017). Through mathematical modeling it was proposed that cell proliferation may contribute to a large part of PSM elongation in quail embryos (Benazeraf et al., 2017). Thus, although the mechanisms that underlie embryo elongation are not yet fully understood, it seems that in chick embryos, PSM is the main candidate to be the tissue driver of embryo elongation.

1.2.3 - Somitogenesis

Even before gastrulation reaches its end, cells begin to differentiate and to form structures along the embryo. As the Hensen's node regresses, while gastrulation keeps occurring in the most posterior part of the embryo, in the anterior part, the somites and the head begin to form. Somite formation is a very interesting process of development (Figure 1.4). Not only is it the first evidence of segmentation of the vertebrate body axis, but it is also a periodic process. Somites appear with a period that is species-specific (90 minutes in the chicken embryo, 2 hours in mice and 30 minutes in zebrafish). The period of somite formation presents different periods of formation along chick development: the period of formation of the somites is 90 minutes from the 15º somite until approximately stage HH21; After, the last somites are formed with higher periods, in stage HH23 the period was suggested to be 150 minutes (Palmeirim et al., 1997; Tenin et al., 2010).

Somites are blocks of mesodermal cells that are formed from the paraxial mesoderm, also known as somitic mesoderm. Somites are formed sequentially along the anterior-posterior axis bilaterally to the notochord and neural tube (Figure 1.4A) (reviewed in Bailey, 2015). When somites are formed, they are composed by a layer of epithelial cells that surround the structure, while the cells in inner part are mesenchymal. The cells that give rise

to somites are mesenchymal, therefore they suffer a mesenchymal-to-epithelial transition to form the epithelial sheet. When each somite is formed, they are separated from the paraxial mesoderm with fissures, individualizing each somite from each other and from the paraxial mesoderm. When matured, somites are subdivided in three major compartments: the sclerotome, the myotome and the dermatome. Somites are transient structures and they will give rise to other structures later in development. The sclerotome will contribute to form vertebrae and rib cartilage. The myotome to musculature of the back, the rib cage and the ventral body wall. The dermatome also contributes to the dermis of the back of the embryo. The tendons, vertebral joints and invertebral discs are also formed from somitic compartments.

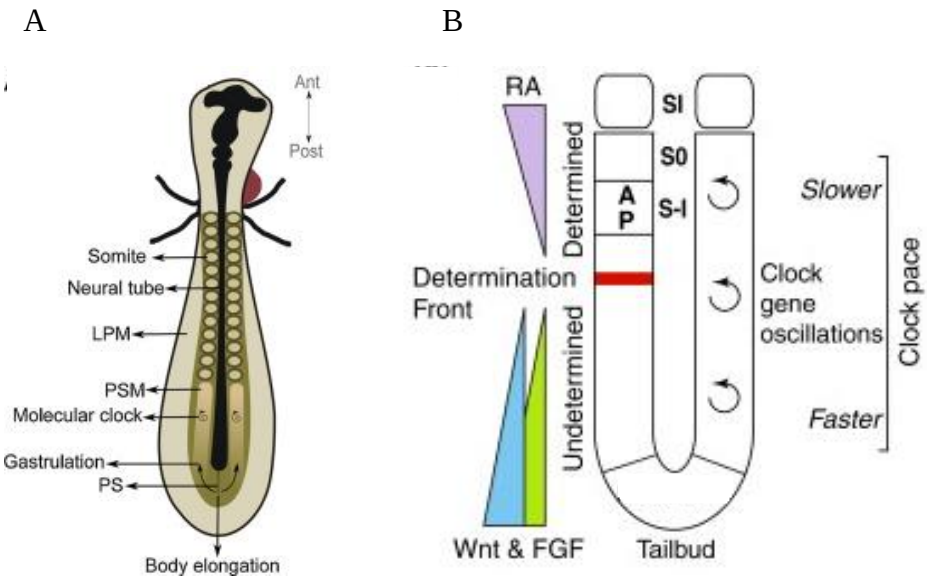

Figure 1.4 – **Somitogenesis – The clock and wave-front model;**

A – Representation of a dorsal view from a chicken embryo in stage HH11; The structures are represented in the antero-posterior axis, where the somites can be observed bilaterally to the neural tube. B – Representation of a caudal part of a chicken embryo during somitogenesis with the components of the clock and wavefront model. The wavefront is represented by the opposing gradients of retinoic acid (RA) and Wnt and FGF signaling pathways. The clock is operating within PSM and the period slows down in a posterior-to-anterior fashion. Figures A and B were adapted from Sheeba et al., 2016; Gibb et al., 2010 respectively.

Somitogenesis is strictly regulated both in time and space. Somites appear on both sides of the embryo at the same time, and even if the paraxial mesoderm is isolated, it segments in the correct time and direction (Palmeirim et al., 1997). Several models were conceptualized to explain such coordination and two of the most discussed were the cell cycle and the clock and wavefront model (Collier et al., 2000; Cooke and Zeeman, 1976). The cell cycle model settles on the idea of the cell cycle as the periodic event that controls the timing of somite formation (Collier et al., 2000). This idea was developed when some experiments showed that heat-shock abnormalities were similar to abnormalities caused by cell cycle progression inhibition. Nowadays, the model used to explain somitogenesis is the clock and wavefront model. However, a link between cell cycle and somitogenesis cannot be discarded. Several studies showed that the molecules regulating somitogenesis and the cell cycle are connected. It was showed that cell cycle progression is important for somite morphogenesis, but not required for the oscillations of the segmentation clock, which will be discussed later (Zhang et al., 2008). Delaune and collaborators also showed that cells tend to enter the M phase of the cell cycle when the oscillation of the molecular clock is in the off phase (Delaune et al., 2012). Those observations suggest that, despite the cell cycle model not being the most used to explain the process of somitogenesis, we cannot discard a link between the two processes. The model used nowadays to explain somitogenesis is the "clock and wavefront" (Figure 1.4B) (reviewed in Bailey, 2015). The "clock and wavefront" model is composed by two different parts: the first one composed by opposing gradients across the PSM that would originate a wavefront which would give positional information for the formation of the somites. The second part of the model is composed by a clock that would give time information to the cells, putting them in a permissive/non-permissive state for morphological somite formation, explaining the periodicity of segmentation (reviewed in Bailey, 2015).

1.3 - The somitogenesis molecular clock

The question of how temporal regulation of somitogenesis is achieved is one of the most interesting questions in developmental biology: how cells in the embryo have the notion of Time and how this translates into biochemical and morphological characteristics. Time

can be considered as the fourth dimension of embryo development and one of the first hints about how cells count/sense time during development was uncovered in 1997 by Isabel Palmeirim and collaborators (Palmeirim et al., 1997), when the first evidence of the clock of somitogenesis was discovered (Figure 1.5). Palmeirim and collaborators discovered that *hairy1*, a member of the Hes proteins and homologous to human Hes1, had an oscillatory expression of its mRNA in the PSM with the same period as somite formation (Palmeirim et al., 1997). This was the first time that the segmentation molecular clock was described. Later on, it was shown that Hes genes presented both mRNA and protein oscillatory expression during somitogenesis in several organisms (reviewed in Bailey, 2015). The period of oscillation of the clock is variable among the species and corresponds to the period of somitogenesis: 90 minutes in the chick, 30 minutes in the zebrafish and 2 hours in the mouse embryos.

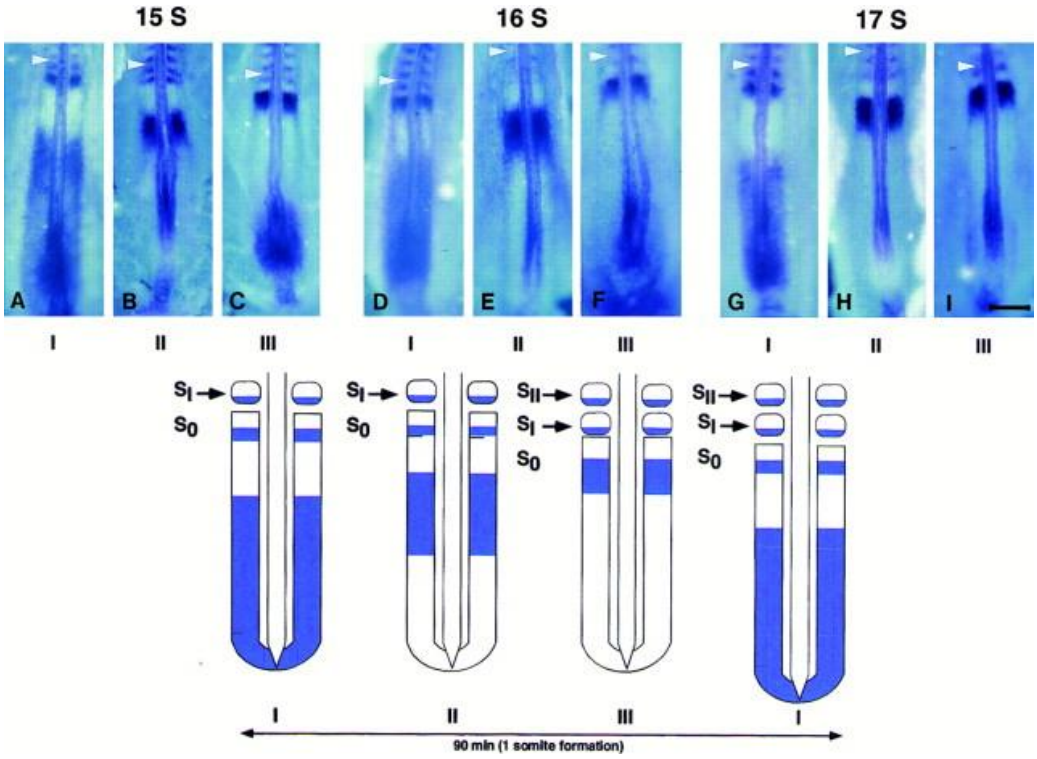

Figure 1.5– **Expression pattern of hairy1 during somitogenesis;**

Expression pattern of *hairy1* in the caudal part of chicken embryos during somitogenesis stages. The expression is dynamic within PSM with a period of 90 minutes, which corresponds to the period of somitogenesis in the chicken embryo (Palmeirim et al., 1997).

It was also shown that the oscillations of the molecular clock were regulated by negative feedback loops that were responsible for maintaining the sustained oscillations of Hes proteins (Figure 1.6) (Hirata et al., 2002). Another important feature of the somitogenesis molecular clock is the synchrony between PSM cells in order to form somites in the desired time and space. It was shown in zebrafish, that in the PSM, Hes oscillations are synchronized through Notch signaling, which also activates Hes expression (Jiang et al., 2000). If synchronization between cells is disturbed, somite formation is impaired (Delaune et al., 2012). Cell movements in the PSM are important to achieve a high level of synchronization between cells (reviewed in Uriu et al., 2010). Another interesting feature of the clock is that the period slows down in a posterior-to-anterior fashion, until it stops when the new somite is formed (Figure 1.4). Another structure that also presents a molecular clock during development is the limb. In limb development the period of the genetic oscillations is 6 hours (Pascoal et al., 2007). The signaling pathways and players involved in the clock of both limb and somitogenesis are conserved, showing that the machinery is reused in two different developmental processes (Sheeba et al., 2016). This highlight the plasticity of these networks that, using conserved players and pathways, can achieve different periods of oscillation.

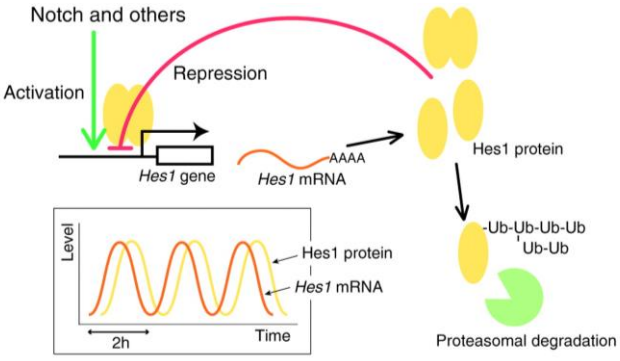

Figure 1.6 – **Hes negative feedback loop;**

Negative feedback loop that underlies the oscillatory expression of Hes genes. Hes genes are activated by Notch and other signaling pathways. After transcription, Hes mRNA is translated and the protein represses its own transcription closing the loop. Hes proteins are degraded by proteossomal degradation. In the mouse, both mRNA and protein of Hes1oscillate with a period of two hours. Figure from Kageyama et al., 2007).

The other part of the "clock and wavefront" model is the wavefront. The wavefront components were only described after the discovery of the clock. It is proposed nowadays

that the wavefront is composed by opposing gradients of retinoic acid and FGF/Wnt signaling (reviewed in Bailey, 2015) along PSM. FGF/Wnt present a posterior-to-anterior gradient. The gradient of FGF is accomplished by mRNA decay along the PSM (Dubrulle and Pourquié, 2004). The expression pattern correlates with activated Erk which is a downstream effector of the FGF signalling pathway (Dubrulle and Pourquié, 2002). Wnt3a also presents the similar expression pattern as FGF8 (Aulehla et al., 2003). Opposing these gradients is the presence of RA that is produced by the enzyme retinaldehyde dehydrogenase 2 (Raldh2). Raldh2 is expressed in the somites and anterior part of the PSM. RA and FGF have opposing effects in cells in the PSM and mutually inhibit each other: the gradient of FGF8 and Wnt3a is responsible for maintaining the cells in an undifferentiated and proliferative state; RA induces the differentiation of the cells (reviewed in Andrade et al.,2005). This balance between RA and FGF/Wnt defines the prospective somitic boundary location within the PSM (reviewed in Andrade et al.,2005). Concordantly, if FGF8 gradient is displaced, the new somites formed are smaller (Dubrulle et al., 2001).

More recently it was shown that the wavefront gradients and the molecular clock are linked in somitogenesis. In the mouse PSM it was shown that pErk oscillates in a hes7-dependent manner (Niwa et al.,2011). Hes7 is one of the members of the molecular clock and also regulates the oscillatory expression of Notch effectors. Hes7 integrates both oscillators in a way that they are synchronous in the posterior PSM and asynchronous in the anterior PSM, thereby linking the wavefront and the clock of somitogenesis (Niwa et al., 2011). Aulehla and co-workers also showed that the activation of Wnt signalling provides a permissive environment and maintains the oscillations of the segmentation clock and suggested that Wnt signalling downregulation in the anterior PSM may regulate the arrest of the oscillations in normal conditions upon somite formation (Aulehla et al., 2007). These observations show that the wavefront and the clock are linked during somitogenesis, providing an additional layer of regulation.

1.3.1 - Hes protein family

Hairy1 is a member of the Hairy and Enhancer of Split (Hes) family of transcription factors (reviewed in Kageyama et al., 2007). This family of proteins has three highly conserved domains: the basic helix-loop-helix (bHLH), the Orange domain and the C-terminal tetrapeptide Trp-Arg-Pro-Trp (WRPW) domain (Figure 1.7). The bHLH domain allows protein binding to the DNA and also homodimerization and heterodimerization through the helix-loop-helix motif. The Orange domain regulates the binding of the bHLH domain to other partners forming heterodimers, although its full role remains unclear. The WRPW domain can repress transcription through the recruitment of co-repressor complexes (Kageyama et al., 2007). Hes proteins are commonly known as transcriptional repressors and can act both directly and indirectly (Sasai et al., 1992a). Direct transcription inhibition is mediated by the recruitment of corepressors such as Groucho and other transducin-like Enhancer of split (TLE) proteins (Fisher et al., 1996; Grbavec and Stifani, 1996; Paroush et al., 1994). Groucho/TLE are complex transcriptional repressors that recruit histone deacetylases (HDACs) to the chromatin but do not bind directly to the DNA, and are important in several cellular processes (Chen and Courey, 2000). Hes proteins can also repress transcription indirectly by competing with other bHLH activators for the binding to DNA through E-boxes (CANNTG) (Kageyama et al., 2007; Sasai et al., 1992b).

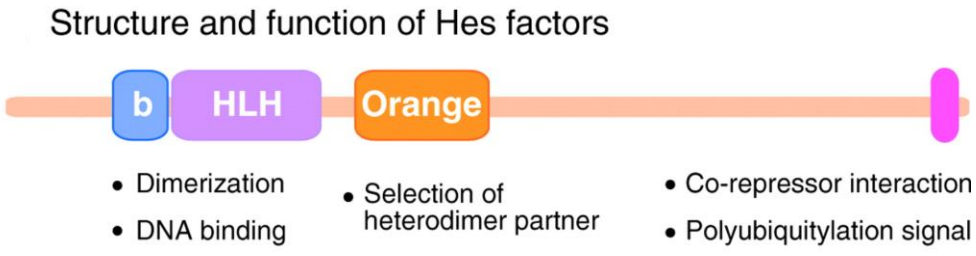

Figure 1.7 – **Conserved domains of the Hairy and Enhancer of Split (Hes) family of proteins;**

Structure and domain function of Hes proteins. Basic (b) helix-loop-helix (HLH) domain is important for dimerization and DNA binding, The Orange domain mediates the selection of partners for heterodimer formation. The pink region represents the WRPW domain that is important for the co-repressor interaction. Figure adapted from Kageyama et al., 2007).

Most bHLH domains bind to E-Boxes, however, Hes family proteins have in the middle of the basic region of the bHLH domain, a proline residue in a conserved position that is proposed to confer affinity to specific target sequences, such as N-boxes (CACNAG)(Akazawa et al., 1992; Ohsako et al., 1994). Hes proteins and their mRNAs both have short half-lifes, around 20 minutes in cultured cells. It was shown that the route of degradation is mediated by ubiquitination (Figure 1.6) and that the proteins are degraded by the proteasome in fibroblast cells (Hirata et al., 2002). The ability of Hes proteins to form homodimers and heterodimers with several partners, to bind to different regions in the DNA, and the short half-lives of both mRNA and protein, allows Hes proteins to have different roles and functions in biological systems and to work as genetic oscillators (reviewed in Kageyama et al., 2007).

1.3.2 - Hes proteins as genetic oscillators

In biological systems, the timing of responses and events is very important. The circadian clock and cell cycle are the most conserved and well-known oscillators that are supported by genetic oscillatory networks. During the last years, other genetic oscillators with ultradian periods have come to light (reviewed in Isomura and Kageyama, 2014), for example the Hes oscillators. These genetic oscillators have important roles is cell responses and regulating timed processes, highlighting the functional correlation between dynamic patterns of expression or activity and cellular responses. There are multiple oscillators (at the level of biological activity or gene expression) that lead to dramatically different cellular responses depending on the dynamics that they present. NF-kB pathway activity oscillations, oscillatory p53 expression, pulsatile Erk activity are some of the examples that, depending on the dynamics can lead to different cellular responses (reviewed in Isomura and Kageyama, 2014). This highlights the importance of understanding how a pathway or molecule is being expressed or activated over time, to deeply understand biological events.

Hes genes are important genetic oscillators in the context of embryo development. Depending on the tissue and context, the differential dynamics of Hes expression is key for

distinct cellular responses, to synchronize events, for timing cellular processes or regulating binary cell fate decisions (Kageyama et al., 2007).

Hes genes have oscillatory expression in several cell types, different organisms and tissues (Kobayashi et al., 2009; Palmeirim et al., 1997; Pascoal et al., 2007; Shimojo et al., 2008; William et al., 2007). The oscillations of Hes proteins are possible due to a set of important characteristics: short half-lives of both mRNA and protein, a delay between mRNA transcription and protein translation and the participation in a regulatory negative feedback loop (Hirata et al., 2002; Uriu, 2016). This negative feedback allows the maintenance of the oscillation during long periods of time inside cells. Hes1 has different periods of oscillation depending on the cells where it is expressed; for example in embryonic stem (ES) cells the period is of 3–5 hours and in neural progenitors the period is of 2–3 hours) (Kobayashi et al., 2009; Shimojo et al., 2008). Also, hairy1 has a period of oscillation in chicken PSM of 90 minutes (Palmeirim et al., 1997) and in the limb of 6 hours (Pascoal et al., 2007).

During the last decades, mathematical formulations and simulations have provided new insights in developmental biology, being very useful to predict and lay down the possible scenarios that could explain what is observed *in vivo*, including in trying to understand how a negative feedback loop could lead to different periods in the clocks. Based on mathematical formulations, the period of a genetic oscillator can be calculated by differential equations that are determined in most part by the time delays involved in the negative feedback loop and the half-lives of both mRNA and protein molecules (reviewed in Uriu, 2016). According to Uriu and collaborators (2016), shorter time delays in the feedback and shorter half-lives of the molecules cause shorter periods of oscillations. So, the same gene can have different periods of expression oscillations by changing the length of time delays, stability of the molecules or changing the timescales of the biochemical reactions involved, such as transcription and translation (reviewed in Uriu, 2016). Therefore, different cell types can adjust the period of the genetic oscillator, employing different levels of regulation. It is also important to understand that, in order to be a reliable clock, the genetic oscillator needs to ensure the precision of oscillation (Uriu, 2016).

Besides the role of Hes proteins in somitogenesis, these oscillators play important roles in other contexts. In nervous system development, Hes proteins are very important for

cell differentiation decisions. In mouse neural stem cells, Hes1 oscillates with a period of 2-3 hours (Shimojo et al., 2008). In this context it has two contradictory functions: proliferation of neural stem cells and differentiation of glial cells into astrocytes (Figure 1.8) (reviewed in Kageyama et al., 2007). The dynamic of expression of Hes1 in these contexts are different: in neural stem cells, Hes1 presents an oscillatory dynamics, while during differentiation it presents higher levels of Hes1 (Harima et al., 2014).

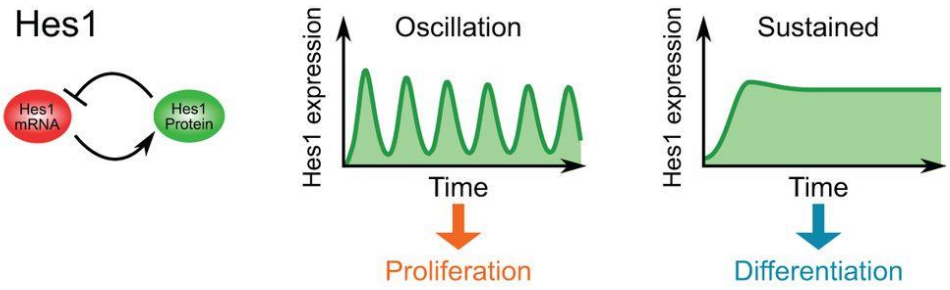

Figure 1.8 - **Different cell responses to different Hes1 expression dynamics;**

Hes1 protein can be differentially expressed in neural stem cells. If Hes1 levels oscillate, neural stem cells proliferate, if Hes1 expression is sustained, neural stem cells differentiate into astrocytes. Figure adapted from Isomura and Kageyama, 2014).

Hes1 negatively regulates the *achaete-scute* homolog 1 (Ascl1) in neural stem cells, therefore, when Hes1 presents an oscillatory dynamics of expression, Ascl1 presents the same dynamics in an inverse pattern. When Hes1 expression is sustained, Ascl1 is downregulated and the contrary also occurs. Ascl1 is a proneural factor that induces cell cycle exit and promotes neuronal differentiation (reviewed in Harima et al., 2014). However, it was showed that Ascl1 could have a role in neuronal stem cell proliferation. An oscillatory expression with a period of 3 hours activates neural stem cell proliferation and sustained expression correlates with neuronal differentiation. Thus, Hes1 expression in neural stem cells drives differential responses also by regulating different dynamics of expression of other genes (reviewed in Harima et al., 2014). Accordingly, overexpression of Hes1 or Hes5 in mouse brains at embryonic day 13.5 inhibits neuronal differentiation (Ohtsuka et al., 2001). On the other hand, in the absence of those factors, radial glial cells (which are neural stem

cells) prematurely differentiate into neurons, leading to a depletion of neural stem cells (Hatakeyama et al., 2004). Therefore, Hes gene expression dynamics are important to regulate robust binary cell fate decisions in progenitor cells (Pfeuty and Kaneko, 2014), where phase differences in Hes1 oscillation between two cells would be important. The role of the dynamics of expression was also highlighted in the work of Shimojo and collaborators (2016). In their work they altered the dynamic of expression of *delta1*, transforming the oscillatory expression to a sustained expression state, without altering the average levels of expression. Delta1 is a Notch ligand that induces Hes1 expression, and Hes1 also regulates delta1. Delta1 presents an oscillatory expression both in somitogenesis an in neural stem cells. Altering delta1 dynamics of expression, altered also Hes1 expression, which leads to fused somites and smaller brains (Shimojo et al., 2016).

Hes1 oscillates in embryonic stem (ES) cells (Kobayashi et al., 2009), with a period that varies from 3-5 hours, and tends to be differentially expressed during the cell cycle: higher levels of Hes1 during S-G2 phase compared to G1 phase (Kobayashi et al., 2009). Hes1-low ES cell tend to more efficiently differentiate into neurons while the Hes1-high cells differentiate into mesodermal cells. Inactivation of Hes1 reduces heterogenous responses to a differentiation signal and leads to a more preferential differentiation into the neural fate of ES cells (Kobayashi et al., 2009). This shows that the cyclic expression is important to achieve multiple cell types even under the same differentiation stimulus.

1.3.2 - Hes proteins and cancer

Hes proteins have important roles during development, so it is very natural that deregulation of those proteins and related pathways can lead to diseases. The role of Hes1 in cancer is not well understood but Hes1 has already been linked to metastasis, stem cell renewal, and drug resistance (reviewed in Liu et al., 2015). The cancer types were Hes1 plays an important role are vast, and only a few examples will be listed. Intestinal carcinomas usually develop from adenomas. It was showed that adenoma cells express Hes1 at high levels. Curiously, when mice are treated with gamma-secretase (Notch signaling inhibitor), adenomas transformed into goblet cells. This shows that Notch-Hes1 signaling may play an important role in intestinal adenomas development (van Es et al., 2005). In colon cancer, it

seems that the expression of Hes1 is higher in poorly differentiated cancer samples, compared with well differentiated samples. Hes1 expression is also correlated with expression of stem cell markers and seems to enhance self-renewal properties of stem-like cancer cells (CSC) (Gao et al., 2015). Hes1 also promotes EMT and enhances invasiveness in colon cancer cells (Gao et al., 2015). Pancreatic cancer is one of the deadliest worldwide. This high mortality rate is mostly due to late detection. In this type of cancer, Hes1 was described to have an important role in maintaining the cancer stem cell population where it has a higher expression in Cancer stem cells (CSC) cells compared to non CSC cells (Abel et al., 2014). In acute myeloid leukemia (AML) Hes1 has been described as an independent prognostic factor where low levels of Hes1 are associated with poor prognosis (Tian et al., 2015). In nasopharyngeal carcinoma, Hes1 can trigger EMT and this effect seems to be mediated by several proteins, such as PTEN which is downregulated by Hes1 (Wang et al., 2015). PTEN is one of the most common mutated genes in cancer (Yin and Shen, 2008). This protein is part of the PI3K pathway which regulates cell cycle progression, cell survival and growth (reviewed in Chalhoub and Baker, 2009). In rhabdomyosarcomas, a tumor from skeletal muscle samples examined showed that every cell line and patient sample had elevated levels of Hes1 compared to the control skeletal muscle, and most with 5-50-fold higher change (Sang et al., 2010).

Reports on Hes1 effects on cancer development are sometimes contradictory but in most cases, it seems to have an important role in maintenance of cells in a relatively undifferentiated state (reviewed in Liu et al., 2015). It is important to consider that the dynamics of expression in each case was not assessed, therefore, we cannot exclude the possibility that different dynamics of Hes1 expression also have an important role during carcinogenesis. This highlights the importance of understanding the biological roles of Hes in different tissues and how the different dynamics of expression/activity influence biological processes and disease initiation and progression.

1.4 - Goals of this work

Previous work from our lab showed that when *hairy1* is overexpressed in chick PSM precursors during gastrulation, the development of the embryo body is delayed relatively to

head development (Andrade et al., under review). This delay can be observed both morphologically and with molecular differentiation markers. Despite this delay, the embryo recovers from the phenotype later on. As mentioned before, *hairy1* is a member of the Hes protein family that acts as a genetic oscillator regulating somite formation in the chick embryo (Palmeirim et al., 1997). There are several hypotheses that could explain why overexpression of *hairy1* delays embryo development. Hairy1 may be affecting cell division, cell differentiation and/or cell migration through the primitive streak during gatrulation. In order to understand how *hairy1* is delaying embryo development and how the embryo recovers from the phenotype, we decided to study embryo elongation using live imaging techniques in WT embryos and in embryos with Hairy1 overexpression.

The main goals of this work are to:

- Characterize Hairy1 expression dynamics in gastrulation stages;
- Describe chicken embryo elongation in wild-type conditions;
- Analyze the impact of Hairy1 overexpression in gastrulation stages on embryo elongation;

2 - MATERIALS AND METHODS

2.1 - Chick embryo incubation and staging

Fertilized chicken (*Gallus gallus)* eggs were provided by commercial sources and incubated in a humidified atmosphere and controlled temperature (37-38ºC). Embryos were staged based on the Hamburger and Hamilton classification (Hamburger and Hamilton, 1951) or by somite number.

2.2 - RNA probe synthesis

hairy1 probe synthesis was performed using a previously described plasmid (Palmeirim et al., 1997). *In vitro* transcription was performed using 1µg of linearized plasmid, 3,5 µl of transcription buffer 10x (NZYtech), 2 µl Dig RNA labelling mix (Roche), 2µl RNA polymerase (NZYtech) and 2µl RNAsin (RNase inhibitor) (Promega) and incubated during three hours at 37ºC. After this period, 2µl of RNasin (Promega) and 4µl of DNase I (Promega) where added and incubated for 30 minutes at 37ºC. 200 µl TE, 20 µl lithium chloride 4M and 600 µl of ethanol (EtOH) were added followed by over-night (o/n) incubation at -20ºC. After o/n incubation the reaction was centrifuged at 14000 rpm for 30 minutes at 4ºC followed by the addition of 1 mL of EtOH (70%) to the pellet. A centrifugation at 14000 rpm during 15 minutes during 4ºC was performed next, the supernatant discarded and followed by the resuspension of the pellet in 50 µl of EDTA 10 mM. The probe was stored at -20ºC. Electrophoresis analysis was performed using 0.8% agarose gel in TAE (Tris-acetate-EDTA) with 2,5 µl greensafe (Nzytech) (Appendix 1). The molecular marker used was λ*Pst*I previously prepared in the lab.

2.3 - *In situ* hybridization

Whole mount *in situ* hybridization was performed as described (Henrique et al., 1995). Chicken embryos were dissected in phosphate buffered saline (PBS) 1% and fixed in 4% formaldehyde (Sigma) in PBS completed with 2mM EGTA, o/n at 4ºC. Embryos were then washed twice in PBT (PBS 1% with 0.1% Tween-20) followed by dehydration. Dehydration was comprised by two sequential washes in 50% methanol (MeOH)/PBT and 100% MeOH. Embryos were then stored at -20ºC for future utilization.

Embryos were rehydrated through sequential washed in 75%, 50%, 25% MeOH/PBT followed by two washes in PBT. Next, a 10µg/mL proteinase K in PBT treatment was performed, followed by rinsing in PBT and post-fixation in 4% formaldehyde complemented with 0.1% glutaraldehyde (Sigma) in PBT. The period of treatment in proteinase K in minutes corresponds to the stage number of the embryo according to the Hamburger and Hamilton stages (Hamburger and Hamilton, 1951). After post-fixation, embryos were washed with 1:1 PBT/Hybridization mix and then with hybridization mix alone. Embryos were then incubated one hour at 70ºC in hybridization mix followed by an incubation o/n in hybridization mix complemented with the probe of interest. The next day, the embryos were rinsed twice with prewarmed hybridization mix and washed with 1:1 hybridization mix/MABT. Two washes in MABT followed by an incubation in the same solution for 15 minutes, were performed. Blocking steps followed: 1 hour in MABT complemented with 2% Boehringer Blocking Reagent (BBR) and 1 hour in MABT complemented with 2% BBR and 20 % heat-treated goat serum (BL). 1/2000 AP-anti-DIG antibody (Roche) in 2% BBR/20%BL/MABT was incubated o/n at 4ºC. Embryos were then washed in MABT for 1 hour, at least three times, followed by two washes during 10 minutes each in NTMT (Tris-HCl with magnesium chloride, sodium chloride and tween-20). Embryos were finally incubated in NTMT with NBT (4-nitro blue tetrozolum chloride, ROCHE) and BCIP (5-Bromo-4-Chloro-3-Indolyl-Phosphate, ROCHE) at room temperature until the signal was developed to the desired extent. Embryos where then washed in PBT and stored in 0.1% azide in PBT. Embryos were photographed using a STEREO Lumar.V12 (Zeiss) in petri dishes with 1% agarose in water.

2.4 - Immunofluorescence

The *whole mount* immunofluorescence protocol used during this work required optimization for use with the custom-made Hairy1 antibody. Two protocols were used as reference with further optimizations.

First protocol used - Embryos were collected in PBS1x and fixed in PFA 4% at room temperature for one hour followed by three washes in PBS1x during ten minutes without agitation. Embryos were permeabilized during 5 minutes without agitation in 0.1% Triton X-100 in PBS1x followed by a blocking step in 10%FBS for one hour at room temperature without agitation. Hairy1 (H1) (1:150, Andrade et al., under review) and Brachyury (T) (1:100, R&D) (positive control) were incubated o/n at 4ºC. The primary antibody incubation was followed by three washes in PBS 1x for ten minutes. Secondary antibody (Alexa Goat-anti-mouse 488, Molecular probes; Alexa Goat anti-rabbit 568, Molecular probes) incubation proceeded for one hour at room temperature after centrifugation (30 minutes, 13000 rpm, 4ºC) with a concentration of 1:2000 followed by 3 washes in PBS 1x for ten minutes. Slide assembly was performed in PBS1x.

Second protocol (Martins et al., 2009; Pinheiro, 2014) - Embryos were collected in PBS1x and fixed in 4% PFA in PBS1x o/n at 4ºC. Embryos were then washed at least 3 times 10 minutes. Two optional steps of blocking and permeabilization followed: 1) 5% BSA for 4 hours at room temperature: 2) 2 hours in ID 1% (1% Triton X-100 1% BSA in PBS1x) at RT. Embryos were then incubated in primary antibody diluted in 1% BSA in PBS 1x o/n at 4ºC: Hairy1 (H1) (1:150, Andrade et al., under review), Brachyury (T) (1:100, R&D) (positive control) or Fibronectin (FN) (1:400, F-3648, Sigma-Aldrich) (positive control) Embryos were then washed in PBS 3 times for 10 minutes. Secondary antibody (Alexa Goat-anti-mouse 488, Molecular probes; Alexa Goat anti-rabbit 568, Molecular probes) was diluted 1:1000 in PBS-BSA 1% and embryos incubated o/n at 4ºC. Embryos were then washed 2 times for 10 minutes and post-fixed in PFA 1% at room temperature for one hour. Finally, embryos were washed two times for 10 minutes in PBS 1x and slides were assembled in PBS1x. All washes and incubations, except in antibody solutions, were performed with agitation.

Embryos were imaged using Axio Imager 2 (Zeiss).

2.5 - Ex-ovo embryo culture

Embryos were cultured using the early chick (EC) culture, also known as Chapman culture (Chapman et al., 2001) setup. The incubated eggs were cooled for 30 minutes at room temperature and cleaned with 70% EtOH. The shell was allowed to dry and then the egg was deposited in a petri dish so that the embryo faced up. The thick albumin was removed from the embryo and a piece of Whatman paper no.3 with a central opening was placed onto the vitelline membrane allowing the embryo to stay framed in the aperture. The vitelline membrane around the paper was cut and then the paper was gently removed with an angle of 45ºC. All yolk attached to the paper was removed and the embryo gently washed with PBS 1x. The embryo was then placed onto an agar-albumen culture dish ventral-sided up. Embryos were then incubated at 38ºC.

Agar-albumen culture dish (10 cm) (Chapman et al., 2001) was prepared following the next steps: 0,24 g of agar were melted in a microwave in 40 mL saline solution (7.19 g NaCl, 1L water); 40 mL of thin albumin was collected; Both the melted agar and the thin albumin were placed at 49 ºC for at least one hour; thin albumin was added to the melted agar and 40µl of Penicilin-Streptomycin (penstrep) (0.05% (v/v); Gibco) was added to the solution. 2 mL of the solution was added to each petri dish (10 mm) and the culture dishes were cooled at RT o/n. Culture dishes were then placed at 4ºC until use for no longer than 2 weeks.

2.6 - Embryo electroporation

Embryos at HH3-4 were electroporated as described (Iimura and Pourquie, 2008) using an empty vector (Sato et al., 2007) and a vector that constitutively activates the expression of hairy1 (pCAT-Hairy1) (Andrade et al., under review). Embryos were

electroporated in the epiblast region containing the presomitic mesoderm precursors (Iimura and Pourquie, 2006), represented in figure 2.1.

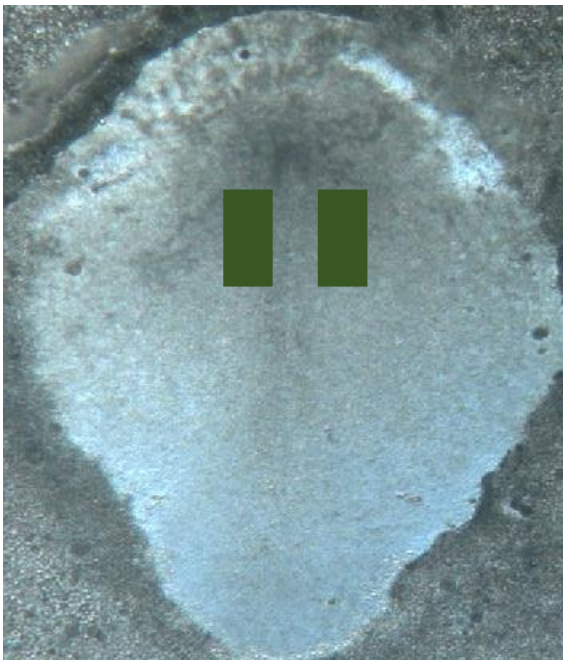

Figure 2.1 – Representation of the electroporated regions in HH4 embryos;

Schematic representation of the regions of the embryo containing the PSM precursors (represented in green). This region was electroporated with the empty or pCAT-Hairy1 vectors. Up – anterior part of the embryo; Down – Posterior part of the embryo; Embryo in stage HH4 according to Hamburger and Hamilton (Hamburger and Hamilton, 1951).

After embryo preparation for Chapman culture (described above), the embryo was placed in a petri dish-type electrode (CUY700-P2E, NEPA GENE) filed with tyrod's saline solution 1x (Voiculescu et al., 2008). The embryo was positioned ventral up was then injected with a glass needle (prepared from glass capillaries using a puller (SUTTER INSTRUMENT CO., Model P-87, Flaming/Brown Micropippete) using the following settings: Time: 150; Heat: 720; Pull: 75; Velocity: 60) prefilled with DNA plasmid with 0.3/1 µl Fastgreen (0.4% wt/v). The injection was performed on the sides of the primitive streak, within 90%-60% extension, between the vitelline membrane and the epiblast with a microinjector IM 300 (Narishige Japan). After the injection, five 50 ms pulses of 10 V, with an interval of 350 ms were applied using the eletroporator BTX ECM 830, Eletro Square Porator (Harvard Apparatus) with the electrodes placed under (-) and above (+) the embryo. The following

control embryos were also prepared: embryos electroporated with empty vector, embryos electroporated without injection, embryos without treatment and embryos injected without electric shock. Embryos were then incubated for 4 hours before imaging and up to a total of 26 hours. A total of 583 embryos were incubated: 206 electroporated with Hairy1 (pCAT-Hairy1) overexpression vector, 261 electroporated with empty vector, 13 controls where all procedure was performed except the injection, 3 controls where all procedure was performed except for the electric shock and 100 embryos cultured in Chapman without any treatment. The embryos that had fluorescence in the region of interest and/or control embryos in good conditions, were dissected from the filter paper, fixed and stored at -20ºC after dehydration in MeOH. Embryos were imaged in a steREO Lumar V12 (Zeiss).

2.7 - Live-imaging

Live imaging of embryos cultured ventrally in Chapman (Chapman et al., 2001) was performed in an incubation chamber (UNO STAGE TOP INCUBATOR, Okolab) with humidified-saturated atmosphere and controlled temperature at 38ºC using steREO Lumar V12 (Zeiss) for 12 to 27 hours. The setup for live-imaging was optimized. A home-made chamber was used to place the embryo in the center, with a ring of paper humidified in water placed around (Figure 2.2). Frames were acquired every three minutes in bright field and with fluorescence. Electroporated embryos were first selected for the presence of fluorescence 4-6 hours after electroporation and then analyzed during a total of 12-24 hours.

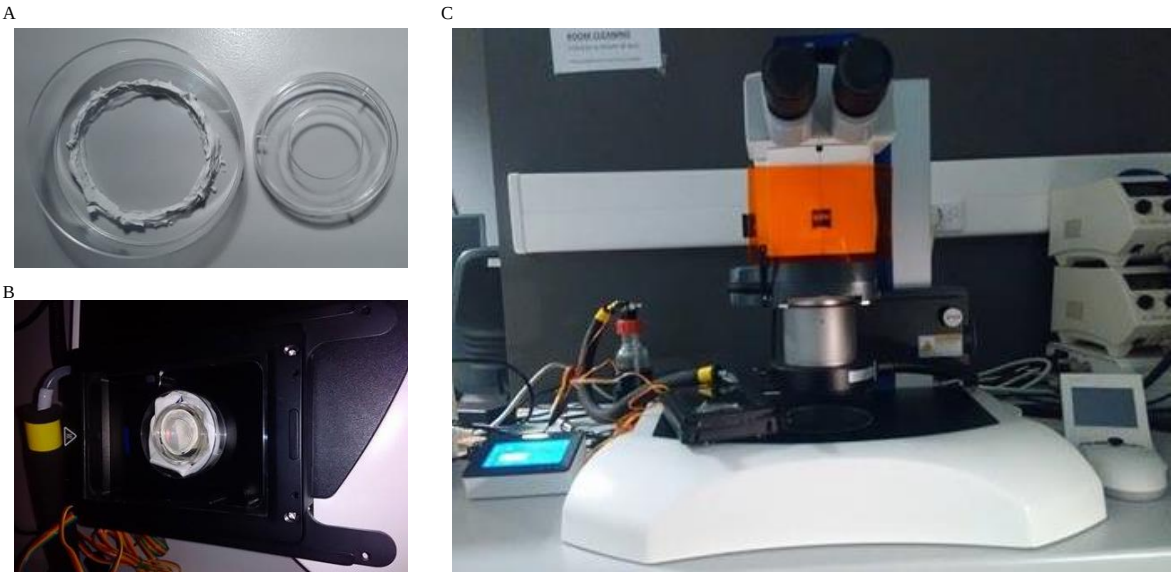

Figure 2.2 – **Set-up used to perform live-imaging of the embryo**

A – Home-made chamber with a ring in the center with the same diameter as the culture; The agar-albumen petri-dish was placed in the center with a paper around humidified with water. B – UNO STAGE TOP Incubator used. The home-made chamber was placed in the center of the incubator. C – Stereo Lumar V12 with the camera placed in the left side.

2.8 - Video analysis

Selected images (representing 1h time intervals) from two sets of videos were analyzed: the first one with the embryos cultured in Chapman (Chapman et al., 2001) (n=7) and the second one of embryos cultured in New (New, 1955) (n=6). The videos of embryos cultured in New were kindly provided by collaborators (T. Azevedo and G. Martins). All analyses and measurements were performed *de novo* within the present work. The following length measurements were performed in each frame: 1) from the most anterior portion of the embryo till the most posterior limit of the embryo adjacent to the *area opaca*; 2) from the most anterior part of the embryo to the end of the primitive streak; 3) from the most anterior part of the embryo until the Hensen's node; 4) from the Hensen's node to the posterior limit of the embryo adjacent to the *area opaca*; 6) From the last formed somitic cleft to the Hensen's node (PSM portion); 7) from the most anterior part of the embryo to the middle of the second somite (head portion); 8) from the first to the last somitic cleft formed (segmented region) (Figure 2.3).

Since each video corresponds to a different individual, the measurements were aligned to allow for comparison. Since no embryo stage was present in all videos, two moments of development were taken as reference: the last frame in all videos in which the embryo was in stage HH4 and the frame of formation of the posterior cleft of the fourth somite, in HH8. All videos containing stage HH4 were aligned by the last frame in this stage which corresponds to time 0 in further analyses. The videos corresponding to embryos already at the beginning of stage HH5 were aligned by the formation of the posterior cleft of the fourth somite (HH8). The two groups of embryos were aligned by adding 13.15 hours to the moment of formation of the posterior cleft of the fourth somite in the videos aligned by the stage HH8. The average of the time of the formation of the posterior cleft of the fourth somite (HH8) was calculated in the videos aligned by stage HH4 that presented stage HH8 (n=4) to achieve the value of 13.15. When required (for analysis comparing means and length) the alignment was adjusted and all time points were rounded to the nearest whole value. The maximum error associated with this procedure is 30 min. All other analyses, including elongation rates were performed with the original alignment.

After the alignment, the elongation rate between two consecutive time points was calculated using the following formula: [length(a+1)-length(a)]/[t(a+1)-t(a)]. The elongation rate for each embryo was calculated by the mean of the elongation rates between all two adjacent points. When the mean of the elongation rates of different embryos was required, the formula was applied considering only the first and last value of each condition (for comparison between groups of embryos).

A

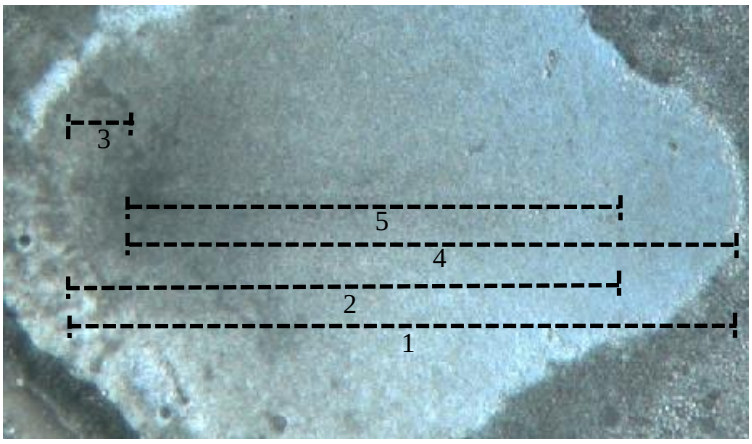

B

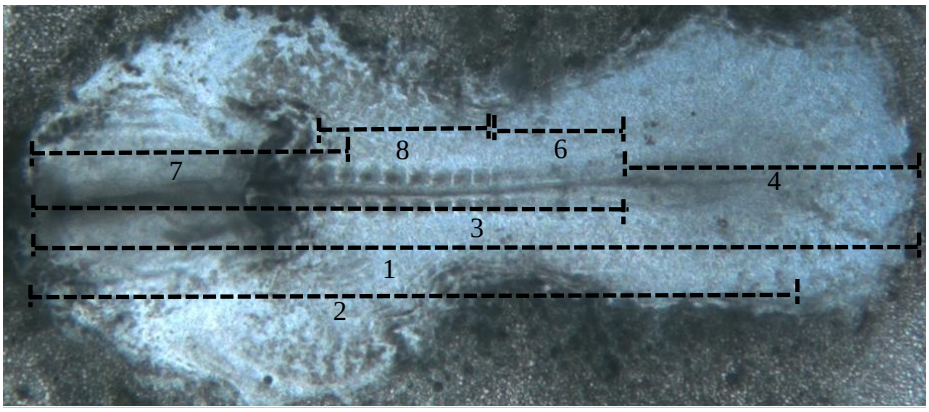

Figure 2.3 – ***Schematic representation of the measurements performed in each embryo;***

Representation of each measurement performed in each frame of the videos. A - Embryo in gastrulation stages B - Embryo in early somitogenesis. Right: posterior portion of the embryo; Left – Anterior part of the embryo; 1) from the most anterior portion of the embryo till the most posterior limit of the *area pellucida*; 2) from the most anterior part of the embryo to the end of the primitive streak; 3) from the most anterior part of the embryo till the Hensen's node; 4) from the Hensen's node to the posterior limit of the *area pellucida*; 6) From the last formed somitic cleft to the Hensen's node (PSM portion); 7) from the most anterior part of the embryo to the middle of the second somite (head portion); 8) from the first somitic cleft to the last somitic cleft formed (segmented region)

2.9 - Statistical analysis

All statistical analyses were performed using the program SPSS. To analyze if the measurements between embryos and if the embryos differentiated by conditions were statistically different the following nonparametric tests were used: Kruskal Wallis (Daniel, 1929) and Jonckheere-terpstra (Pérez, 2001). Nonparametric tests were applied due to the

low number of embryos and since the data didn´t followed a normal distribution. Both tests were also applied to compare the two culture techniques (Chapman and New). A hierarchical classification cluster analysis according to the Ward method and fixing the squared euclidian distance (Pérez, 2001) was applied to understand if the embryos were different in clustering behavior when the rates of variation of length having time in consideration were taken into account. This analysis was performed considering the time period: t0 to t14.

2.10 - Light-sheet microscopy

Live-imaging of an chicken embryo cultured in Chapman (Chapman et al., 2001) (HH4) electroporated with pCAT empty vector was performed in a Zeiss Light Sheet Z1 Microscope. The embryo was placed onto the microscope support by gluing the paper into the metal piece of the support. The embryo was then placed in the microscope chamber that was previously filled with thin albumen at 37ºC. The setup and conditions were prepared with the assistance of a Zeiss expert.

2.11 - Vital Dye labelling

Draq5 (BioLegend) and syto 62,64 (Syto Red Fluorescent Nucleic Acid Stains, Termofisher) were tested in chicken embryos in stage HH4. After embryo *ex ovo* culture in Chapman (Chapman et al., 2001) as described above, embryos were incubated with 50 µl of the following vital dyes diluted in PBS 1x: 1:1000 (Syto 62,64) and 1:5000, 1:1000, 1:2500 (Draq5), placed on top of the embryo. After incubating the embryos for 15 minutes (DRAQ5) and 15 minutes or 1 hour (Syto 62,64), embryos were gently washed twice with PBS 1x and then imaged using Axio Imager 2 (Zeiss).

3 - RESULTS

3.1 - Characterization of Hairy1 expression during chick embryo gastrulation

3.1.1 - Dynamics of *hairy1* mRNA expression

The dynamics of some clock genes, such as *hairy2*, was already addressed in chick gastrulation stages (Jouve et al., 2002). *hairy2* is expressed in pulses after the ingression of cells in the primitive streak in stage HH4 (Jouve et al., 2002). The same work, mentioned that *hairy1* is expressed in the paraxial mesoderm prospective territory, in the rostral primitive streak and in the forming neural plate, but the data was not shown. We are interested in understanding how *hairy1* is expressed during gastrulation, hence, using *situ* hybridization, we addressed if the expression of *hairy1* in gastrulation stages is also dynamic.

In stages HH3-5 *hairy1* m*RNA* is expressed in the region of the Hensen's node, along the primitive streak and in the most posterior part of the embryo with different dynamics (Figure 3.1). In stages HH3 (n=12) and HH4 (n=27), *hairy1* it was detected in the Hensen's node and in the most posterior part of the primitive streak in 87% of the embryos (n= 34/39). In a very small number of embryos, *hairy1* was exclusively present in the Hensen's node (n=2/39)., *hairy1* was present along all the primitive streak extension in 62% of the embryos (n=24/39). In the cases where expression is present in the primitive streak extension, in one third of the embryos (n=9/24), expression is absent in the primitive groove but present in the primitive ridge. On the other hand, when expression is present in the primitive groove, it is always present in the primitive ridge. This shows that the cells in the primitive groove and in the primitive ridge are asynchronous with each other. It is interesting to note that the cells in those two regions are in different moments of the epithelial-to-mesenchymal transition (EMT): the cells in the epiblast around the groove are getting ready to gastrulate but are organized in an epithelial sheet; in the region of the groove, cells are already adopting a mesenchymal behavior (reviewed in Nakaya and Sheng, 2008). In stage HH5 (n=7) *hairy1* expression pattern is also dynamic. In early moments within this stage (n=3/6) the expression is similar to the one in stage HH4. However, when the Hensen's node has regressed further,

hairy1 expression can be seen in the head process, in the Hensen's node and in the full extension of the primitive streak (Figure 3.1). Nevertheless, the number of embryos analyzed within stage HH5 is low, therefore it would be important to perform the same analysis in a higher number of embryos to confirm those results and to explore more tissues where hairy1 expression may be dynamic.

Altogether, our results show that *hairy1* expression is very dynamic during gastrulation along the anterior-posterior and medial-lateral axes.

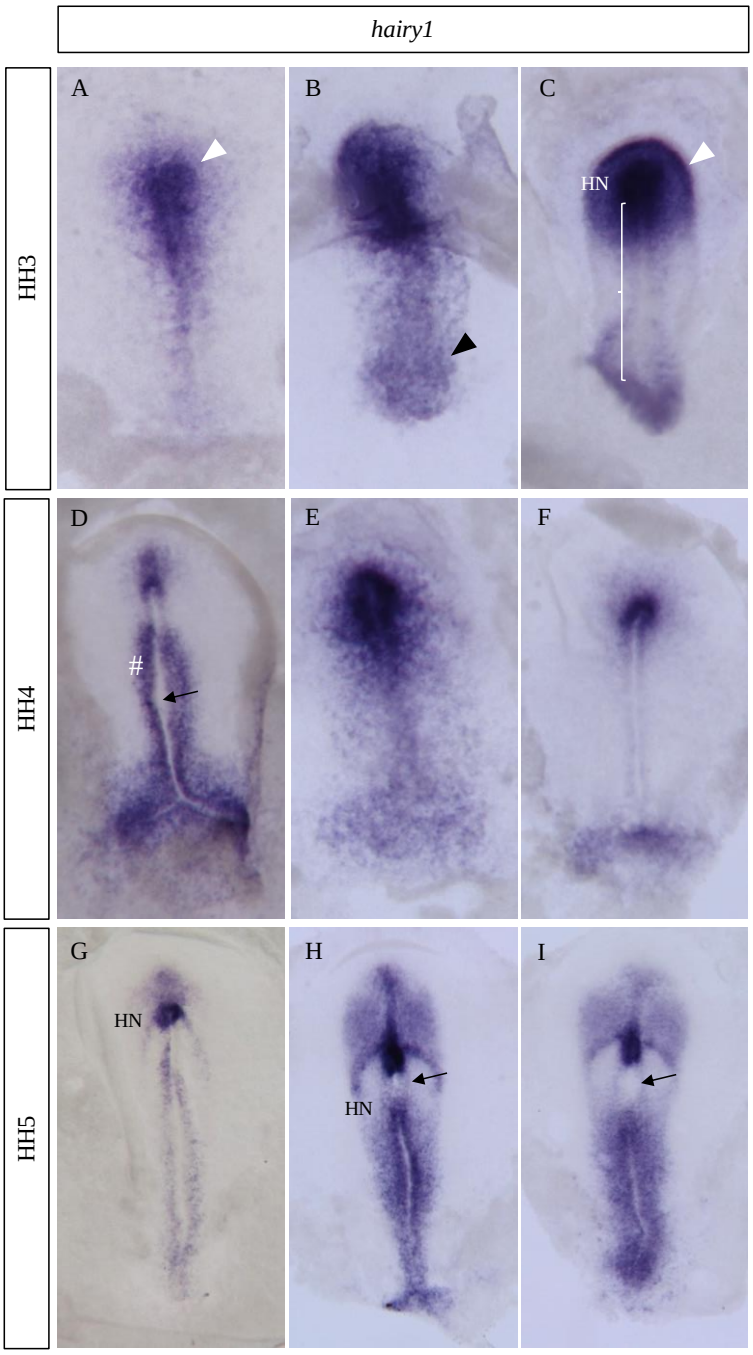

Figure 3.1 - ***D*ynamic *hairy1* expression during chick gastrulation stages (HH3-5);**

hairy1 in situ hybridization of whole-mount chick embryos in stages HH3 (A-C), HH4 (D-F) and HH5 (G-I). *hairy1* expression is present in the Hensen's node region (A, C; white arrowhead), in the primitive streak (C, {) and in the posterior region of the embryo (B, black arrowhead). In the primitive streak (C, {) expression is dynamic. When is present along this region, if is present in the primitive groove (D, black arrow) is always present in the primitive ridge (D, #). However, in one third of the embryos that present expression along the primitive streak, expression is present in the primitive ridge (D, #) but absent in the primitive groove (D, arrow) In early stage HH5 (G), *hairy1* expression resembles that of HH4 but when the Hensen's node has regressed a higher extent, expression is visible in the head process, Hensen's node and primitive streak (H,I). In the region immediately before the Hensen's node, expression also seems dynamic in late HH5 (I and J, black arrow). HN – Hensen's node; Anterior to the top.

3.1.2 - Hairy1 protein distribution: Optimization of a Hairy1 Immunofluorescence protocol

mRNA levels do not always correspond to protein levels. Therefore, it is important to address how, when and where the protein is being expressed directly. Our lab has a custom-made monoclonal Hairy1 antibody available already successfully tested in Western blot and immunohistochemistry in sections (unpublished). In the present work, several conditions were evaluated in order to optimize a whole-mount immunofluorescence protocol.

The most important steps in the immunofluorescence protocol are: fixation, sample permeabilization, blocking and antibody incubation. Initially, a protocol previously used in the lab for whole mount samples was employed, and despite the positive control working well (using a commercial antibody for T), it was not possible to distinguish specific signal from the background noise for Hairy1 (Figure 3.2). We used two different conditions to improve the signal-to-noise ratio: higher primary antibody concentrations (1:100 and 1:50) and different solution to dilute the primary antibody (PBS 1x versus blocking solution) in order to reduce background. None of the conditions improved the signal-to noise ratio of Hairy1 (Figure 3.2).

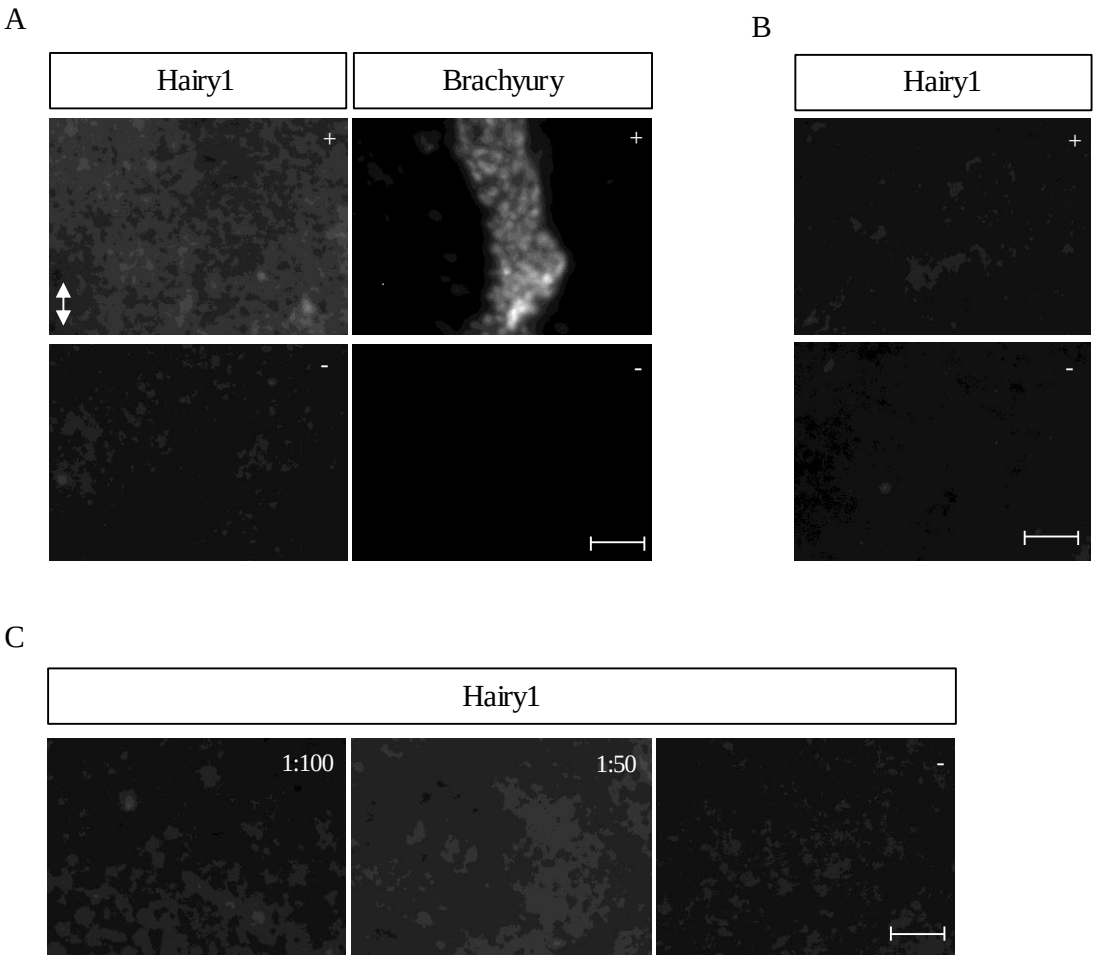

Figure 3.2 - **Whole mount immunofluorescence in chick embryos (HH4-6) using Protocol 1**;

A – Immunofluorescence for Hairy1 (1:150) and Brachyury (positive control; 1:100) in the presence (+) and absence (-) of primary antibody. B – Immunofluorescence for Hairy1 where the antibody was diluted in blocking solution instead of PBS 1x. C – Different antibody concentrations for Hairy1 were tested: 1:100 and 1:50. Double-head arrow: anterior-posterior axis. Scale bar: 50 µm

The low signal-to-noise ratio could be due two several conditions such as: inappropriate fixation of the sample, low sample permeabilization and the use of inappropriate blocking steps. Therefore, we decided to test a second protocol which was already used to perform immunofluorescence in chick embryos within the same stages (Martins et al., 2009; Pinheiro, 2014). The major differences between the two protocols resided in the fixation, permeabilization and blocking steps, which were some of the most prominent problems identified in the first protocol.

The second protocol was performed using fibronectin as positive control since it was one of the antibodies successfully used in other works using the same protocol (Pinheiro,

2014). The results for Hairy1 showed some speckles that could be specific staining, however the results were not clear since high levels of background were present (Figure 3.3). Despite that, the result achieved with protocol 2 was better compared with the resulted achieved using the first protocol. Therefore, we decided to perform further optimizations using the second protocol.

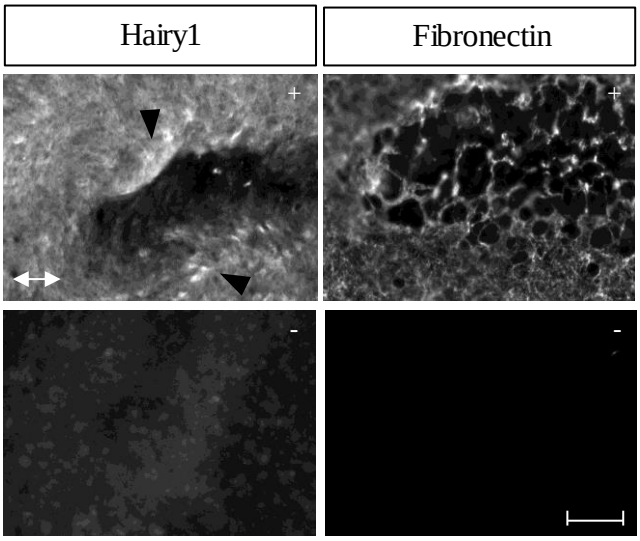

Figure 3.3 - **Whole mount immunofluorescence in chick embryos (HH4) using Protocol 2;**

Immunofluorescence for Hairy1 (1:150) and fibronectin (positive control, 1:400) in the presence (+) and absence of primary antibody (-). Hairy1 treated embryos show some speckles (white arrowheads) with higher intensity. Double-head arrow: anterior-posterior axis. Scale bar: 50 µm

To optimize the protocol, 2 different conditions were tested. First, different blocking steps (optional step 2 versus optional step 1+2, see Methods) and a higher concentration of BSA (5% versus 1%) were tested. From all conditions, optional step 1+2 was the best approach, since it produced less background, although the levels of specific staining remained undetectable (not shown). Therefore, all the following experiments were performed with blocking step 1+2 and 1% BSA.

It is known that proteins expressed in low levels and with high dynamics are not easily detectable, which is the case of Hairy1. Meanwhile, a new method, that was used to detect low-level proteins with dynamic expression in mouse PSM, was published (Bailey et al., 2017). The main difference remained in the period of antibodies incubations: 3-5 days at 4ºC

instead of o/n. We decided to test protocol 2 with 3 days of antibody incubations at 4ºC and we obtained better results for the positive control. However, no specific signal from Hairy1 antibody was detected and high levels of background were present (not shown and Figure 3.4).

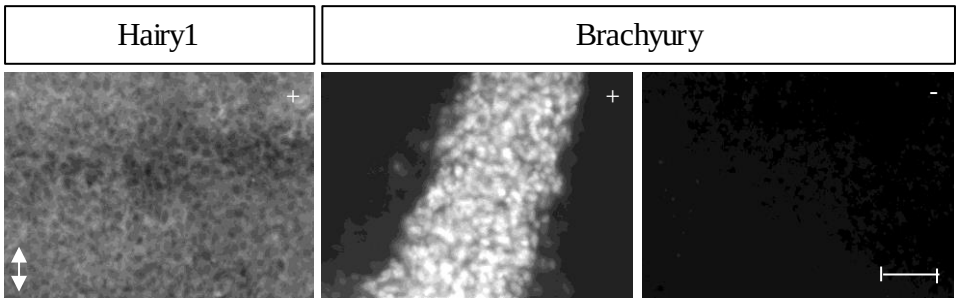

Figure 3.4 - **Whole mount immunofluorescence in chick embryos (HH4-6) using Protocol 2 with three days of incubation with antibodies.**

Immunofluorescence for Hairy1 (1:150) and Brachyury (positive control, 1:100) in the presence (+) and absence (-) of primary antibody, using protocol 2 with three days of incubation for the antibodies steps instead of o/n. T was used as positive control. A-P: anterior-posterior axis. Double-head arrow: anterior-posterior axis. Scale bar: 50 µm

Due to the high levels of background, the secondary antibody time of incubation was reduced to overnight. In these conditions, the positive control showed specific binding and low levels of background but no clear specific signal for Hairy1 expression was detected (Figure 3.5).

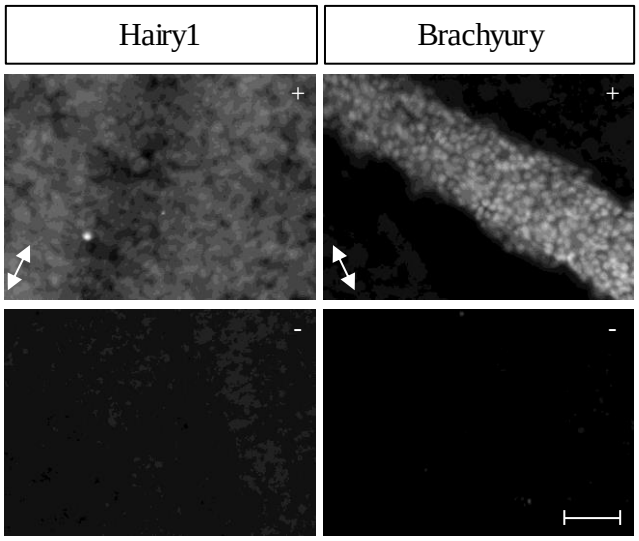

Figure.3.5 – **Whole mount immunofluorescence in chick embryos (HH4-6) using Protocol 2 with three days of incubation of the primary antibody;**

Immunofluorescence for Hairy1 (1:150) and Brachyury (positive control, 1:100) in the presence (+) and absence (-) of primary antibody using protocol 2, with 3 days of incubation for the primary antibody an o/n incubation step for the secondary protocol. Double-head arrow: anterior-posterior axis. Scale bar: 50 µm

In order to improve the levels of background, the washes after antibody incubation and post-fixation were performed with PBS1x, 0.1% Tween-20, plus an additional wash with PBS 1x only, in order to remove Tween-20 from the embryos. We found that the addition of Tween-20 to the washing steps improved the levels of background (Figure 3.6).

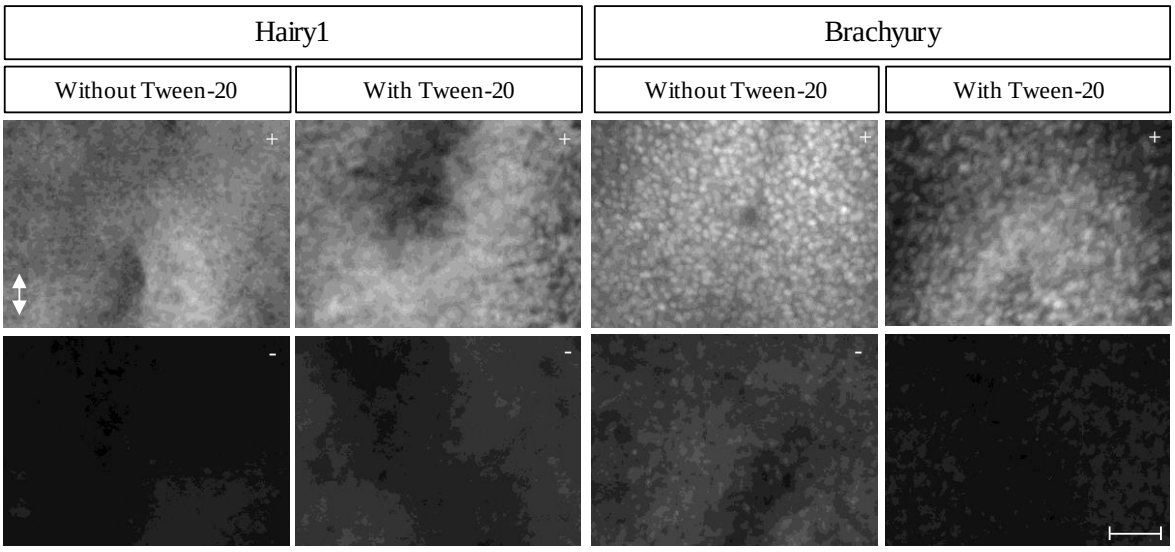

Figure 3.6 - **Whole mount immunofluorescence in chick embryos (HH4-6) using Protocol 2 with Tween-20 added to wash steps;**

Immunofluorescence for Hairy1 (1:150) and Brachyury (positive control, 1:100) in the presence (+) and absence (-) of primary antibody using protocol 2, with and without Tween-20 during wash steps. Double-head arrow: anterior-posterior axis. Scale bar: 50 µm

At this point, the levels of background were lowered but still no specific binding was achieved for Hairy1. Xiao and collaborators (2017) showed that incubation of antibodies at 37 ºC could improve both quality and efficiency of immunolabelling of free-floating thick tissue sections (Xiao et al., 2017). Hence, we performed the antibody incubation step at 37ºC. The immunolabelling of the positive control was improved, however no specific binding for Hairy1 was achieved (Figure 3.7).

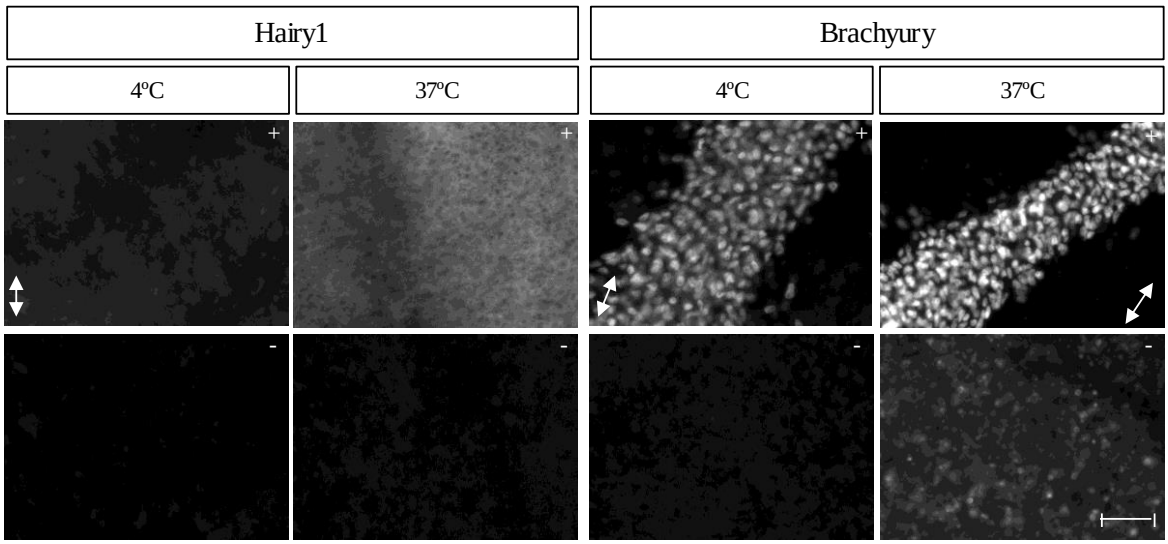

Figure 3.7 - **Whole mount immunofluorescence in chick embryos (HH4-6) using Protocol 1 with antibody incubations at 37 ºC and 4ºC;**

Immunofluorescence for Hairy1 (1:150) and Brachyury (positive control, 1:100) in the presence (+) and absence (-) of primary antibody using protocol 2. Antibody incubation were performed at 37ºC and 4ºC for comparison. Double-head arrow: anterior-posterior axis. Scale bar: 50 µm

In all the tests that were performed, PFA was used as fixing agent. PFA is widely use in immunofluorescence protocols; however, since it causes crosslinking (reviewed in Hoffman et al., 2015), in some cases it can mask the epitope and inhibit the binding of the antibody to the protein of interest. To solve this problem, antigen retrieval protocols are commonly used, however this is not applicable to whole-mount samples, such as embryos, since the high temperatures would destroy the sample. Another solution is to fix samples for reduced periods of time or use an alternative reagent for fixing agent. Therefore, embryos were fixed for only 20 minutes on ice in PFA and a few positive staining regions for Hairy1 binding were present (Figure 3.8A). However, embryos were too fragile, and none remained intact until the end of the protocol. A different fixing agent that does not induce protein crosslinking was also assayed: 95% EtOH, 4% water and 1 % acetic acid. Still, we could not see any specific binding for Hairy1 antibody (Figure 3.8B).

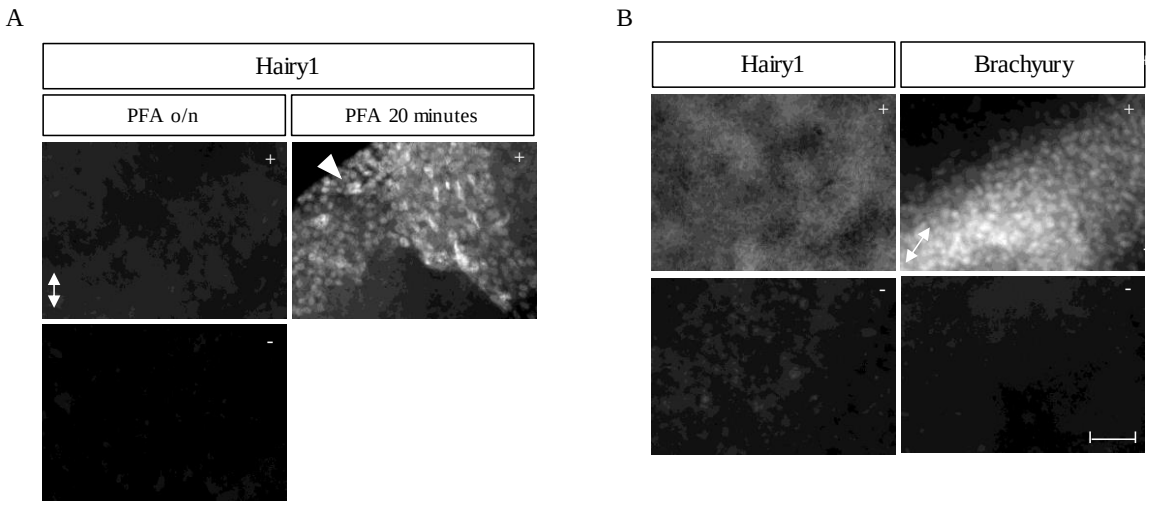

Figure 3.8 - **Whole mount immunofluorescence in chick embryos (HH4-6) using Protocol 2 with different fixation conditions;**

Immunofluorescence for Hairy1 (H1) and Brachyury (T) in the presence (+) and absence (-) of primary antibody with: A – different periods for PFA 4% fixation (o/n versus 20 minutes) and B – with a different fixative agent (95% EtOH, 4% water and 1% glacial acetic acid). T was used as positive control.

In this work, an immunofluorescence protocol for Hairy1 was attempted to be optimized, however without success. Two different protocols were tested, with further optimizations of fixing agent, time of fixation, blocking and permeabilization steps, antibody concentrations and washing steps. Since none of the conditions were successful for Hairy1 antibody, it is possible that the antibody used is not able to recognize the protein in its native condition. Hairy1 protein is also expressed in low levels and in a very dynamic way, which could render its detection difficult. The use of complementary steps to amplify any specific signal could be useful. Also, in the future, it would be important to try different conditions and to test other antibodies against Hairy1 in order to assess the dynamics of expression of Hairy1 protein during chicken embryo development.

3.2 - Characterization of the anterior-to-posterior elongation of the early chicken embryo

One of the main goals of this work is to understand how Hairy1 overexpression affects the growth of the chicken embryo. In order to answer this question, we first needed to characterize the elongation of the chick embryo along the anterior-to-posterior (AP) axis in wild-type (WT) conditions. With this purpose, live imaging of chick embryos cultivated *ex ovo* using Chapman culture (Chapman et al., 2001) was performed from stage HH3 to HH10. We also analyzed videos of embryos grown in New culture (New, 1955) encompassing developmental stages from HH5 to HH9 (Table 3.1), previously obtained from a collaborating lab (T. Azevedo and G. Martins). To determine the elongation rate of the embryo, as well as which portions of the embryo mostly contributed to total elongation, eight measurements were performed in each video on frames corresponding to 60 min intervals.

Table 3.1 - **Embryos analyzed in the present study, cultured using two different culture methods;**

Embryos analyzed in the present study encompass stages HH3-HH10. Embryos were cultured in two different *ex ovo* cultures systems: Chapman (C) and New (N) and staged according to Hamburguer and Hamilton (HH). Each number corresponds to a different embryo/video.

Embryo	Culture method	Initial stage (HH)	Final stage (HH)
1C	Chapman	HH3+	HH5
2C	Chapman	HH3	HH7
3C	Chapman	HH4	HH10
4C	Chapman	HH4	HH9
5C	Chapman	HH5	HH10
6C	Chapman	HH4	HH9
7C	Chapman	HH3+	HH5
8N	New	HH6	HH8
9N	New	HH6	HH8
10N	New	HH5	HH9
11N	New	HH5	HH8
12N	New	HH5	HH8
13N	New	HH5	HH9

The chick embryo elongates along the anterior-posterior axis while tissues begin to differentiate. In the stages included in the analyses, the primitive streak can be seen elongating, until it reaches its maximum length at stage HH4 (Figure 3.9, SupMovie 1). After HH4, the Hensen's node regresses while structures in the anterior portion begin to develop, primarily the head and then the somites, budding off periodically from the PSM on both sides of the notochord, which is being laid down as the Hensen's node regresses (Figure 3.10, SupMovie 2)

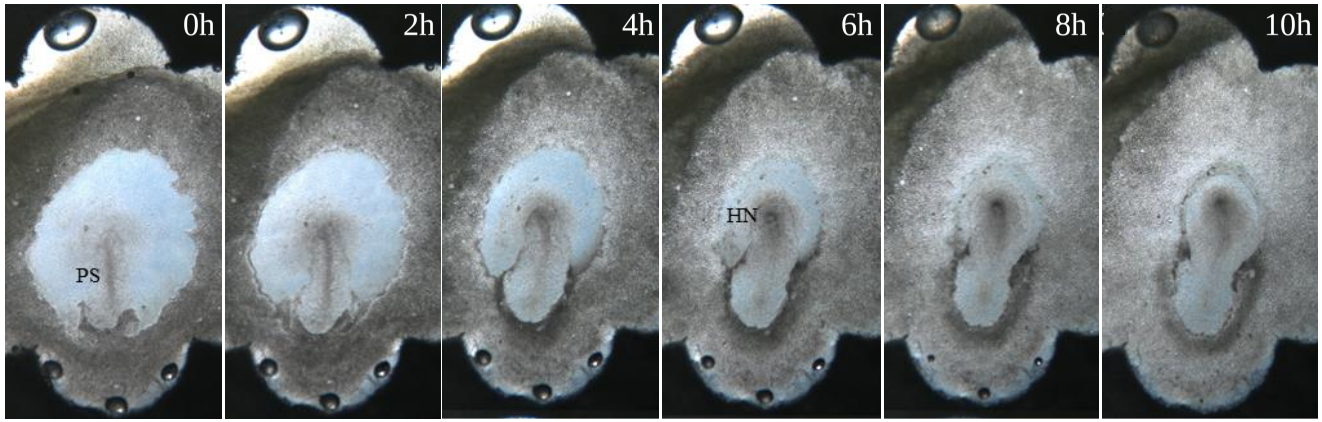

Figure 3.9 - **Primitive streak extension in a chick embryo from HH3-HH4.**

Sequential images obtained along a total of 10 hours. It is possible to visualize the primitive streak (PS) extension until it reaches is maximum extent at stage HH4. HN – Hensen's node; PS – Primitive streak

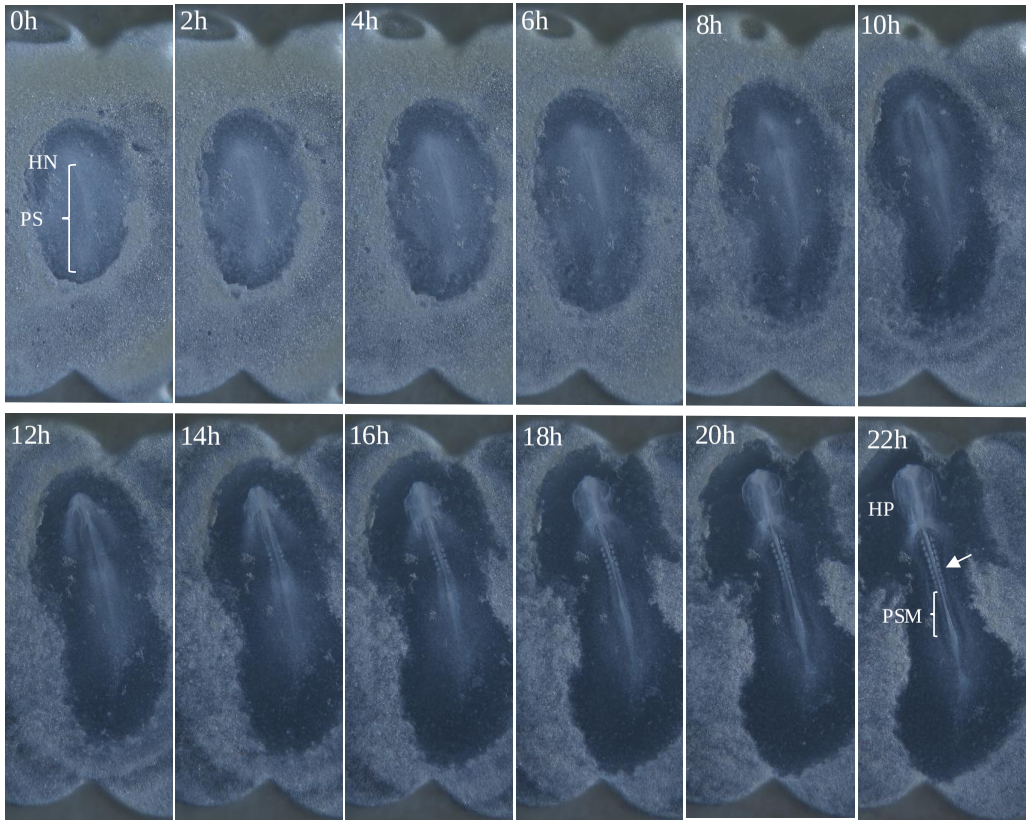

3.10 - **Chicken embryo development from HH4-HH9;**

Sequential images obtained along a total of 24 hours. Primitive streak (PS) elongates until it reaches its maximum length around 10h. After t6 the Hensen's node (HN) and PS begin to regress while in the most anterior region of the embryo the Head (HP) and somites (arrow) are formed, which are formed from the PSM ({). Anterior to the embryo to the top.

To determine the total elongation rate of the embryo, two different measurements were performed on frames corresponding to 60 min intervals: from the anterior-most part of the embryo to the posterior limit adjacent to the *area opaca* (measurement 1) or to the end of the primitive streak (measurement 2). The posterior limit of measurement 1 is an easily detectable feature for the operator, which implies less errors associated to the measurements. However, the region between the end of the primitive streak and the posterior limit adjacent to the *area opaca* is very variable among different embryos. On the other hand, the posterior limit of measurement 2 is difficult to determine visually. Both measurements were plotted for each embryo over time and the corresponding elongation rates compared (Figure 3.11, 3.12 and Table 3.2) in order to understand if they are equivalent in terms of elongation rate and behavior.

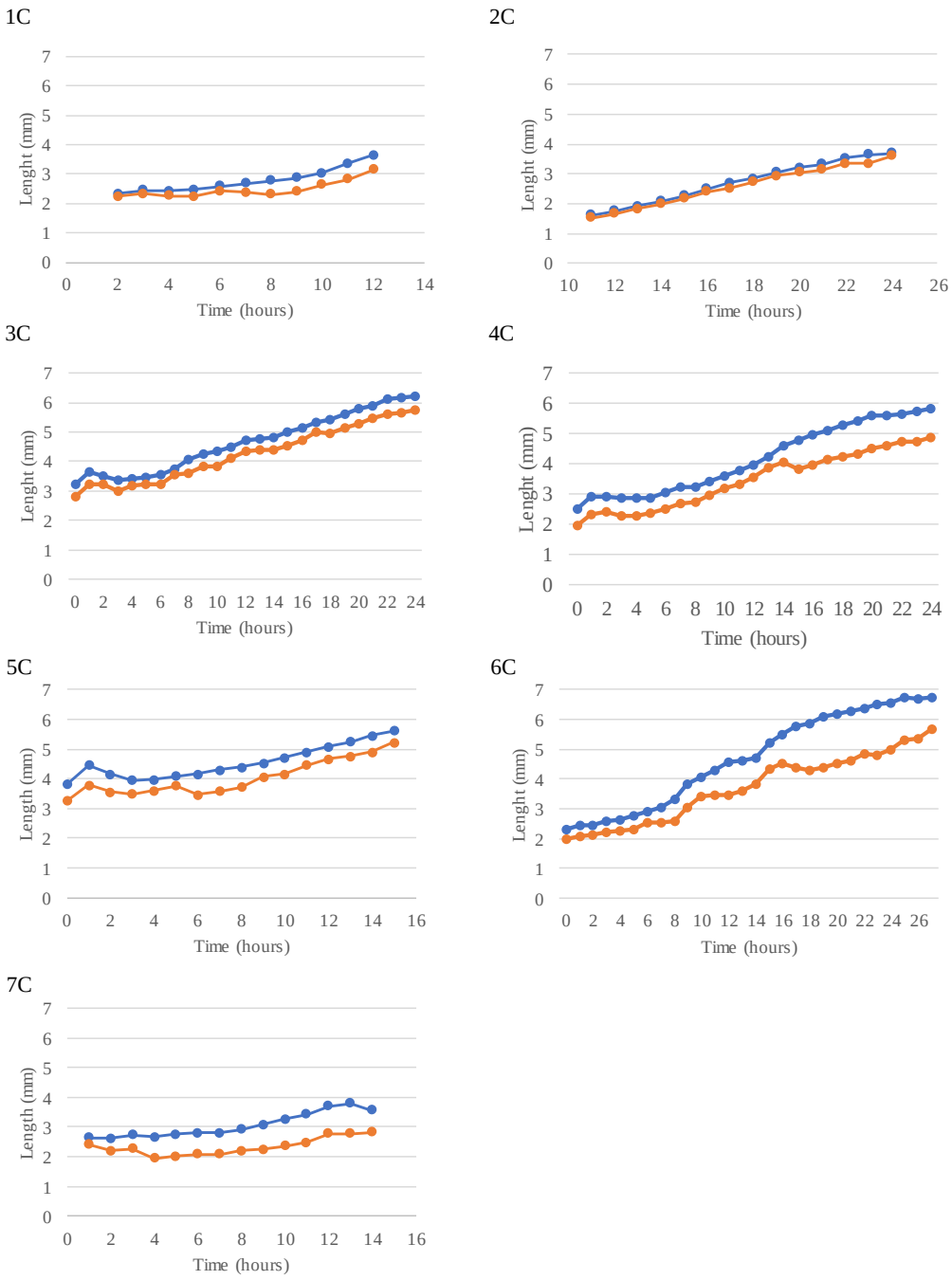

Figure 3.11 – **Chick embryo elongation using two different measurements**: **measurement 1 and 2 for the embryos cultured in Chapman culture;**

Each embryo corresponds to one video with measurements performed in frames corresponding to 60 minutes interval. Measurement 1 – from the most anterior part of the embryo to the most posterior part of the *area pelucida* (blue lines); Measurement 2 – from the most anterior part of the embryo to the end of the primitive streak (orange lines). Graphs were plotted considering the distance between the two reference points (mm) over time (hours).

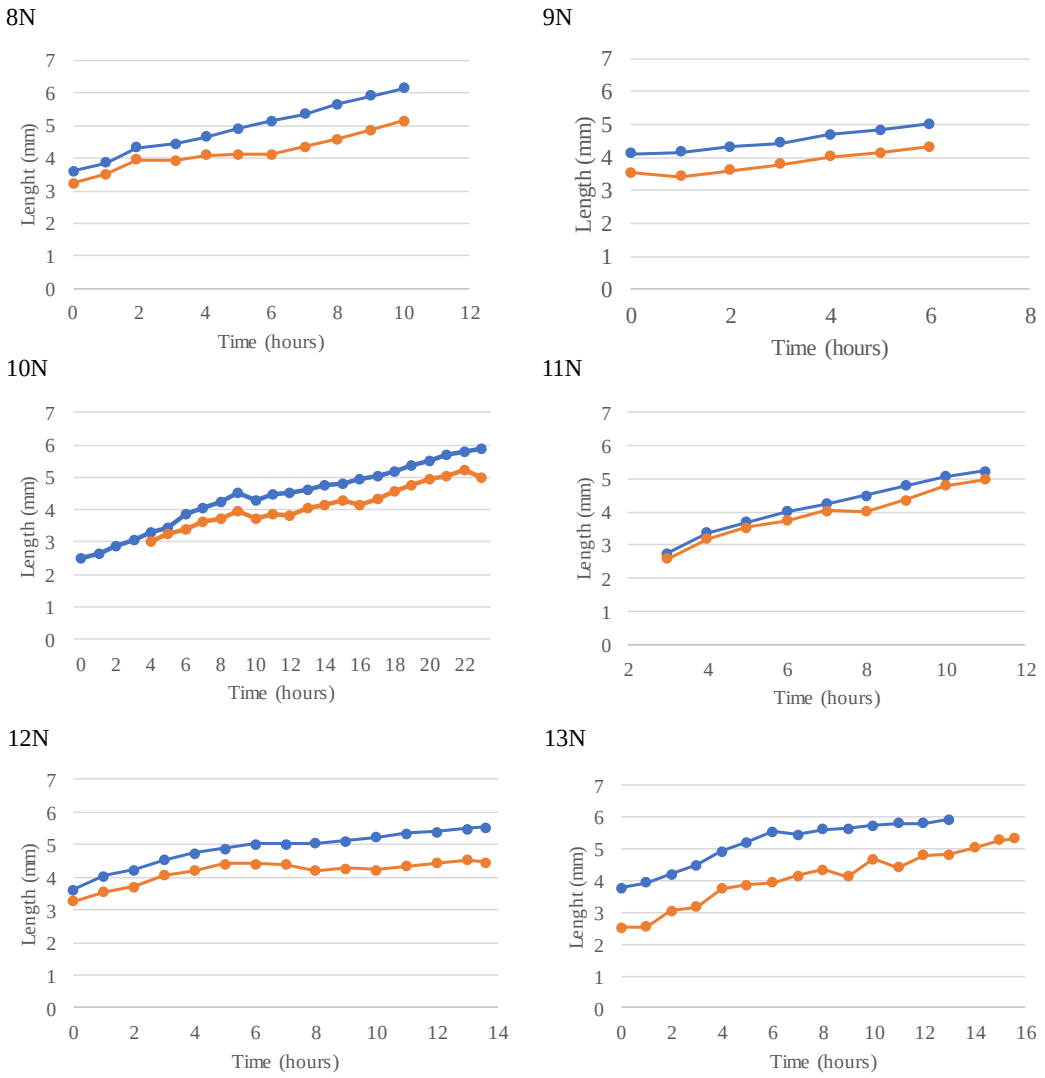

Figure 3.12 – **Chick embryo elongation using two different measurements: measurement 1 and 2 for the embryos cultured in New culture;**

Each embryo corresponds to one video with measurements performed in frames corresponding to 60 minutes interval. Measurement 1 – from the most anterior part of the embryo to the most posterior part of the *area pelucida* (blue lines); Measurement 2 – from the most anterior part of the embryo to the end of the primitive streak (orange lines). Graphs were plotted considering the distance between the two reference points (mm) over time (hours).

Table 3.2 - **Embryo elongation rate considering two different measurements: measurement 1 and 2;**

Total elongation rates considering measurement 1 and 2 for each embryo; Measurement 1 – from the most anterior part of the embryo to the most posterior part of the *area pelucida*; Measurement 2 – from the most anterior part of the embryo to the end of the primitive streak; C refers to Chapman culture and N to New culture; Each elongation rate results from the mean of the elongation rates between each two adjacent points.

Embryo	Elongation rate measurement 1	Elongation rate measurement 2
1C	0.119 ± 0.079	0.092 ± 0.120
2C	0.159 ± 0,053	0.158 ± 0.049
3C	0.125 ± 0.089	0.123 ± 0.109
4C	0.140 ± 0.090	0.123 ± 0.094
5C	0.122 ± 0.124	0.134 ± 0.152
6C	0.164 ± 0.098	0.137 ± 0.125
7N	0.091 ± 0.107	0.033 ± 0.100
8N	0.262 ± 0.061	0.200 ± 0.124
9N	0.153 ± 0.045	0.131 ± 0.092
10N	0.148 ± 0.068	0.104 ± 0.114
11N	0.286 ± 0.102	0.299 ± 0.134
12N	0.143 ± 0.086	0.084 ± 0.117
13N	0.168 ± 0.122	0.177 ± 0.177

As shown in Figures 3.11 and 3.12, the progression of embryo elongation assessed using measurement 1 is very similar to that of measurement 2. To confirm this, the ratio between measurement 1 and measurement 2 for each time point was also calculated. As expected, the ration was higher than 1 for all embryos. However, it varies among embryos, which confirms the observation that the distance between the end of the primitive streak and the most posterior part of the embryo adjacent to the *area opaca* is variable among embryos within the same stage. Despite that, in the same embryo this distance remains constant over time in the developmental stages considered in the analysis (HH3-HH10), as shown in Table 3.3: the standard deviation of the mean ratio for each time point is around 0.01-0.096. This

corroborates what can be seen in Figures 3.11 and 3.12. Also, the elongation rates obtained from the two measurements are not significantly different per embryo (Table 3.2). Thereby, we decided to use measurement 1 as a proxy for total embryo size since it is more reliable considering that the most posterior part of the embryo adjacent to the *area opaca* is a more easily detectable feature for the operator.

Table 3.3 – Mean ratio of measurement 1 and 2 over time;

For each video the length of measurement 1 was divided by the length of measurement 2 for each time point considered and the mean and standard deviation calculated. The standard deviation of the mean for each embryo varies between 0.01 and 0.096. Each embryo corresponds to one video. Measurement 1 – most anterior part of the embryo to the most posterior part of the embryo adjacent to the *area pellucida.* Measurement 2 – most anterior part of the embryo to the end of the primitive streak.

Embryos	Mean of the ratio between time point for measurement 1 and 2
1C	1.123 ± 0.06
2C	1.051 ± 0.01
3C	1.096 ± 0.02
4C	1.200 ±0.04
5C	1.130 ± 0.04
6C	1.250 ± 0.075
7C	1.308 ± 0.080
8N	1.170 ± 0.057
9N	1.178 ± 0.022
10N	1.136 ± 0.031
11N	1.067 ± 0.025
12N	1.160 ± 0.050
13N	1.346 ± 0.096

3.2.1 - Chapman *versus* New culture systems

Having established the spatial cues for measuring embryo total elongation, the goal was to compare the two *ex ovo* culturing techniques and to understand if we could use the two sets of embryos indistinctly for posterior analysis. As shown in Table 3.2 the elongation rates of the embryos cultured in New tend to be descriptively higher compared to the embryos cultured in Chapman. However, the embryos cultured in New encompass later developmental stages than the ones cultured in Chapman (Table 3.1). Hence, the differences could be due to different behaviors/elongation rates during different stages of development; *i.e.*, early stages of development (HH3/4) could elongate at lower rates than later stages. We decided therefore to only include measurements from stage HH5 onwards since the videos of embryos cultured in New encompass stages from this stage onwards. To graphically compare measurements obtained from different videos, these were aligned considering the stages HH4 and HH8. In Figure 3.13 it can be seen that the embryos cultured using New culture elongate in a similar fashion as the embryos cultured using Chapman. Also, the mean of the elongation rates is similar for the two techniques (Table 3.4).

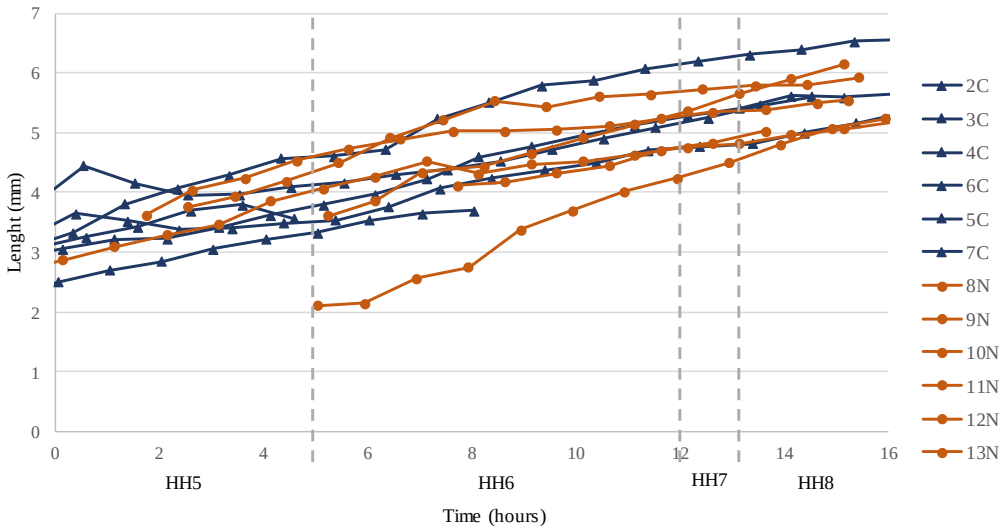

Figure 3.13 - **Chick embryo elongation using Chapman and New culture systems;**

The distance between the most anterior part of the embryo and the most posterior limit of *area pelucida* was measured in frames corresponding to one-hour intervals. Embryos cultured in Chapman (C)are represented in orange and embryos cultivated in New (N) are represented in blue. Stages were defined according to Hamburger and Hamilton (Hamburger and Hamilton, 1951). Embryos were aligned considering the stages HH4 and HH8.

Two nonparametric statistical tests were further applied to compare the elongation of the embryos. We found that the embryos presented statistically significant differences in growth behavior among them (Kruskal Wallis - $p=1.814e^{-7}$; Jonckheere-terpstra - p=0.027). Embryos cultured in Chapman culture have statistically significant different behaviors among them (Kruskall Wallis – p= 0.000; Jonckheere-terpstra – p=0.005). For the New culture the same was not observed (Kruskal Wallis - p=0.000; Jonckheere-terpstra - p=0.203), which means that embryos cultured in New culture have more similar growth behaviors between them. This can be due to the developmental stages included in the analysis for both cultures. The embryos cultured in Chapman encompass more early stages than the embryos cultured in New, which are also more variable in elongation behavior. Also, when comparing the standard deviation among embryos, the same was not observed, since embryos cultured in New have a higher standard deviation between them when compared with the embryos cultured in Chapman (Table 3.4). The different results could be due to the methodology. Standard deviation only gives us a notion of the variability between embryos considering the total rate of elongation. The statistical tests were performed considering the length of the embryos in each time point thus giving complementary information related with

the overall behavior of the embryos. Importantly, no statistically significant differences in growth were detected when comparing culture methods (Kruskal Wallis - p=0.427; Jonckheere-terpstra - p=0.427).

Table 3.4 - E**longation rates of embryos cultured in Chapman and New systems**;

Elongation rates were calculated considering the first and last time point measured for each video. The mean and standard deviation of the elongation rates of the embryos cultured in each cultured were calculated.

Culture System	**Embryo**	**Elongation Rate (mm/h)**	**Mean (mm/h)**
Chapman	2C	0.150	0.133 ± 0.037
	3C	0.112	
	4C	0.154	
	5C	0.120	
	6C	0.181	
	7C	0.078	
New	8N	0.256	0.193 ± 0.06
	9N	0.154	
	10N	0.148	
	11N	0.288	
	12N	0.142	
	13N	0.167	

All the tests mentioned above were performed having in consideration the length of the embryos in the different time points. However, it is also important to compare the elongation rate (ratio between the length variation and time variation per time point), between the two culture methods. For that we executed a hierarchical cluster analysis to dendographically visualize how embryos cluster among themselves. The configuration of the embryos in the dendogram does not segregate the embryos in the two different cultures systems (Figure 3.14). Instead, the dendogram evidences the formation of three different groups. Embryos of the different cultures are distributed by two clusters while embryo 11N is isolated (considering the computational distance of 5 as indicated in black). It is interesting to find that this analysis was able to identify the embryo that also presents a different behavior in Figure 3.13.

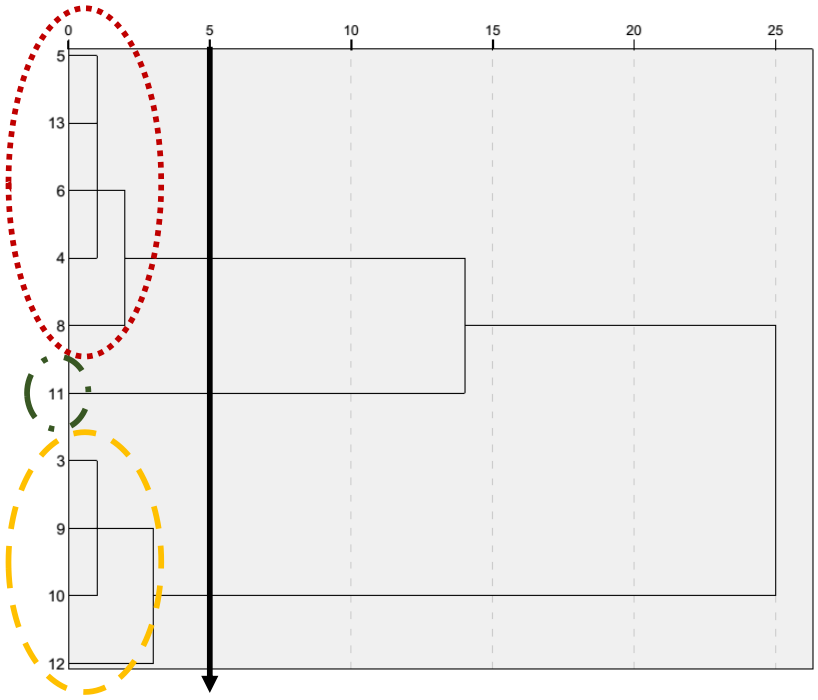

Figure 3.14 – **Hierarchical cluster analysis of the chick embryo elongation rates using Chapman and New culture systems.**

Hierarchical cluster analysis following the Ward method and fixing the squared Euclidian distance. Considering the computational distance of 5 (in black) the embryos segregate among themselves in three clusters. Five different embryos constitute the first cluster: 5C, 13N, 6C, 4C and 8N (magenta). The second cluster is comprised by embryo 11N (green). The last cluster comprises four different embryos: 3C, 9N, 10N and 12N (yellow). Each number corresponds to one embryo: 3 – 3C; 4 – 4C; 5 – 5C; 6 – 6C; 8 – 8N; 9 – 9N; 10 – 10N; 11 – 11N; 12 – 12N; 13 – 13N

Overall, our analysis strongly supports the hypothesis that embryos cultured in Chapman or New culture systems grow in a similar fashion in the developmental stages analyzed. This may be a surprising result, considering the characteristics of both techniques. The main advantages of Chapman culture compared with New culture reside on the easiness of the execution and in the tension applied. In Chapman culture, the correct tension is accomplished by placing the paper directly onto the vitelline membrane, so the tension applied is very similar to the tension *in ovo* (Chapman et al., 2001*)*. In New culture, tension is applied by the operator which means that the correct amount of tension is empirical (Chapman et al., 2001). Therefore, different elongation behaviors might be expected between embryos cultivated in the two cultures. However, this was not observed, which reinforces the applicability of both techniques for chicken embryo studies.

Since our results show that embryo elongation is independent of the culture system used, we considered all 13 embryos to infer further results in this study. Considering all the embryos, it was observed that the chicken embryo elongates with an average rate of 159 ± 55 µm/h from stages HH3-HH10.

3.2.2 - Stage-specific characteristics: total duration and elongation rates

Next, we sought to understand how the chicken embryo elongates in each stage of development, from HH3 to HH10. First, the precise duration of each developmental stage was investigated. In the analysis we only included data from videos where both the beginning and end of each stage were clearly visible. Exceptionally, when a stage that was not included in the video from beginning to the end, presented higher period of time than the respective calculated mean, the duration of this stage was included in the analysis. This implies that the mean of the duration of each stage may be underestimated. Such is the case for stages HH4 - HH6.

In average, the embryos remain in stage HH4 for 6.2 hours and in stage HH5, 6.4 hours (Figure 3.15). Developmental stages HH6-HH9 presented lower periods of duration. Stage HH6 lasts in average 3.3 hours, stage HH7 3.5 hours, stage HH8 4.1 and 5.1 hours at stage HH9. Stages HH4, HH5 and HH6 were the ones that presented higher standard

deviations (Figure 3.15), most probably due to biological variability. Embryos were imaged ventrally, which makes the detection of the transition from HH5 to HH6 more difficult. It was confirmed that the variation wasn't due to problems in detecting the stage transition, since the duration of these two developmental stages is not inversely proportional in each embryo (Appendix 3).

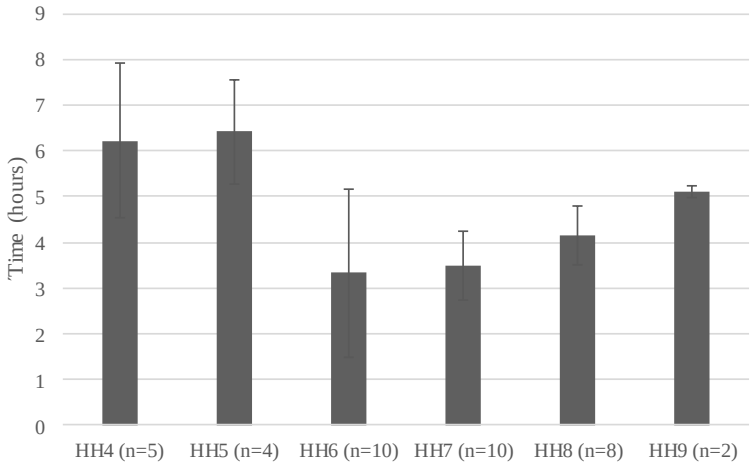

Figure 3.15 - **Period of duration of stages HH4 to HH9;**

The duration of each developmental stage was calculated considering the mean of the duration of the respective stage in all embryos. Only embryos that had all the respective stage imaged were included in the analysis. This criterion was followed excluding cases when the period of the respective developmental stage was higher than the mean. Embryos were staged according to (Hamburger and Hamilton, 1951)

The total duration predicted for the developmental stages according to the Hamburger and Hamilton (1951) are shorter than the periods calculated in the present study. Hamburger and Hamilton staging system was developed by analyzing hundreds of embryos dissected in specific intervals of incubation. This approach has the disadvantage that the same embryo is not visualized in more than one timepoint and the initial stage before incubation cannot be controlled, so high errors are likely to be associated with stage duration. In our work, the same embryo was analyzed over time, allowing a more precise analysis. This also highlights the advantages of live-imaging in the study of embryo development.

Having this system as an advantage, and considering that the period of formation of the first somites is not known we decided to calculate the period of formation of the first 2-

10 somites. The period was calculated by performing the mean of the formation of three consecutive somites corresponding to the mean of duration of stage HH7-10. Thus, the data presented is an average value and not a direct measurement of each individual somite. The first three somites presented an average periodicity of 1.16 hours (~70,0 min), the following three somites 1.38 hours (~83 min) and next three somites 1.70 hours (~102 min) (Figure 3.16). The periods calculated are different from 90 minutes, which is the somite formation period for somites 15-20 (Palmeirim et al., 1997). The periodicity calculated for the formation of the first three somites considered is particularly lower. Thus, these results suggest that the first somites are formed at higher rates, and the velocity of somite formation increases until it stabilizes at the ~90 minutes characteristics for chicken embryos around 15-20 somites. Those results are interesting since it was already described that the last somites have higher periods of formation (Tenin et al., 2010). This suggests that over somitogenesis the period of somite formation is variable and seems to be slowing down as development progresses: the first somites are formed faster and the last ones are formed at slower rates.

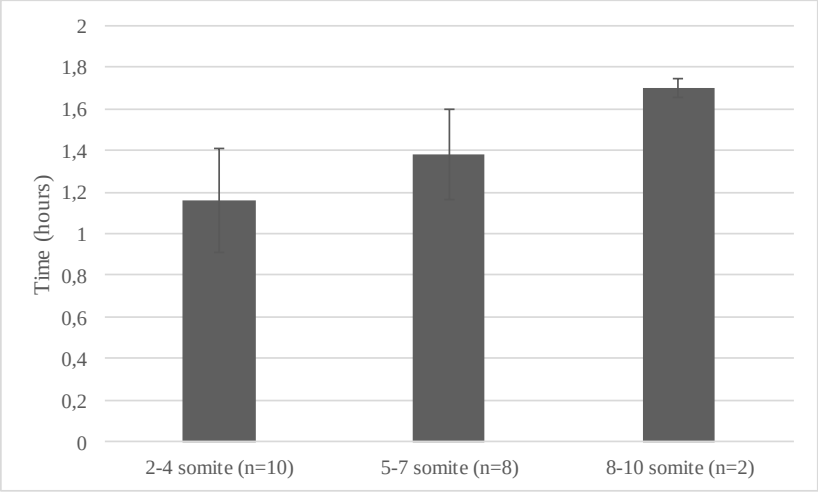

Figure 3.16 - **Period of formation of the first 9 somites;**

Somite period formation was calculated from the period of duration of stages HH7-HH9. The duration of each developmental stage was calculated considering the mean of the duration of the respective stage in all embryos. Only embryos that had all the respective stage imaged were included in the analysis. This criterion was followed excluding cases when the period of the respective developmental stage was higher than the mean. Embryos were staged according to Hamburger and Hamilton (Hamburger and Hamilton, 1951)

Finally, the total elongation rates were calculated *per* developmental stage. In Figure 3.13, embryos length in function of time is plotted. The developmental stages in the graph were aligned by defining the entire value were more than half of the embryos were already in the stage considered. As seen in Figure 3.13 the embryos have different elongation behaviors along the developmental stages, where the rates vary. Considering that observation we decided to perform the 1st derivate for each embryo elongation curve. The 1st derivate gives us a measure of how the rate of each curve alters along time and when. Therefore, when the rate is constant, the derivate present a steady line with same values of y. When the rate varies over time several picks can be observed. After plotting all the derivates it was not possible to take any conclusions, since they present a lot of noise and it was not possible to choose e cut-off point (Appendix 4). Therefore, we decided to calculate the elongation rate per developmental stage (Figure 3.17).

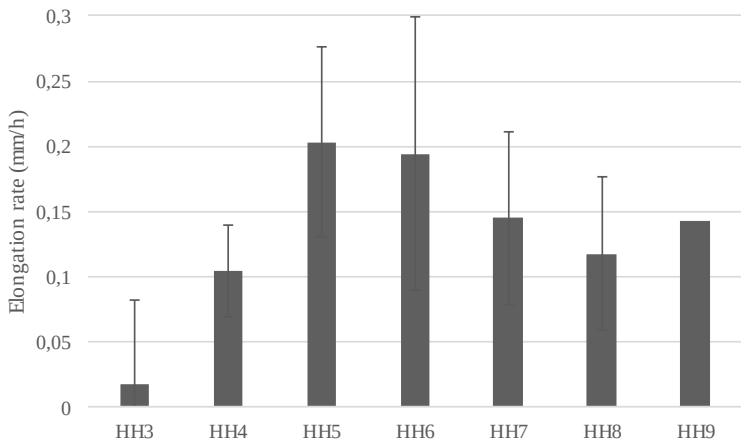

Figure 3.17- **Chick embryo stage-specific elongation rates from HH3-HH9;**

Elongation rates of the different stages of development included in the analysis (HH3-HH9). The embryos were aligned by the last frame in the stage considered and the elongation rates calculated considering the first and last time point included in the analysis. In the x axis are represented the stages of development (Hamburger and Hamilton, 1951) and in the y axis the elongation rates (mm/h).

As shown in Figure 3.17, the different developmental stages present different rates of elongation. Stage HH3 presents the lowest elongation rate from all stages comprised. This is not surprising, since during this stage the major event happening is the elongation of the primitive streak. During stage HH4, the elongation rate is almost 10 times higher than stage

HH3. Stages HH5 and HH6 present the highest elongation rates. In stages HH7,8,9 the rate of elongation is lower and more stable. Stages HH5-6 are characterized by the regression of the Hensen's node and the elongation of the notochord and precede the beginning of somitogenesis. This shows that the period of time when the embryo elongates at higher rates occurs in gastrulation stages after the beginning of the regression of the Hensen's node which can indicate an important role for the gastrulation movements and for notochord elongation in driving embryo elongation during these stages.

3.2.3 - Tissue-specific characteristics: elongation of different portions of the embryo

To understand the driving force of chicken embryo elongation we asked which portions of the embryo where contributing more to the total elongation by assessing the dynamics of the different portions of the embryo. The different portions considered in the analysis were: 1) Notochord elongation – measured from the most anterior part of the embryo to the Hensen's node; 2) Node regression – measured from the Hensen's node to the most posterior part of the embryo adjacent to the *area opaca*; 3) Head portion elongation – measured from the most anterior part of the embryo to the middle of the second somite; 4) Segmented region elongation – measured from the first to the last somitic clefts formed; 5) PSM elongation – measured from the last somitic cleft formed to the Hensen's node. Figure 3.18 and 3.19 represent the variation of the length of the whole embryo and of the different portions measured over time. As can be observed in the Figure 3.19, the head portion and the most posterior part of the embryos contribute the least to total embryo elongation. The notochord elongates continuously over time in a linear fashion. After the beginning of somitogenesis, the PSM and segmented region are the ones that contribute more for embryo elongation. The elongation rates of each one of these portions was calculated. From stage HH3 to HH10 the embryo elongates at a rate of 159 ± 55 μm/h. The notochord extends at 203 ± 71 μm/h, a slightly higher rate than the total elongation rate. The Hensen's node regresses with a rate of -34 ± 4 μm/h. The sum of the notochord elongation rate and the Hensen's node regression rate gives a value that is approximately the total elongation rate. This was according to what was expected, since the two measurements are equivalent to the

measurement 1, which is equivalent to the total elongation of the embryo. The head portion of the embryo is the tissue that presents the lowest elongation rate: 31± 28 µm/h which is very similar to the regression of the Hensen's node rate. The PSM elongates with a rate of 76 ± 28 µm/h and the segmented region with 101± 18 µm/h. The sum of the elongation rates of the PSM and segmented region is close to the total elongation rate showing that those regions are the ones contributing more to the total elongation rate after the beginning of somitogenesis.

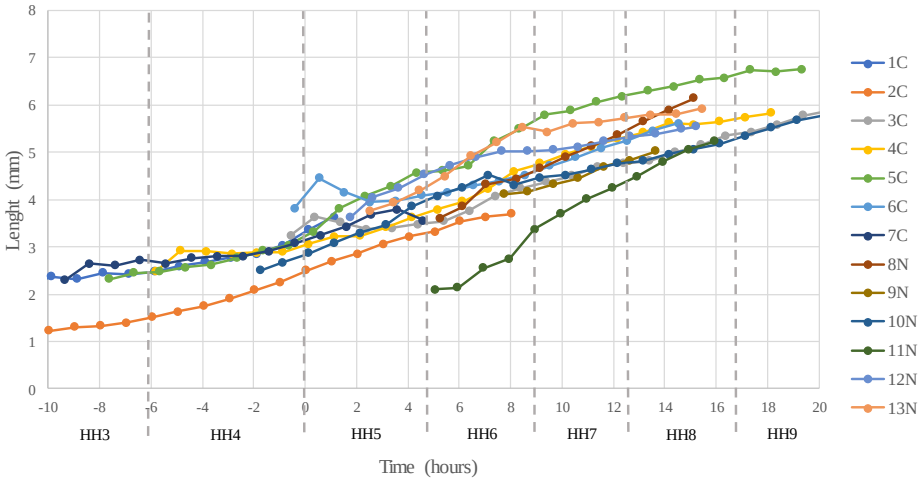

Figure 3.18 - **Chick embryo elongation from stage HH3-HH9**

The distance between the most anterior part of the embryo to the most posterior limit of *area pelucida* was measured in frames corresponding to one-hour intervals. Each line corresponds to one embryo. Embryos 1A-7A were cultured using Chapman culture and embryos from 8B to 13B were cultured using New culture. Stages were defined according to Hamburger and Hamilton (Hamburger and Hamilton, 1951). Embryos were aligned considering the stages HH4 and HH8.

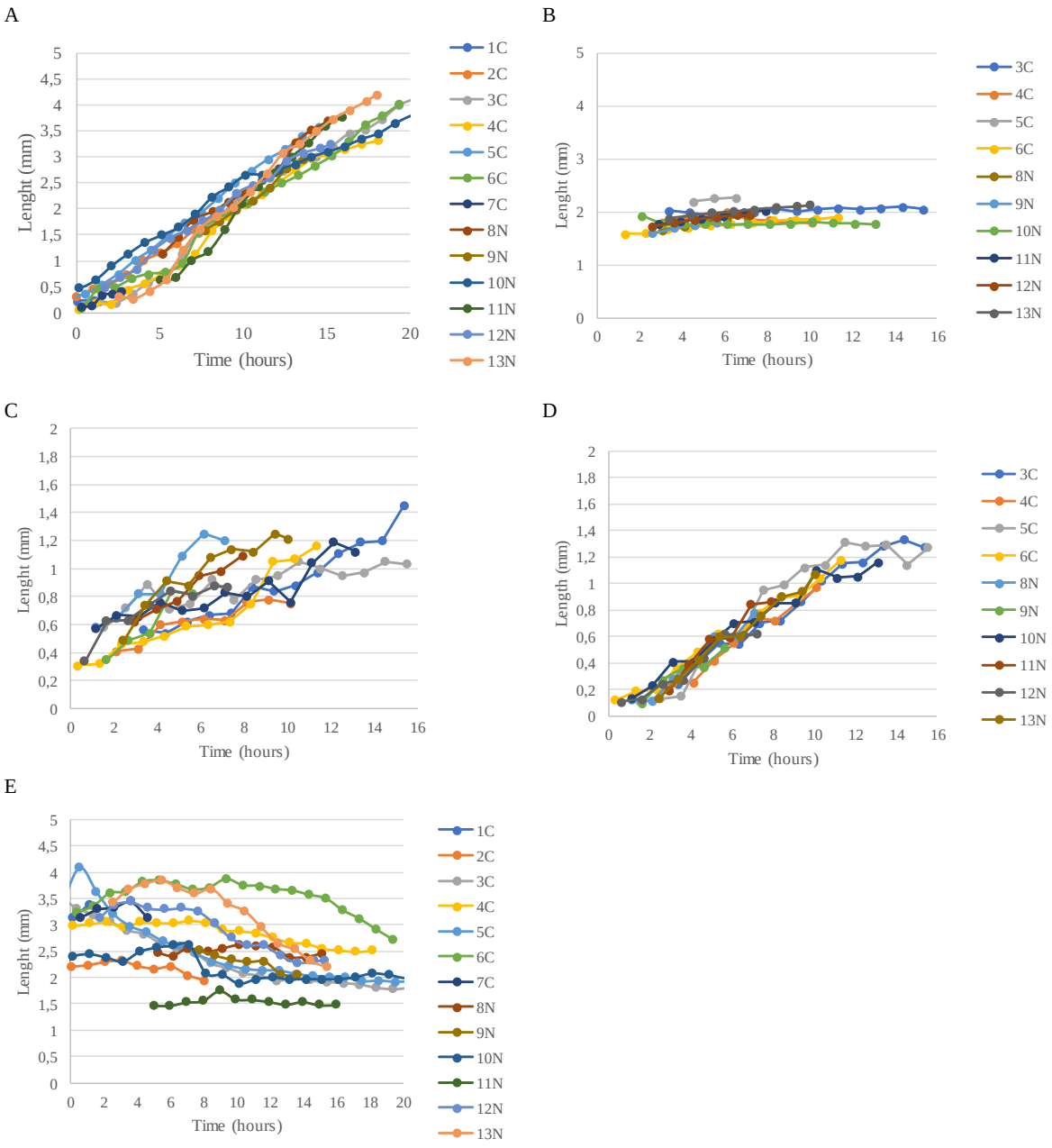

Figure 3.19 – **Elongation of the different portions of the embryo from stage HH5-HH9;**

A – Notochord elongation; B – Head portion; C – PSM; D – Segmented region; E – Most posterior part of the embryo; Each measurement was performed in frames corresponding to one-hour intervals. Each line corresponds to one embryo. Stages were defined according to Hamburger and Hamilton (Hamburger and Hamilton, 1951). Embryos were aligned considering stages HH4 and HH8.

The contribution of each portion for total embryo elongation after the beginning of somitogenesis is shown in Figure 3.20. In the kymogram, the contribution of each portion considered to embryo elongation can be seen. The segmented region and the PSM are contributing more for total embryo elongation while the head portion and the most posterior part of the embryo contribute less. Somites, which comprise the segmented region, are formed from segmentation of the rostral most-PSM over time. This suggests that the mechanisms driving PSM extension are the important mechanisms driving chick embryo elongation.

	Elongation rate (μm/h)
Total embryo	159 ± 55
Notochord	203 ± 55
Hensen's node regression	-34 ± 40
Head portion	31± 28
PSM	76 ± 28
Segmented region	101± 19

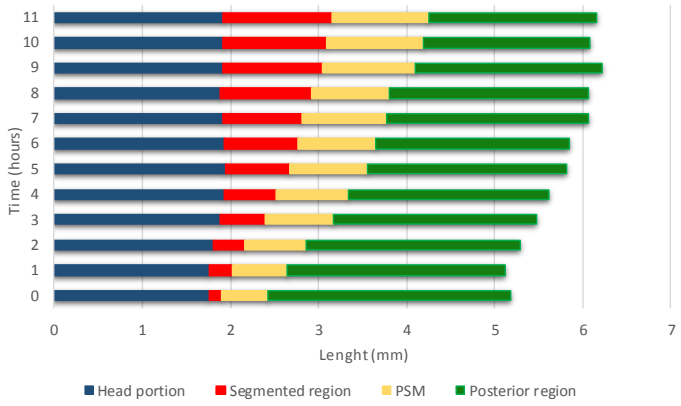

Figure 3.20 – **Elongation rates and contribution of each region of the embryos to the total elongation (somitogenesis stages);**

The table shows the elongation rate of each portion of the embryo measured. The contribution of each portion is represented in the kymogram. Blue – Head portion; Red – segmented region; Yellow – PSM; Green – posterior region of the embryo. Embryos were aligned considering stages HH4 and HH8.

3.3 - Impact of Hairy1 overexpression in chick embryo elongation

Previous work of the lab showed that when Hairy1 is overexpressed in the precursors of PSM in gastrulating stages (HH4), the development of the trunk of the embryo is delayed compared to the head (Andrade et al., under review). There are several hypotheses that could explain the phenotype described, such as: 1) Hairy1 is affecting cell division; 2) Hairy1 is affecting differentiation of the cells, and/or 3) Hairy1 is affecting cell migration and ingression through the primitive streak. All these processes would affect embryo elongation, therefore we decided to address if embryo elongation was being affected by Hairy1 overexpression.

Early chick embryos were electroporated with an overexpression vector of Hairy1 (pCAT-Hairy1) in PSM precursors in stage HH4. In order to confirm Hairy overexpression, *in situ* hybridization was performed showing ectopic expression of *hairy1* in the same localization as GFP (Figure 3.21).

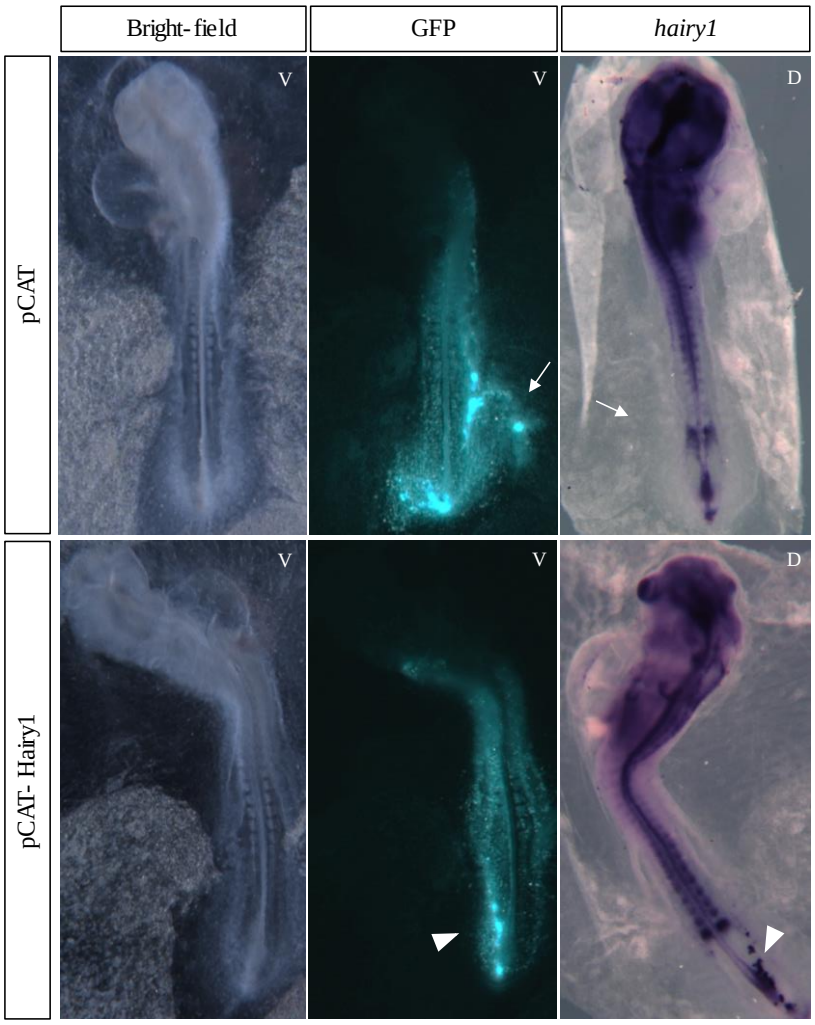

Figure 3.21 – **pCAT-Hairy1 embryos present ectopic expression of *hairy1* mRNA corresponding to electroporated regions;**

Embryos electroporated with the control and pCAT-Hairy1 vectors photographed in bright-field and with fluorescence (green) corresponding to the regions of overexpression of the vectors electroporated. Embryo in situ hybridized with a probe for *hairy1* showing that embryos electroporated with pCAT-Hairy1 present ectopic expression of hairy1 mRNA. Expression of the control vector does not lead to ectopic expression of *hairy1* mRNA

.

In the present work, the phenotype described previously (Andrade et al., under review) was never detected, however in our experimental design, embryos were incubated for long periods of time before imaging (until 5-16 somites). The previously described phenotype was detected in the transition from HH7 to HH8 and was already known to be transient (Andrade et al., under review). We decided therefore to use live-imaging to follow the development of the electroporated embryos. Embryos were incubated for 4-6 hours after electroporation in order to allow fluorescence to develop. Next, the best embryo, considering

the fluorescence location and the viability of the embryo, was imaged for 12-24 hours (Appendix 7,6: supMovie3). The total elongation of the embryo, as well as the elongation of PSM and segmented region were analyzed. PSM and the segmented region are the ones that are contributing more to the total elongation rates of the WT embryo and those are the tissues where the expression of Hairy1 is being altered. The total length of each region considered is graphically represented as a function of time for the embryos analyzed in Figure 3.22. Considering the length variation over time (Figure 3.22) the total length of the embryo does not present differences between the embryos electroporated with the empty vector and with pCAT-Hairy1. However, the length of the PSM and of the segmented region tend to be smaller in embryos pCAT-Hairy1.

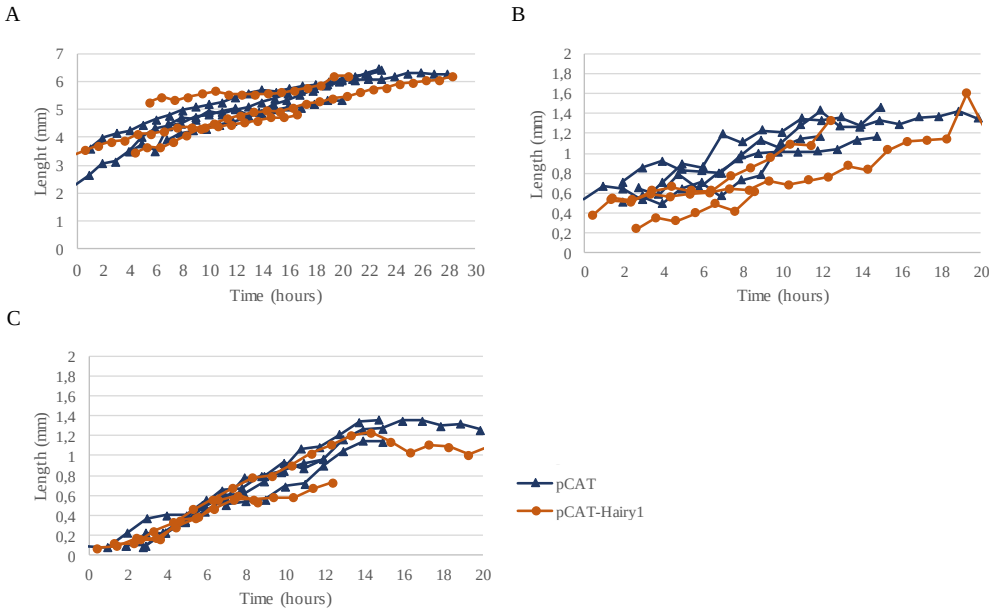

Figure 3.22 – **Elongation of embryos electroporated with empty vector and pCAT-Hairy1;**

Elongation of the total embryo, PSM region and segmented region in embryos electroporated with empty vector (green), and electroporated with H1 overexpression vector (brown). Embryos pCAT-Hairy1 seem to have lower slopes in the total embryo elongation.

Furthermore, the elongation rate of the total embryo, PSM and segmented region was calculated. As shown in Table 3.5 pCAT-Hairy1 embryos present significantly lower elongation rates than the control embryos. Electroporation with empty vector didn't affected

embryo elongation (Table 3.2 and 3.5). Regarding the elongation of the PSM, pCAT-Hairy1 tend to have higher elongation rates than the embryos electroporated with the empty vector (Table 3.5). The segmented region elongation rate is significantly lower in pCAT-Hairy1 embryos. This difference could be due to either a smaller length of each somites or to a higher period of somite formation leading to fewer number of somites. In the graph, in the first hours, the length of the segmented region seems similar between all the embryos, therefore it can be concluded that in this window the somites have the same size, but further analysis is required to confirm. Regarding the PSM, the elongation rate of the PSM tends to be higher in pCAT-Hairy1 and the length of the tissue tends to be smaller. This is an interesting result because if the elongation rate as a tendency to be higher, we would expect the same regarding the total length of the tissue. This implies that PSM is substantially smaller since the beginning of somitogenesis and that somehow the embryo is trying to recover. Also, the segmented region presents a lower elongation rate in the pCAT-Hairy1 embryo. Considering that, we would also expect a higher length of the PSM tissue. All those observations suggest that PSM elongation is being altered upon Hairy1 overexpression. However, the differences observed in PSM elongation rate and length are not significant and the number of embryos analyzed is low. Thus, it would be very important to increase the number of embryos analyzed to confirm if those differences are significant.

Table 3.5 – **Elongation rate (µm/h) of the total embryo, PSM and segmented region of embryos electroporated with empty vector and with overexpression of Hairy1 vector;**

Total elongation rate of the embryo, PSM and segmented region considering the first and last point measured. Elongation of both total embryo and segmented region are lower in pCAT-Hairy1 embryos, however, elongation of PSM seems higher in the pCAT-Hairy1 embryos. Elongation rate in mm/hour.

Total embryo	140 ± 22	95 ± 27
PSM	49 ± 8	59 ±16
Segmented region	82 ± 19	56 ± 5

Considering our data, we have strong suggestions that the total elongation of the embryo, the PSM elongation and the segmented region segmentation are being compromised when Hairy1 is being overexpressed. However, the impact in somitogenesis is also important to consider. Our methodology didn't allow to detect alterations in somitogenesis. Therefore, it would be interesting to perform some adjustments to the alignment performed to compare the videos. These embryos were aligned considering stage HH8. Stage HH8 already has 4 somites formed. Despite that, align the videos by early stage of development (perhaps HH6 since HH4/5 are not present in all videos) would allow to address if the beginning of somitogenesis is delayed in comparison to the control group. We could also measure the extent of the head development in the moment of formation of the first somite, which would also allow to identify a delay in development of the posterior part of the embryo in the pCAT-Hairy1 embryos.

To confirm that the embryos pCAT-Hairy1 have differences in elongation compared with the control group two nonparametric statistical tests were applied considering the length of each portion over time. In the statistical analysis, the wild-type embryos cultured in Chapman were included. The behavior of elongation of the embryos between conditions presented statistically significant differences (Kruskal Wallis - $p=0.013$; Jonckheere-terpstra - $p=0.037$). Considering the data from the elongation rates (Table 3.5) and the average of the total length (Appendix 7.5) of each group of embryos, is clear that the embryos pCAT-Hairy1 have different elongation behaviors from the control and WT embryos which are more similar among them. This gives strength to the hypothesis that Hairy1 is affecting the total elongation rate of the embryo. However further analysis is required, as well as a higher number of treated embryos, to fully understand the phenotype and the recovery, and confirm if and how Hairy1 is affecting embryo elongation.

3.4 - Preliminary results for Future Work on Hairy1 impact on cell migration and proliferation

One of the goals of the present work is to add some new insights of how Hairy1 is affecting the development of the early chick embryo. Previously we analyzed the impact of Hairy1 in embryo elongation, which gave some insights on how the whole system is being affected. However, we are also interested in understanding what is going on at the single cell level and if we are affecting cell division, differentiation, or migration, or several of these processes.

Live-imaging is a strong tool that would allow us to assess some of our questions. Among the available techniques, light sheet imaging has some advantages. It allows to film live specimens for long periods, to live image at the single cell level and to control the temperature conditions (Power and Huisken, 2017). In order to understand if it would be possible to perform live imaging of chicken embryos in the stages of interest (from early stages of gastrulation onwards) some tests were performed in a commercial light sheet microscope (Zeiss). The culture setup was optimized with the assistance of a technician from Zeiss. We used embryos electroporated with GFP cultured in chapman. In order to live-image the embryos, the paper of the chapman culture was glued to the support of the microscope. The setup was then submerged in thin albumin at 37ºC in the sample chamber. This setup allowed to live-image embryos in stage HH4 for around 6 hours. As seen in Figure 3.23 it is possible to live image at the single cell level without losing whole embryo perspective. It is also possible to follow cell movement and to visualize cell divisions (Figure 3.23). With our approach, the basal conditions to perform light-sheet are settled. However, further optimization will be required to ensure that the embryo remains in focus for longer periods. Thus, light sheet microscopy will be a very useful tool to study how Hairy1 is affecting cell division and movement in electroporated embryos in future studies.

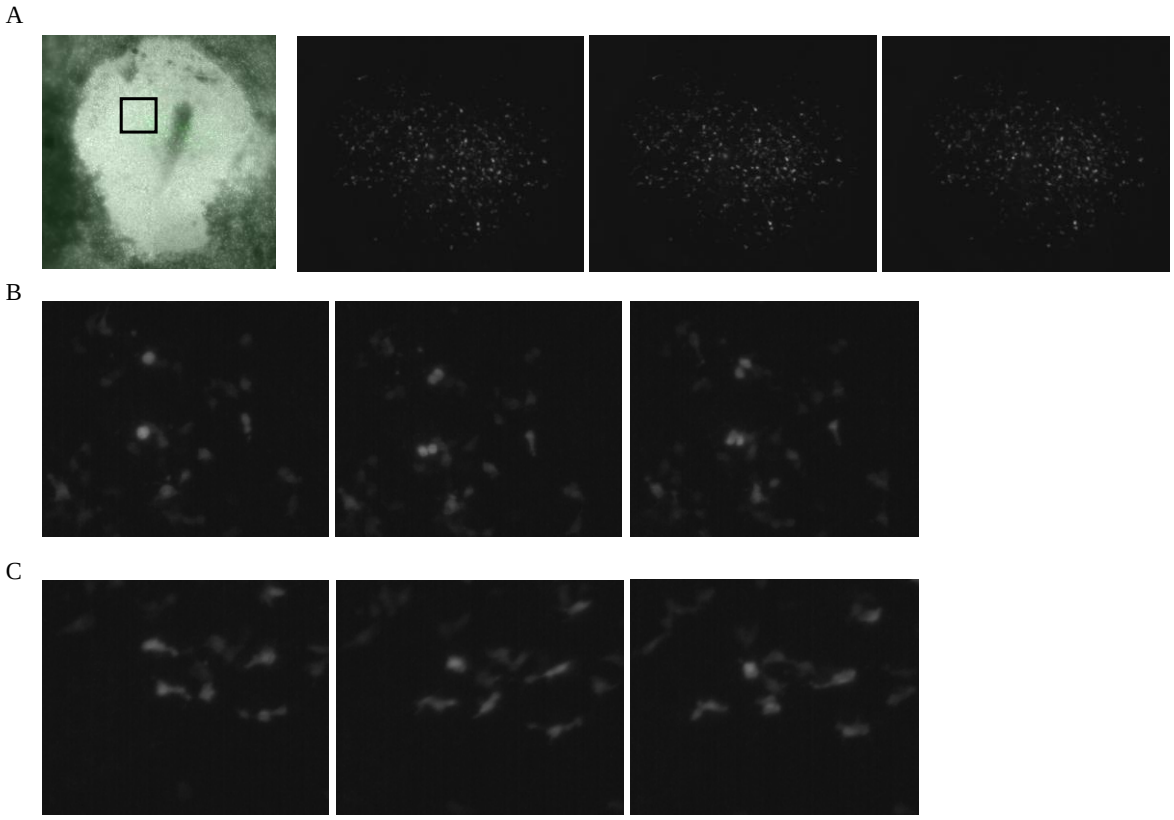

Figure 3.23 – **Light sheet microscopy allows to live image chicken embryos**;

Chicken embryo (HH4) electroporated with empty vector was live imaged using light sheet microscopy. A – whole embryo perspective. B – The region in the black square in A was zoom in in order to observe two cells dividing. C - The region in the black square in A was zoom in to visualize two cells migrating in the epiblast.

To be able to live-image embryos and to follow cell movements and divisions it is important to label the cells. In our experimental design it would be useful to avoid electroporation and to use tools that have different wavelengths from GFP. There are several tools available nowadays that are useful to evaluate cell migration and cell division and that can be used in both fixed and live samples. Some of the tools more commonly in the last years used are summarized Appendix 7. The methods vary from immunolabelling techniques, constructs that can be electroporated to vital dyes. In the present work we decided to begin testing vital dyes. They are advantageous because they don't require electroporation and because they are easily used. Vital dyes are chemical compounds that mark structures inside cells without requirement to fix samples, allowing live imaging. Three different dyes

were tested to stain embryos in HH4 – syto 62,64 and Draq5 (Figure 3.24). Draq5 didn't labeled all the cells. From the syto dyes tested syto 64 presented the most promising result (Figure 3.24). However, signal was lost rapidly due to photobleaching (Figure 3.24). This would not allow to perform live imaging of embryos for long periods. Despite that, it is recommended to use buffers without phosphate to dilute those compounds, because phosphate can compromise the stability of the dye leading to photobleaching. PBS 1x was used to dilute the dyes, so it would be recommended to, in the future test again the syto dyes with other buffers.

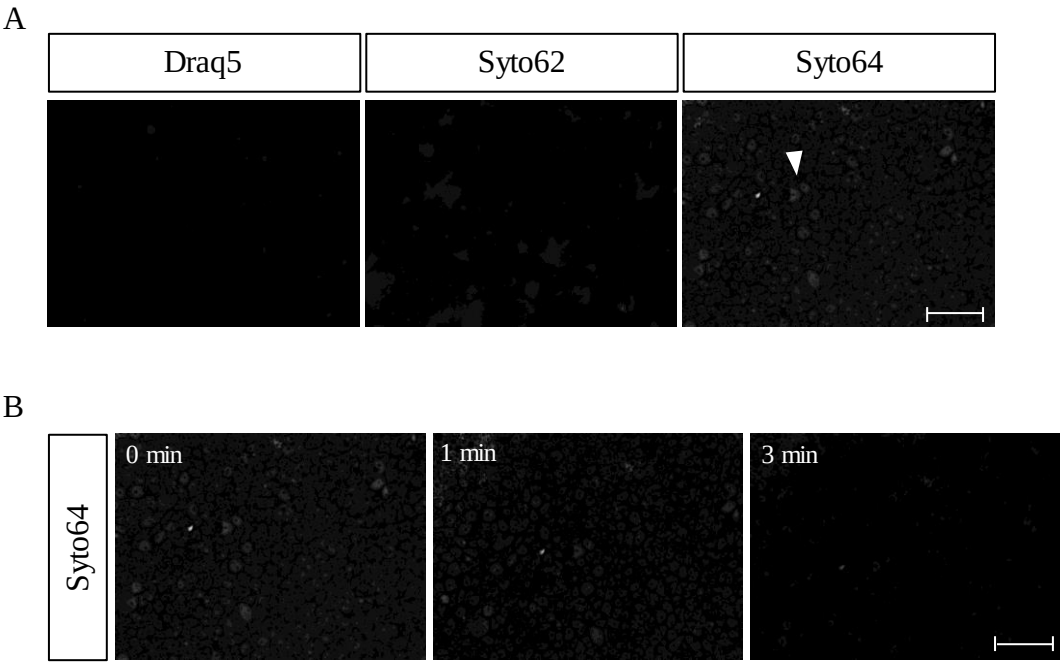

Figure 3.24 – **Test performed with three different vital dyes: Draq5, Syto 62 and 64;**

A **-** Three different vial dyes were tested in HH4 embryos. Draq5, Syto 62 and Syto 64. B – Frames taken each minute show that syto64 photobleachs rapidly.

Thereby, in the present work, we also tested some tools that are going to be useful in the future to assess the impact of Hairy1 overexpression in early chick embryo development.

4 - Discussion

4.1 - Dynamic expression of Hairy1 in early chick embryo

The main goal of the present study focused on understanding the role of Hairy1 in early chick embryo development. It was already known from previous work in the laboratory, that, when Hairy1 is overexpressed in PSM precursors, in gastrulation stages, the development of the trunk is delayed. Hairy1 is expressed in the PSM in a dynamic manner, being part of the molecular clock that regulates somitogenesis (Palmeirim et al., 1997). The role of dynamics in expression or biological activity, is gaining more and more attention since it was showed that it can elicit differential biological responses (Isomura and Kageyama, 2014)

In the present work, it was shown that *hairy1* also presents a dynamic expression pattern in gastrulation stages, both along the anterior-posterior and medial-lateral axes using *in situ* hybridization. Along the anterior-posterior axis, *hairy1* is present with different dynamics in the Hensen's node and in the primitive streak. The epiblast cells, were *hairy1* is expressed, is going to give rise to the three embryonic layers that will form all tissues of the embryo. Is already known that the embryonic clock functions in the central nervous system, in the PSM and in the limb with different periods (Palmeirim et al., 1997; Pascoal et al., 2007; Shimojo et al., 2008). We show that in gastrulation stages, *hairy1* is already dynamic along the embryo, therefore it can be contributing to all lineages and tissues.

The PSM presents a dynamic expression of *hairy1* which is important for somite formation (Palmeirim et al., 1997). The precursors of the somite cells are located at two different regions in the embryo: the most medial part of the somites are formed from a population of stem cells that are present in the Hensen's node; the cells that will give rise to the most lateral part of the somites will gastrulate through the most anterior part of the primitive streak (Iimura et al., 2007; Psychoyos and Stern, 1996). The two populations of cells are differently committed to become somites. The medial part is able to segment in the absence of the lateral part of the PSM. On the other hand, the lateral PSM does not segment in the absence of the medial portion (Freitas et al., 2001). Freitas and collaborators (2001)

showed that in stage HH9-, *hairy1* is already oscillating, in cells in the prospective territory of the PSM, before they incorporate into the PSM tissue. In the same work was also showed that the precursors of cells that originate the medial and lateral somite are not synchronous: instead they observed a "wave" of expression along the future medial/lateral PSM axis. Concordantly, the expression of *hairy1* across the PSM is also asynchronous along the medial-lateral axis, which is evidenced by the presence of cross-stripes in the expression pattern (Freitas et al., 2001). Freitas and collaborators (2001) proposed therefore that the expression of *hairy1* is giving positional information both in the antero-posterior and medial-lateral axes. In stages of gastrulation, in the present work we observed that the expression of *hairy1* presented different dynamics of expression in the Hensen's node and in the primitive streak. These results show that, in gastrulating stages (HH3-5), the cells that will originate the somites, already have different dynamics of expression. This shows that the uncoupling of expression described (Freitas et al., 2001), that could underlie the asynchrony along the medial-lateral axis during somitogenesis and the positioning information along the medio-lateral axis, is already present in early gastrulation stages (HH3-4). This novel observation, adds new insights in the understanding of somite formation, giving the suggestion that the medial and lateral PSM precursors are already receiving different signals in early gastrulation.

We also observed that the region of the primitive groove and the primitive ridge present different dynamics of *hairy1* expression, showing differential medial to lateral expression dynamics in the primitive streak. Thus, the cell in the primitive rigde, and in the primitive groove are asynchronous for *hairy1* expression. The cells in the epiblast are going to gastrulate in order to form the three embryonic layers, thus they suffer an epithelial-to-mesenchymal transition (EMT) (Gilbert, 2014). Along the medial-lateral axes the cells are in different status of this process. The cells in the epiblast ridge outside the middle of the streak are in an epithelioid organization (Nakaya and Sheng, 2008). The cells in the primitive groove are entering a mesenchymal state (Lim and Thiery, 2012; Nakaya and Sheng, 2008; Voiculescu et al., 2014). Expression of EMT related markers also show that the cells in the primitive groove express N-cadherin while the cells in the rest of the epiblast majorly express E-cadherin (Thiery et al., 1984; Nakayama et al., 2008). Thus, the cells where we observed an asynchronous dynamism of *hairy1* expression present very different status in the EMT

transition. Therefore, we hypothesize that *hairy1* might be involved in the EMT in epiblast cells during gastrulation. In the chicken embryo, Hairy1 was already shown to influence the EMT through the downregulation of responsiveness to BMP signaling in roof plate cells. BMP is important to neural crest cell induction and EMT and Hes1/Hairy1 misexpression downregulates neural crest migration (Nitzan et al., 2016). Also, Hes1, the human homolog of hairy1, was already described as having an important role in the regulation of the EMT (Wang et al., 2015; Gao et al., 2015). In human colon cancer, Hes1 induced EMT phenotype and cytoskeleton reconstruction, enhancing the metastatic potential of cells (Gao et al., 2015). In nasopharyngeal carcinoma, Hes1 was shown to induce EMT-like cellular markers alterations and promoted migration and invasiveness in vitro (Wang et al., 2015). In both cases, the alteration in EMT was mediated by PTEN. Thus, we hypothesize that hairy1 can be modulating the epithelial to mesenchymal transition in the epiblast cells, regulating the migration and ingression of the cells. The influence of *hairy* expression in the EMT could explain the observed phenotype when hairy1 is overexpressed, where we could be impairing gastrulation through the impairment of the EMT, leading to a delay in development.

In order to understand the functional role of Hairy1, it is very important to be able to analyze and understand what is happening at the protein level. Where it is located?; at what levels?; with which dynamics? All of these are very relevant questions. First, because mRNA does not always correspond to protein levels. Second, because most of the known gene functions relevant for biology are mediated by the protein. Namely, during somitogenesis, the negative feedback loop used to explain the sustained oscillatory expression of *hairy1* implies that the protein of Hairy1 needs to be also inhibiting the transcription of its own mRNA transiently and cyclically. However, the localization of the protein, the levels of the protein and other functions could be important to understand all its roles. Therefore, it would be crucial to optimize the immunofluorescence protocol and/or to obtain better antibodies against Hairy1. This would represent an important tool to better understand the function of Hairy1 during development.

4.2 - Somite periodicity over time

In the present work we addressed how early chicken embryo elongates and which are the portions of the embryo that contribute most to the total elongation. We also addressed the periods and rates of different developmental stages (HH3-HH9), as well as the period of somite formation. We observed that for the first 2-10 somites the period of formation increases over time. The periods calculated were also different from the 90 minutes described for the 15-20 somites (Palmeirim et al., 1997). Namely, the period of formation of the first 6 somites considered is inferior to 90 minutes. Somites seem very similar, however they will later differentiate in different types of bones along the antero-posterior axis (Gilbert, 2014). Therefore, the first somites that have different periods of formation, also give very different structures. Later in development, when the elongation and somitogenesis are reaching its end, it was showed that somite formation period is longer than the period described for the formation of the 15-20 somites that remains constant until HH21. The period for the formation of the somites at stage HH23 was shown to be around 150 minutes. (Tenin et al., 2010). This already evidences that all somites are not formed with the same period in the chicken embryo. It is common knowledge that, in the chick embryo, the first three somites are formed at higher rates than the further ones, but the period was never determined. In fact, in the literature it is considered that the first somite to be formed is actually the second since the first is not yet visible (Hamburger and Hamilton, 1951). In this work, we corroborate that the first somites are formed at a faster rate than the others. This indicates that, in the chicken embryo, the formation of the somites has different periods depending on the phase of development. The data from the present work and from the work of Tenin and collaborators also suggests that the period tends to increase during development (Tenin et al., 2010).

It would be also interesting to address the period of the somitogenesis clock underlying the formation of those somites to understand if the alteration in somite formation period is accompanied by an alteration in the clock period. This would be also useful to study the levels of regulation and the interplays between pathways that are applied to the clock inside cells that would drive to different periods of the clock. The main players in the somitogenesis clock within PSM and in the limb are the same (Sheeba et al., 2016), highlighting also that the differences that give rise to the different periods may in the

regulation mechanisms underlying both processes. During gastrulation the period is not known, but seems to be smaller than 90 minutes (not published), the first somites are formed at lower rates until they reach the period of 90 minutes which is stable until approximately the stage HH21. In the limb of the chicken embryo, *hairy1* oscillates with a period of 6 hours (Pascoal et al., 2012). The clock is also present in several cell types with periods of Hes1/Hairy1 of 2-5 hours (Kobayashi et al., 2009; Shimojo et al., 2008). The change in the period of oscillation, with a tendency to be higher over development could underlie a higher level of complexity of the regulatory mechanism or extra-levels in between the negative feedback-loop. Another very important molecular clock is the circadian clock, which the discovery of its molecular mechanisms was awarded with the Nobel prize in physiology or Medicine in 2017. The circadian clock period is 24 hours in humans allowing us to anticipate and adapt to the different phases of the day. Despite the different outputs of the molecular clocks described, they rely in negative feedback loops (reviewed in Uriu, 2016). The different levels of regulation may be what underlies the different periods. Considering that in the same cells, the same players can be involved in different clock/periods, it is interesting to try to understand how they are regulated and how they are related. It must be easier to create a sustained clock from a pre-existent clock than from a non-oscillatory network. Taking this view in mind we could think about clock like sprockets in a watch, where we have different molecular clocks, entrained in other molecular clocks, transforming the periods, or giving rise to new networks.

4.3 - Chick early embryo elongation

In order to understand how the chicken embryo develops over time, the elongation of the embryo and of different portions of the embryo was addressed. Regarding the elongation of different portions of the embryo we observed that more differentiated tissues present less variability among them in length over time. On the other hand, more undifferentiated tissues present more differences in total length over time. This observation suggests that more differentiated tissues have a more strict control in total length, which requires that the embryo needs to tightly regulate the length of those tissues.

During stages of gastrulation the major events occurring are the ingression and rearrangements of cells from the epiblast that are going to form the three embryonic layers, the elongation of the primitive streak and later the regression of the primitive streak accompanied by the formation of the notochord (Gilbert, 2014). In this study it was observed that the notochord elongates with a higher velocity than total embryo elongation. This suggests that the notochord elongates without forcing all embryo to elongate. On the other hand it could also push the adjacent tissues to elongate until the tensions between the two tissues would cause shredding. To assess this, it would be needed to measure tensions among tissues and inside tissues over time to confirm if this could explain embryo elongation. The notochord is formed between the neural tube and the endoderm by the deposition of cells from the Hensen's node to the posterior end of the notochord (Gilbert, 2014). While cells are added to the notochord, the rearrangements and cell division within the notochord also contribute to its extension (Sausedo and Schoenwolf, 1993). Considering that the notochord elongates with a higher velocity than whole embryo it suggests that notochord elongates and slides between the tissues. Regarding the whole embryo, it elongates continuously over time, where cell division and cell ingression, migration and rearrangements seem to play an important role.

During somitogenesis stages, we observed that the PSM and the segmented region are contributing most the embryo elongation. The segmented region is formed by differentiation of PSM cell into somites periodically. Thus, the mechanisms driving PSM elongation, may be the key mechanisms driving embryo elongation. PSM cells are originated from cells that are ingressing through the primitive streak and due to cell division, that present a period in the PSM around 9 hours (Benazeraf et al., 2017). Considering that PSM elongation is mostly driven through addition of new cells from the Hensen's node and from the epiblast, gastrulation should still be the engine of elongation accompanied by cells rearrangements and cell division. Bénazeráf and collaborators proposed that PSM was the most important tissue for embryo elongation in embryos from 13-15 somites. We obtained similar results for earlier stages which suggests that the same processes described by Benazeraf and collaborators, may already be acting earlier.

Our work also contributed with a new set of data of WT early chick embryo elongation that could be further explored and used to assess the impact of several conditions in chicken embryo elongation. We collected this set of information in order to be able to study the impact of Hairy1 in early embryo elongation. However, we can use the set to study other questions such has the impact of other genes and treatments. This information will be made available in the future to be used by other groups (Maia-Fernandes, AC and Pais de Azedevo, T., et al., manuscript in preparation). This new dataset could also contribute to update the Hamburger and Hamilton (HH) staging system. Hamburger and Hamilton stager was made taking as base hundreds of embryos that were dissected and staged in different time points of egg incubations. Therefore, periods of stage duration are approximations calculated considering the percentage of embryos within a stage after a certain period of incubation. Live imaging techniques opened a new window of opportunity from which we could obtain more information. In the HH stager the morphological characteristics used to define the stage of development were visualized without considering that they are evolving constantly. Since nowadays we apply live imaging in various studies it would be very useful to use all the information that can be extracted from seeing and embryo develop to better define stages and acquire better pictures as reference.

4.3 - Understanding the role Hairy1 in early embryo development

Understanding how Hairy1 overexpression is affecting early embryo development was one of the goals of the present work. Previous work from the lab showed that when Hairy1 is overexpressed in the PSM precursors the developmental of the trunk is delayed compared with the head development. We performed live-imaging of embryos electroporated with an overexpression vector for Hairy1. Due to the low number of embryos analyzed, it was not possible to reach definitive conclusions however we have suggestions that the embryo elongation is being affected. In this work we observed that chicken embryo elongation is delayed by Hairy1 overexpression. The total embryo and segmented region elongation rates are delayed and the PSM total length seems to be shorter. The segmented region elongation could be altered due to smaller somites or to a lower segmentation rate. It

would be interesting to deeply analyze the videos to see if: the period of somite formation is delayed in treated embryos compared to control embryos; if somite length is different in the two conditions and if different somites have different lengths in the same embryo.

Since hairy1 is expressed cyclically in the PSM, overexpression of Hairy1 would ultimately lead to the dampening of the oscillations, thus altering its expression dynamic. Thus, we would be affecting the dynamics of expression which was already described as having important roles in biological cellular responses. However, in the present work, we couldn't assess the levels of protein and the dynamics of both protein and mRNA. Therefore, it is crucial to assess in the future: if the dynamic of its mRNA is being affected; the levels of protein, its dynamics and cellular localization. To evaluate mRNA, we could perform the same experiment that lead to the discovery of the oscillations in the first place with electroporated embryos: perform half-embryo explants and *in situ* hybridization in one half without incubation and in the second in the half incubated for 90 minutes. This would allow us to confirm if the oscillations are maintained or not upon overexpression. To assess the protein status we would need to first optimize the IHC protocol.

The alteration of expression of Hairy1 is affecting embryo development delaying it. In a previous work (Shimojo et al., 2016) where the dynamics of *delta1* was altered, the dynamics of expression of Hes1 was also impacted. This lead to defects in somitogenesis and the embryos also seem smaller suggesting that the somitogenesis clock might have a role in elongation. Considering that we observed an impact in embryo elongation, we hypothesize that the impact on embryo elongation could be due to alterations in: 1) cell differentiation and or germ layer specification; 2) cell migration; 3) cell division. There are already evidences that Hes members and Hairy1 homologs can affect these processes in chicken, other models and contexts. Regarding cell differentiation, inhibiting cell differentiation into mesodermal precursors leads to embryo truncation (Oginuma et al., 2017). We also know that Hes genes play an important role in cell differentiation. Sustained expression in ES cells leads to a preferential differentiation choice towards the mesodermal fate (Kobayashi and Kageyama, 2010). In the nervous system development, Hes proteins maintain the neuronal stem cell population. In cancer, Hes1 was described to have an important role in maintaining the cancer stem cell population where it has a higher expression in cancer stem cells (CSC)

cells compared to non CSC cells (Abel et al., 2014). Considering that we electroporate in gastrulation stages, we could be impairing germ layer specification by affecting cellular decisions or/and EMT. As discussed above, Hairy1 and its homolog Hes1 can influence EMT (Gao et al., 2015) (Nitzan et al., 2016) which could affect germ layer specification and/or migration of cells during gastrulation. Altering cell migration would lead to embryo truncation, since the ingression of cells from the primitive streak is needed to embryo elongation (reviewed in (Benazeraf and Pourquie, 2013). There is also some evidence that if we affect cell migration in the PSM (through altering glycolysis) embryos are truncated showing that cell migration impairment leads to embryo elongation delay (Oginuma et al., 2017). On the other hand, we could also be affecting cell division. It was showed in zebrafish that mitosis tends to occur during the off phase of Hes expression which indicates that Hes can inhibit the transition of G2/M (Delaune et al., 2012). In ES cells, Hes1 tends to be differentially expressed during cell cycle and is present in higher levels during S-G2 phase (Kobayashi et al., 2009). Furthermore, Hes1 was shown to regulate Gadd45g, p57 and Cdk inhibitor p27kip1 that are cell cycle regulators (Kobayashi et al., 2009; Murata et al., 2005). In 2006, it was also shown by Baek and collaborators that Hes1 retards G1 phase progression in developing mouse embryos (Baek et al., 2006). In zebrafish, Sugiyama and co-workers showed that the initial G1/S transition in the notochord is always observed posteriorly to the newly formed somites. They suggested that G1/S transition in notochordal cells could be related with the embryonic body axis elongation and segmentation (Sugiyama et al., 2014). Also, in the chicken embryo Hes1/Hairy1 missexpression in neural crest cell stage in the neural tube, promotes a premature cell cycle exit (Nitzan et al., 2016). Despite that cellular division could be affected, it was already shown that inhibiting cell division didn't alter much embryo elongation in chick embryo during somitogenesis stages (Benazeraf et al., 2010). However, this was shown in later stages than the ones comprised in our study. Therefore, an effect in cell division could delay embryo elongation in earlier embryos. Affecting one of those processes, or more than one, could explain the phenotype observed upon Hairy1 overexpression. Thus, it would be very important, to in the future assess how, when and where those processes are being affected, and what is the impact on chicken early development. In the case of the EMT it would be important to address the role of hairy1 in the EMT in epiblast cells during gastrulation. This could be possible by assessing the levels

of EMT markers such as N-cad and E-cad in cells overexpressing Hairy1 versus WT cells. We could also image those cells are assess if they present the phenotypic appearance of normal epiblast cells. To assess cell migration we could perform migration assays to understand if cell overexpressing Hairy1 or with downregulating Hairy1 present different migration properties and potentials. Considering cell differentiation and germ layer specification we could perform immunohistochemistry with specific lineages and cell types markers and assess if they present altered expression in electroporated embryos with Hairy1 overexpression vector. In the present work we already tested some tools that would be very useful to answer our questions regarding Hairy1 effect in early embryo development more specifically regarding cell division and migration. From the live-imaging techniques available nowadays Light sheet microscopy would be a very useful tool to address the levels of cell division and migration through the embryo, at the single level without losing the total embryo perspective and we already settled the basal tools to perform light sheet imaging in early chicken embryos. We tested vital dyes that would allow to identify cellular components, allowing the analysis of cell migration and division. However, recently a transgenic quail line with all cells expressing markers for nucleus was developed (Huss et al., 2015). Quail model is very similar to chicken embryo model, so it could be useful to address the questions of interest mentioned above.

5 - Conclusion

In the present work we performed a characterization of the expression pattern of *hairy1* mRNA, an attempt to optimize an IHC protocol, a characterization of the early chicken embryo elongation and analyzed the impact of Hairy1 overexpression in the chicken embryo. We also gathered some tools that will be useful to study Hairy1 impact in cell division and migration.

Using in situ hybridization we showed that *hairy1* is expressed dynamically along the antero-posterior and medio-lateral axes which can be correlated with the differential location of the precursors of the medial-lateral somite and with different status of the EMT respectively in the embryo. Through live-imaging we obtained a new quantitative framework to study wild-type (WT) early embryo development. We observed that the first 2-10 somites are formed with different periods. We also could also assess that the PSM and segmented region are the portions that contribute most to the total embryo elongation. Using ex-ovo electroporation, and live-imaging we showed that Hairy1 affects total embryo and segmented region elongation rates and that the length of the PSM seems to be also affected. This effect on embryo elongation can be due to alterations in cell division, migration and differentiation.

Assessing the role of Hairy1 in cell division, migration and differentiation could give new insights to developmental biology and also to human disease such as Cancer. Hes1, the human homolog of Hairy1 has been linked to cancer progression, metastasis, drug resistance and cancer stem cells maintenance. Understanding the role of Hairy1 in cellular processes in the context of development could ultimately give an important contribution to understand the role of Hes1 and of it’s dynamics in cancer.

6 - Bibliography

Abel, E. V., Kim, E. J., Wu, J., Hynes, M., Bednar, F., Proctor, E., Wang, L., Dziubinski, M. L. and Simeone, D. M. (2014). The Notch pathway is important in maintaining the cancer stem cell population in pancreatic cancer. *PLoS One* **9**, e91983.

Akiyama, R., Masuda, M., Tsuge, S., Bessho, Y. and Matsui, T., (2014) An anterior limit of FGF/Erk signal activity marks the earliest future somite boundary in zebrafish. Development **141**: 1104-1109

Akazawa, C., Sasai, Y., Nakanishi, S. and Kageyama, R. (1992). Molecular characterization of a rat negative regulator with a basic helix-loop-helix structure predominantly expressed in the developing nervous system. *J Biol Chem* **267**, 21879-85.

Aulehla, A., Wiegraebe, W., Baubet, V., Wahll, M. B., Deng. C., Taketo, M., Lewandoski, M. and Pourquié, O. (2008). A β-catenin gradient links the clock and wavefront systems in mouse embryo segmentation. Nature Cell Biology **10:2:**186-193

Bachvarova, R. F., Skromne, I. and Stern, C. D. (1998). Induction of primitive streak and Hensen's node by the posterior marginal zone in the early chick embryo. *Development* **125**, 3521-34.

Baek, J. H., Hatakeyama, J., Sakamoto, S., Ohtsuka, T. and Kageyama, R. (2006). Persistent and high levels of Hes1 expression regulate boundary formation in the developing central nervous system. *Development* **133**, 2467-76.

Bailey, C. and Dale, K. (2015). Somitogensis in Vertebrate Development. eLS 1–15

Bailey, C. S., Bone, R. A., Murray, P. J. and Dale, J. K. (2017). Temporal Ordering of Dynamic Expression Data from Detailed Spatial Expression Maps. *J Vis* Exp. **(120)**: 55127

Benazeraf, B., Beaupeux, M., Tchernookov, M., Wallingford, A., Salisbury, T., Shirtz, A., Huss, D., Pourquie, O., Francois, P. and Lansford, R. (2017). Multiscale quantification of tissue behavior during amniote embryo axis elongation. *Development*. **1;144(23)**:4462-4472

Benazeraf, B., Francois, P., Baker, R. E., Denans, N., Little, C. D. and Pourquie, O. (2010). A random cell motility gradient downstream of FGF controls elongation of an amniote embryo. *Nature* **466**, 248-52.

Benazeraf, B. and Pourquie, O. (2013). Formation and segmentation of the vertebrate body axis. *Annu Rev Cell Dev Biol* **29**, 1-26.

Chalhoub, N. and Baker, S. J. (2009). PTEN and the PI3-kinase pathway in cancer. *Annu Rev Pathol* **4**, 127-50.

Chapman, S. C., Collignon, J., Schoenwolf, G. C. and Lumsden, A. (2001). Improved method for chick whole-embryo culture using a filter paper carrier. *Dev Dyn* **220**, 284-9.

Chen, G. and Courey, A. J. (2000). Groucho/TLE family proteins and transcriptional repression. *Gene* **249**, 1-16.

Collier, J. R., McInerney, D., Schnell, S., Maini, P. K., Gavaghan, D. J., Houston, P. and Stern, C. D. (2000). A cell cycle model for somitogenesis: mathematical formulation and numerical simulation. *J Theor Biol* **207**, 305-16.

Cooke, J. and Zeeman, E. C. (1976). A clock and wavefront model for control of the number of repeated structures during animal morphogenesis. *J Theor Biol* **58**, 455-76.

Cui, C., Yang, X., Chuai, M., Glazier, J. A. and Weijer, C. J. (2005). Analysis of tissue flow patterns during primitive streak formation in the chick embryo. *Dev Biol* **284**, 37-47.

Czirok, A., Rongish, B. J. and Little, C. D. (2004). Extracellular matrix dynamics during vertebrate axis formation. *Dev Biol* **268**, 111-22.
Daniel, W. W. (1929). Biostatistics: A Foundation For Analysis in the Health Sciences: John Wiley & sons, Inc.
Delaune, E. A., Francois, P., Shih, N. P. and Amacher, S. L. (2012). Single-cell-resolution imaging of the impact of Notch signaling and mitosis on segmentation clock dynamics. *Dev Cell* **23**, 995-1005.
DeLuca, S. M., Gerhart, J., Cochran, E., Simak, E., Blitz, J., Mattiacci-Paessler, M., Knudsen, K. and George-Weinstein, M. (1999). Hepatocyte growth factor/scatter factor promotes a switch from E- to N-cadherin in chick embryo epiblast cells. *Exp Cell Res* **251**, 3-15.
Duband, J. L., Dufour, S., Hatta, K., Takeichi, M., Edelman, G. M. and Thiery, J. P. (1987). Adhesion molecules during somitogenesis in the avian embryo. *J Cell Biol* **104**, 1361-74.
Dubrulle, J., McGrew, J. M., and Pourquie, O. (2001) FGF Signaling Controls Somite Boundary Position and Regulates Segmentation Clock Control of Spatiotemporal Hox Gene Activation. Cell **106**, 219-232
Dubrulle, J., Pourquié, O., (2004). fgf8 mRNA decay establishes a gradient that couples axial elongation to patterning in the vertebrate embryo. Nature Jan **29;427(6973)**:419-22
Dubrulle, J., and Pourquié, O., (2002). From head to tail: links between the segmentation clock and antero-posterior patterning of the embryo. Genetics & Development **12**:519–523
Firmino, J., Rocancourt, D., Saadaoui, M., Moreau, C. and Gros, J. (2016). Cell Division Drives Epithelial Cell Rearrangements during Gastrulation in Chick. *Dev Cell* **36**, 249-61.
Fisher, A. L., Ohsako, S. and Caudy, M. (1996). The WRPW motif of the hairy-related basic helix-loop-helix repressor proteins acts as a 4-amino-acid transcription repression and protein-protein interaction domain. *Mol Cell Biol* **16**, 2670-7.
Gao, F., Huang, W., Zhang, Y., Tang, S., Zheng, L., Ma, F., Wang, Y., Tang, H. and Li, X. (2015). Hes1 promotes cell proliferation and migration by activating Bmi-1 and PTEN/Akt/GSK3beta pathway in human colon cancer. *Oncotarget* **6**, 38667-80.
George, E. L., Georges-Labouesse, E. N., Patel-King, R. S., Rayburn, H. and Hynes, R. O. (1993). Defects in mesoderm, neural tube and vascular development in mouse embryos lacking fibronectin. *Development* **119**, 1079-91.
Georges-Labouesse, E. N., George, E. L., Rayburn, H. and Hynes, R. O. (1996). Mesodermal development in mouse embryos mutant for fibronectin. *Dev Dyn* **207**, 145-56.
Gibb, S., Maroto, M. and Dale, J. K. (2010). The segmentation clock mechanism moves up a notch. *Trends Cell Biol* **20**, 593-600.
Gilbert. (2014). Developmental Biology. Sunderland: Andrew D. Sinauer. 286-292, 416-424, 655-660
Giros, A., Grgur, K., Gossler, A. and Costell, M. (2011). alpha5beta1 integrin-mediated adhesion to fibronectin is required for axis elongation and somitogenesis in mice. *PLoS One* **6**, e22002.
Glickman, N. S., Kimmel, C. B., Jones, M. A. and Adams, R. J. (2003). Shaping the zebrafish notochord. *Development* **130**, 873-87.
Graper, L. (1926). *Wilhelm Roux Arch Entwickl Mech Org* **107**, 162-176.
Grbavec, D. and Stifani, S. (1996). Molecular interaction between TLE1 and the carboxyl-terminal domain of HES-1 containing the WRPW motif. *Biochem Biophys Res Commun* **223**, 701-5.

Hamburger, V. and Hamilton, H. L. (1951). A series of normal stages in the development of the chick embryo. *J Morphol* **88**, 49-92.
Hanahan, D. and Weinberg, R. A. (2000). The hallmarks of cancer. *Cell* **100**, 57-70.
Harima, Y., Imayoshi, I., Shimojo, H., Kobayashi, T. and Kageyama, R. (2014). The roles and mechanism of ultradian oscillatory expression of the mouse Hes genes. *Semin Cell Dev Biol* **34**, 85-90.
Hatakeyama, J., Bessho, Y., Katoh, K., Ookawara, S., Fujioka, M., Guillemot, F. and Kageyama, R. (2004). Hes genes regulate size, shape and histogenesis of the nervous system by control of the timing of neural stem cell differentiation. *Development* **131**, 5539-50.
Hendrix, M. J., Seftor, E. A., Seftor, R. E., Kasemeier-Kulesa, J., Kulesa, P. M. and Postovit, L. M. (2007). Reprogramming metastatic tumour cells with embryonic microenvironments. *Nat Rev Cancer* **7**, 246-55.
Henrique, D., Adam, J., Myat, A., Chitnis, A., Lewis, J. and Ish-Horowicz, D. (1995). Expression of a Delta homologue in prospective neurons in the chick. *Nature* **375**, 787-90.
Hirata, H., Yoshiura, S., Ohtsuka, T., Bessho, Y., Harada, T., Yoshikawa, K. and Kageyama, R. (2002). Oscillatory expression of the bHLH factor Hes1 regulated by a negative feedback loop. *Science* **298**, 840-3.
Huss, D., Benazeraf, B., Wallingford, A., Filla, M., Yang, J., Fraser, S. E. and Lansford, R. (2015). A transgenic quail model that enables dynamic imaging of amniote embryogenesis. *Development* **142**, 2850-9.
Hoffman, A., Frey, L., Smith, M., Auble, T. (2015). Formaldehyde Crosslinking: A toll for the Study of Chromatin Complexes. J Biol Chem. **290(44)**: 26404-26411
Iimura, T. and Pourquie, O. (2006). Collinear activation of Hoxb genes during gastrulation is linked to mesoderm cell ingression. *Nature* **442**, 568-71.
Iimura, T. and Pourquie, O. (2008). Manipulation and electroporation of the avian segmental plate and somites in vitro. *Methods Cell Biol* **87**, 257-70.
Iimura, T., Yang, X., Weijer, C. J. and Pourquie, O. (2007). Dual mode of paraxial mesoderm formation during chick gastrulation. *Proc Natl Acad Sci U S A* **104**, 2744-9.
Illmensee, K. and Mintz, B. (1976). Totipotency and normal differentiation of single teratocarcinoma cells cloned by injection into blastocysts. *Proc Natl Acad Sci U S A* **73**, 549-53.
Isomura, A. and Kageyama, R. (2014). Ultradian oscillations and pulses: coordinating cellular responses and cell fate decisions. *Development* **141**, 3627-36.
Iulianella, A., Beckett, B., Petkovich, M. and Lohnes, D. (1999). A molecular basis for retinoic acid-induced axial truncation. *Dev Biol* **205**, 33-48.
Jiang, Y. J., Aerne, B. L., Smithers, L., Haddon, C., Ish-Horowicz, D. and Lewis, J. (2000). Notch signalling and the synchronization of the somite segmentation clock. *Nature* **408**, 475-9.
Jouve, C., Iimura, T. and Pourquie, O. (2002). Onset of the segmentation clock in the chick embryo: evidence for oscillations in the somite precursors in the primitive streak. *Development* **129**, 1107-17.
Kageyama, R., Ohtsuka, T. and Kobayashi, T. (2007). The Hes gene family: repressors and oscillators that orchestrate embryogenesis. *Development* **134**, 1243-51.
Kasemeier-Kulesa, J. C., Teddy, J. M., Postovit, L. M., Seftor, E. A., Seftor, R. E., Hendrix, M. J. and Kulesa, P. M. (2008). Reprogramming multipotent tumor cells with the embryonic neural crest microenvironment. *Dev Dyn* **237**, 2657-66.

Keller, R., Davidson, L. A. and Shook, D. R. (2003). How we are shaped: the biomechanics of gastrulation. *Differentiation* **71**, 171-205.
Kessel, M. and Gruss, P. (1991). Homeotic transformations of murine vertebrae and concomitant alteration of Hox codes induced by retinoic acid. *Cell* **67**, 89-104.
Kobayashi, T. and Kageyama, R. (2010). Hes1 regulates embryonic stem cell differentiation by suppressing Notch signaling. *Genes Cells* **15**, 689-98.
Kobayashi, T., Mizuno, H., Imayoshi, I., Furusawa, C., Shirahige, K. and Kageyama, R. (2009). The cyclic gene Hes1 contributes to diverse differentiation responses of embryonic stem cells. *Genes Dev* **23**, 1870-5.
Kondoh, H. and Takemoto, T. (2012). Axial stem cells deriving both posterior neural and mesodermal tissues during gastrulation. *Curr Opin Genet Dev* **22**, 374-80.
Lawson, A. and Schoenwolf, G. C. (2001a). Cell populations and morphogenetic movements underlying formation of the avian primitive streak and organizer. *Genesis* **29**, 188-95.
Lawson, A. and Schoenwolf, G. C. (2001b). New insights into critical events of avian gastrulation. *Anat Rec* **262**, 238-52.
Lee, S. T., Welch, K. D., Panter, K. E., Gardner, D. R., Garrossian, M. and Chang, C. W. T. (2014). Cyclopamine: From Cyclops Lambs to Cancer Treatment. *Journal of Agricultural and Food Chemistry* **62**, 7355-7362.
Lim, J. and Thiery, J. P. (2012). Epithelial-mesenchymal transitions: insights from development. *Development* **139**, 3471-86.
Liu, Z. H., Dai, X. M. and Du, B. (2015). Hes1: a key role in stemness, metastasis and multidrug resistance. *Cancer Biol Ther* **16**, 353-9.
Ma, Y., Zhang, P., Wang, F., Yang, J., Yang, Z. and Qin, H. (2010). The relationship between early embryo development and tumourigenesis. *J Cell Mol Med* **14**, 2697-701.
Martins, G. G., Rifes, P., Amandio, R., Rodrigues, G., Palmeirim, I. and Thorsteinsdottir, S. (2009). Dynamic 3D cell rearrangements guided by a fibronectin matrix underlie somitogenesis. *PLoS One* **4**, e7429.
Matsui, T. and Bessho, Y., (2016) Analyzing ERK signal dinamics during zebrafish somitogenesis. ERK Signalling **1487**:367-378
Murata, K., Hattori, M., Hirai, N., Shinozuka, Y., Hirata, H., Kageyama, R., Sakai, T. and Minato, N. (2005). Hes1 directly controls cell proliferation through the transcriptional repression of p27Kip1. *Mol Cell Biol* **25**, 4262-71.
Naganathan, S. R. and Oates, A. C. (2017). The Sweetness of Embryonic Elongation and Differentiation. *Dev Cell* **40**, 323-324.
Nakaya, Y. and Sheng, G. (2008). Epithelial to mesenchymal transition during gastrulation: an embryological view. *Dev Growth Differ* **50**, 755-66.
New, D. A. T. (1955). A New Technique for the Cultivation of the Chick Embryo Invitro. *Journal of Embryology and Experimental Morphology* **3**, 320-&.
Nitzan, E., Avraham, O., Kahane, N., Ofek, S., Kumar, D. and Kalcheim, C. (2016). Dynamics of BMP and Hes1/Hairy1 signaling in the dorsal neural tube underlies the transition from neural crest to definitive roof plate. *BMC Biol* **14**, 23.
Niwa, Y., Shimojo, H., Isomura, A., González, A., Miyachi, H. and Kageyama, R., (2011) Different types of oscillations in Notch and FGF signalling regulate the spatiotemporal periodicity of somitogenesis. Genes Dev. **Jun 1;25(11)**: 1115-1120

Oginuma, M., Moncuquet, P., Xiong, F., Karoly, E., Chal, J., Guevorkian, K. and Pourquie, O. (2017). A Gradient of Glycolytic Activity Coordinates FGF and Wnt Signaling during Elongation of the Body Axis in Amniote Embryos. *Dev Cell* **40**, 342-353 e10.
Ohsako, S., Hyer, J., Panganiban, G., Oliver, I. and Caudy, M. (1994). Hairy function as a DNA-binding helix-loop-helix repressor of Drosophila sensory organ formation. *Genes Dev* **8**, 2743-55.
Ohtsuka, T., Sakamoto, M., Guillemot, F. and Kageyama, R. (2001). Roles of the basic helix-loop-helix genes Hes1 and Hes5 in expansion of neural stem cells of the developing brain. *J Biol Chem* **276**, 30467-74.
Palmeirim, I., Henrique, D., Ish-Horowicz, D. and Pourquie, O. (1997). Avian hairy gene expression identifies a molecular clock linked to vertebrate segmentation and somitogenesis. *Cell* **91**, 639-48.
Paroush, Z., Finley, R. L., Jr., Kidd, T., Wainwright, S. M., Ingham, P. W., Brent, R. and Ish-Horowicz, D. (1994). Groucho is required for Drosophila neurogenesis, segmentation, and sex determination and interacts directly with hairy-related bHLH proteins. *Cell* **79**, 805-15.
Pascoal, S., Carvalho, C. R., Rodriguez-Leon, J., Delfini, M. C., Duprez, D., Thorsteinsdottir, S. and Palmeirim, I. (2007). A molecular clock operates during chick autopod proximal-distal outgrowth. *J Mol Biol* **368**, 303-9.
Pérez, C. (2001). Técnicas Estatisticas con SPSS. Madrid Pearson Educación.
Pfeuty, B. and Kaneko, K. (2014). Reliable binary cell-fate decisions based on oscillations. *Phys Rev E Stat Nonlin Soft Matter Phys* **89**, 022707.
Pinheiro, G. (2014). Somitogenesis and Fibronectin: United by tension? In *Animal Biology Department*, vol. Master (ed. Lisboa: University of Lisboa.
Postovit, L. M., Margaryan, N. V., Seftor, E. A., Kirschmann, D. A., Lipavsky, A., Wheaton, W. W., Abbott, D. E., Seftor, R. E. and Hendrix, M. J. (2008). Human embryonic stem cell microenvironment suppresses the tumorigenic phenotype of aggressive cancer cells. *Proc Natl Acad Sci U S A* **105**, 4329-34.
Power, R. M. and Huisken, J. (2017). A guide to light-sheet fluorescence microscopy for multiscale imaging. *Nat Methods* **14**, 360-373.
Psychoyos, D. and Stern, C. D. (1996). Fates and migratory routes of primitive streak cells in the chick embryo. *Development* **122**, 1523-34.
Andrade, R. P., Pascoal, S., Palmeirim, I., (2005) Thinking clockwise. Brain Reserch Reviews **49:2**, 114-119
Resende, T. P., Ferreira, M., Teillet, M. A., Tavares, A. T., Andrade, R. P. and Palmeirim, I. (2010). Sonic hedgehog in temporal control of somite formation. *Proc Natl Acad Sci U S A* **107**, 12907-12.
Rifes, P., Carvalho, L., Lopes, C., Andrade, R. P., Rodrigues, G., Palmeirim, I. and Thorsteinsdottir, S. (2007). Redefining the role of ectoderm in somitogenesis: a player in the formation of the fibronectin matrix of presomitic mesoderm. *Development* **134**, 3155-65.
Rifes, P. and Thorsteinsdottir, S. (2012). Extracellular matrix assembly and 3D organization during paraxial mesoderm development in the chick embryo. *Dev Biol* **368**, 370-81.
Rosenquist, G. C. (1966). A radioautographic study of labeled grafts in the chick blastoderm: Development from primitive-streak stages to stage 12. *Carnegie Inst. Wash. Contrib. Embryol.*, 38:31-100.

Rosenquist, G. C. (1972). Endoderm movements in the chick embryo between the early short streak and head process stages. *J Exp Zool* **180**, 95-103.
Rosenquist, T. H., Ratashak, S. A. and Selhub, J. (1996). Homocysteine induces congenital defects of the heart and neural tube: effect of folic acid. *Proc Natl Acad Sci U S A* **93**, 15227-32.
Sang, L., Roberts, J. M. and Coller, H. A. (2010). Hijacking HES1: how tumors co-opt the anti-differentiation strategies of quiescent cells. *Trends Mol Med* **16**, 17-26.
Sasai, Y., Kageyama, R., Tagawa, Y., Shigemoto, R. and Nakanishi, S. (1992a). 2 Mammalian Helix Loop Helix Factors Structurally Related to Drosophila Hairy and Enhancer of Split. *Genes & Development* **6**, 2620-2634.
Sasai, Y., Kageyama, R., Tagawa, Y., Shigemoto, R. and Nakanishi, S. (1992b). Two mammalian helix-loop-helix factors structurally related to Drosophila hairy and Enhancer of split. *Genes Dev* **6**, 2620-34.
Sato, Y., Kasai, T., Nakagawa, S., Tanabe, K., Watanabe, T., Kawakami, K. and Takahashi, Y. (2007). Stable integration and conditional expression of electroporated transgenes in chicken embryos. *Dev Biol* **305**, 616-24.
Sausedo, R. A. and Schoenwolf, G. C. (1993). Cell behaviors underlying notochord formation and extension in avian embryos: quantitative and immunocytochemical studies. *Anat Rec* **237**, 58-70.
Schoenwolf, G. C. (1978). Effects of complete tail bud extirpation on early development of the posterior region of the chick embryo. *Anat Rec* **192**, 289-95.
Schoenwolf, G. C., Garcia-Martinez, V. and Dias, M. S. (1992). Mesoderm movement and fate during avian gastrulation and neurulation. *Dev Dyn* **193**, 235-48.
Sheeba, C. J., Andrade, R. P. and Palmeirim, I. (2016). Mechanisms of vertebrate embryo segmentation: Common themes in trunk and limb development. *Semin Cell Dev Biol* **49**, 125-34.
Shimojo, H., Isomura, A., Ohtsuka, T., Kori, H., Miyachi, H. and Kageyama, R. (2016). Oscillatory control of Delta-like1 in cell interactions regulates dynamic gene expression and tissue morphogenesis. *Genes Dev* **30**, 102-16.
Shimojo, H., Ohtsuka, T. and Kageyama, R. (2008). Oscillations in notch signaling regulate maintenance of neural progenitors. *Neuron* **58**, 52-64.
Shum, A. S., Poon, L. L., Tang, W. W., Koide, T., Chan, B. W., Leung, Y. C., Shiroishi, T. and Copp, A. J. (1999). Retinoic acid induces down-regulation of Wnt-3a, apoptosis and diversion of tail bud cells to a neural fate in the mouse embryo. *Mech Dev* **84**, 17-30.
Stemple, D. L. (2005). Structure and function of the notochord: an essential organ for chordate development. *Development* **132**, 2503-12.
Stern, C. D., Ireland, G. W., Herrick, S. E., Gherardi, E., Gray, J., Perryman, M. and Stoker, M. (1990). Epithelial scatter factor and development of the chick embryonic axis. *Development* **110**, 1271-84.
Stewart, T. A. and Mintz, B. (1981). Successive generations of mice produced from an established culture line of euploid teratocarcinoma cells. *Proc Natl Acad Sci U S A* **78**, 6314-8.
Sugiyama, M., Saitou, T., Kurokawa, H., Sakaue-Sawano, A., Imamura, T., Miyawaki, A. and Iimura, T. (2014). Live imaging-based model selection reveals periodic regulation of the stochastic G1/S phase transition in vertebrate axial development. *PLoS Comput Biol* **10**, e1003957.

Sweetman, D., Wagstaff, L., Cooper, O., Weijer, C. and Munsterberg, A. (2008). The migration of paraxial and lateral plate mesoderm cells emerging from the late primitive streak is controlled by different Wnt signals. *BMC Dev Biol* **8**, 63.
Tam, P. P. (1981). The control of somitogenesis in mouse embryos. *J Embryol Exp Morphol* **65 Suppl**, 103-28.
Tenin, G., Wright, D., Ferjentsik, Z., Bone, R., McGrew, M. J. and Maroto, M. (2010). The chick somitogenesis oscillator is arrested before all paraxial mesoderm is segmented into somites. *BMC Dev Biol* **10**, 24.
Thiery, J. P., Delouvee, A., Gallin, W. J., Cunningham, B. A. and Edelman, G. M. (1984). Ontogenetic expression of cell adhesion molecules: L-CAM is found in epithelia derived from the three primary germ layers. *Dev Biol* **102**, 61-78.
Tian, C., Tang, Y., Wang, T., Yu, Y., Wang, X., Wang, Y. and Zhang, Y. (2015). HES1 is an independent prognostic factor for acute myeloid leukemia. *Onco Targets Ther* **8**, 899-904.
Uriu, K. (2016). Genetic oscillators in development. *Dev Growth Differ* **58**, 16-30.
Uriu, K., Morishita, Y. and Iwasa, Y. (2010). Random cell movement promotes synchronization of the segmentation clock. *Proc Natl Acad Sci U S A* **107**, 4979-84.
van Es, J. H., van Gijn, M. E., Riccio, O., van den Born, M., Vooijs, M., Begthel, H., Cozijnsen, M., Robine, S., Winton, D. J., Radtke, F. et al. (2005). Notch/gamma-secretase inhibition turns proliferative cells in intestinal crypts and adenomas into goblet cells. *Nature* **435**, 959-63.
Voiculescu, O., Bertocchini, F., Wolpert, L., Keller, R. E. and Stern, C. D. (2007). The amniote primitive streak is defined by epithelial cell intercalation before gastrulation. *Nature* **449**, 1049-52.
Voiculescu, O., Bodenstein, L., Lau, I. J. and Stern, C. D. (2014). Local cell interactions and self-amplifying individual cell ingression drive amniote gastrulation. *Elife* **3**, e01817.
Voiculescu, O., Papanayotou, C. and Stern, C. D. (2008). Spatially and temporally controlled electroporation of early chick embryos. *Nat Protoc* **3**, 419-26.
Wang, S. C., Lin, X. L., Wang, H. Y., Qin, Y. J., Chen, L., Li, J., Jia, J. S., Shen, H. F., Yang, S., Xie, R. Y. et al. (2015). Hes1 triggers epithelial-mesenchymal transition (EMT)-like cellular marker alterations and promotes invasion and metastasis of nasopharyngeal carcinoma by activating the PTEN/AKT pathway. *Oncotarget* **6**, 36713-30.
Wei, Y. and Mikawa, T. (2000). Formation of the avian primitive streak from spatially restricted blastoderm: evidence for polarized cell division in the elongating streak. *Development* **127**, 87-96.
William, D. A., Saitta, B., Gibson, J. D., Traas, J., Markov, V., Gonzalez, D. M., Sewell, W., Anderson, D. M., Pratt, S. C., Rappaport, E. F. et al. (2007). Identification of oscillatory genes in somitogenesis from functional genomic analysis of a human mesenchymal stem cell model. *Dev Biol* **305**, 172-86.
Wolpert, L. (2008). The triumph of the embryo.
Xiao, X., Feng, Y. P., Du, B., Sun, H. R., Ding, Y. Q. and Qi, J. G. (2017). Antibody incubation at 37 degrees C improves fluorescent immunolabeling in free-floating thick tissue sections. *Biotechniques* **62**, 115-122.
Yang, J. T., Bader, B. L., Kreidberg, J. A., Ullman-Cullere, M., Trevithick, J. E. and Hynes, R. O. (1999). Overlapping and independent functions of fibronectin receptor integrins in early mesodermal development. *Dev Biol* **215**, 264-77.

Yang, J. T., Rayburn, H. and Hynes, R. O. (1993). Embryonic mesodermal defects in alpha 5 integrin-deficient mice. *Development* **119**, 1093-105.
Yang, X., Dormann, D., Munsterberg, A. E. and Weijer, C. J. (2002). Cell movement patterns during gastrulation in the chick are controlled by positive and negative chemotaxis mediated by FGF4 and FGF8. *Dev Cell* **3**, 425-37.
Yin, Y. and Shen, W. H. (2008). PTEN: a new guardian of the genome. *Oncogene* **27**, 5443-53.
Zhang, L., Kendrick, C., Julich, D. and Holley, S. A. (2008). Cell cycle progression is required for zebrafish somite morphogenesis but not segmentation clock function. *Development* **135**, 2065-70.

7 - Appendix

7.1 - Confirmation of *hairy1* probe for *in situ* hybridization integrity

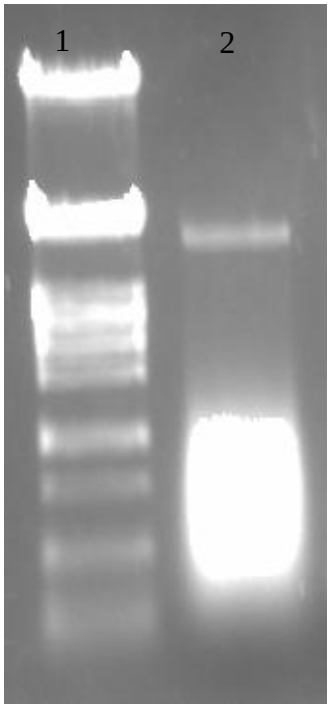

Figure 7.1 – **The probe synthesized for *hairy1 in situ* hybridization was not degraded;**

0.8% agarose gel electrophoresis was performed to confirm the integrity of the synthesized probe for *hairy1*. Lane 1 corresponds to the ladder (λ*Pst*I) and lane 2 to the *hairy1* probe.

7.2 - Movies WT embryos

SupMovie1 - Live imaging of embryo (1C) cultured in Chapman culture from stage HH3 to stage HH5 corresponding to 12 hours. Embryo was staged according to Hamburger and Hamilton (Hamburger and Hamilton, 1951).

SupMovie2 - Live imaging of embryo (6C) cultured in Chapman culture from stage HH4-HH9 corresponding to 27 hours. Embryos was staged according to Hamburger and Hamilton (Hamburger and Hamilton, 1951).

7.3 - 1st derivates of total embryo elongation

In order to confirm that the chicken embryo elongates with different rates along the developmental stages we decided to perform the 1st derivate of the total elongation curves. The 1st derivate gives the alterations in the rate in a curve. Therefore, when we perform the 1st derivate from the length per time if the rate is equal along the curve, the 1st derivate is going to present a steady value. On the other hand, if the rate varies over time, the 1st derivate is going to present different values in each interval. We calculated the first derivate using [length(a+1)-length(a)]/[t(a+1)-t(a)] for each time point. It is important to consider that each x value in the graphs represent an interval of two consecutive time points. Therefore, in the graphs presented, in each x value, the value presented is the interval of the value and the precedent one (Figure 7.2 and 7.3).

We couldn't conclude that the embryos have different elongation rates nor when the elongation rates change with this methodology. The graphs present a lot of noise, therefore, it was not possible to choose a cut-off-point to differentiate noise from significant changes.

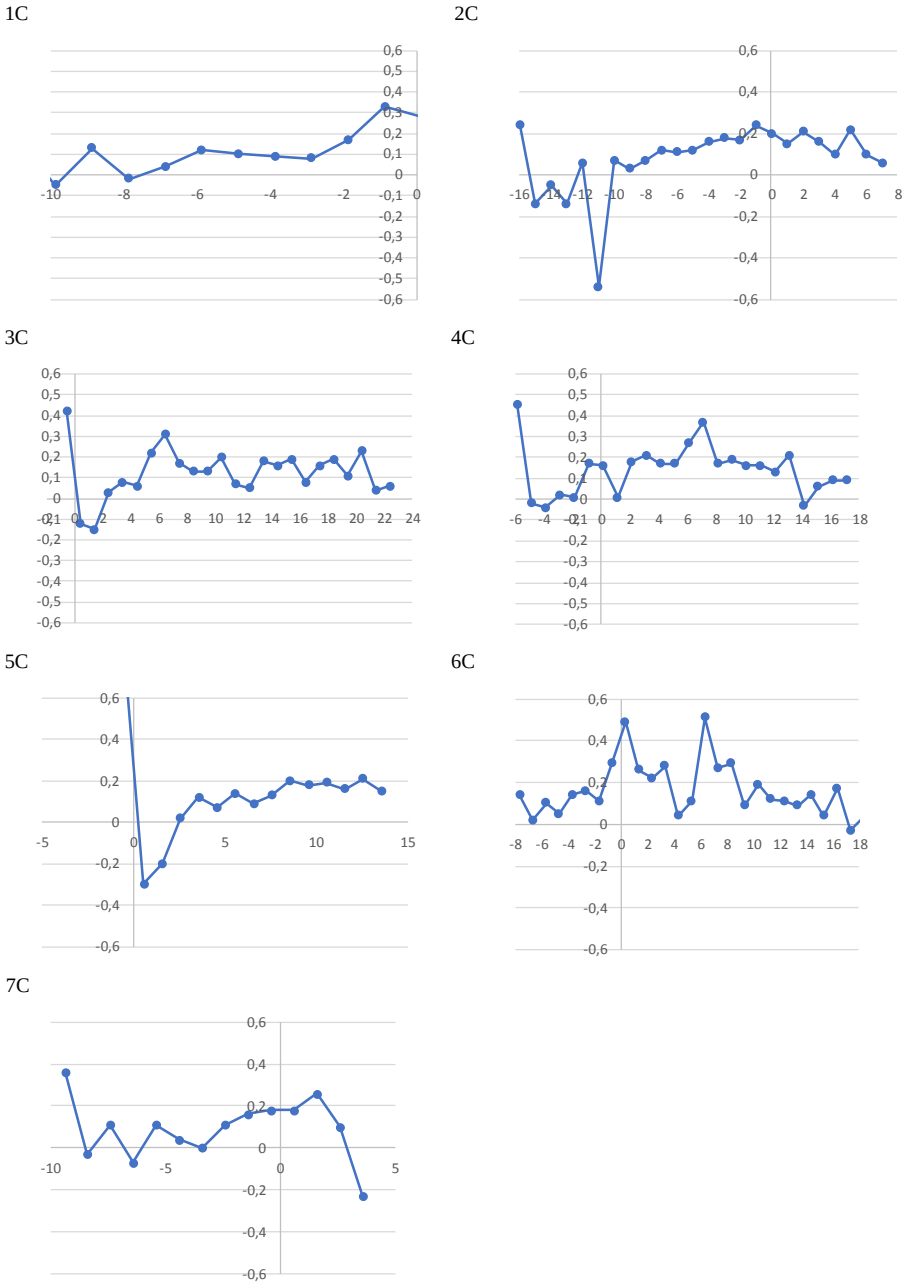

Figure 7.2 – **1st derivate of embryo total elongation curves of embryos cultivated in chapman culture**

1st derivate of the total length per interval was calculated for each time point measured. The rate (y axis) in each interval (x axis) is represented in the graphs.

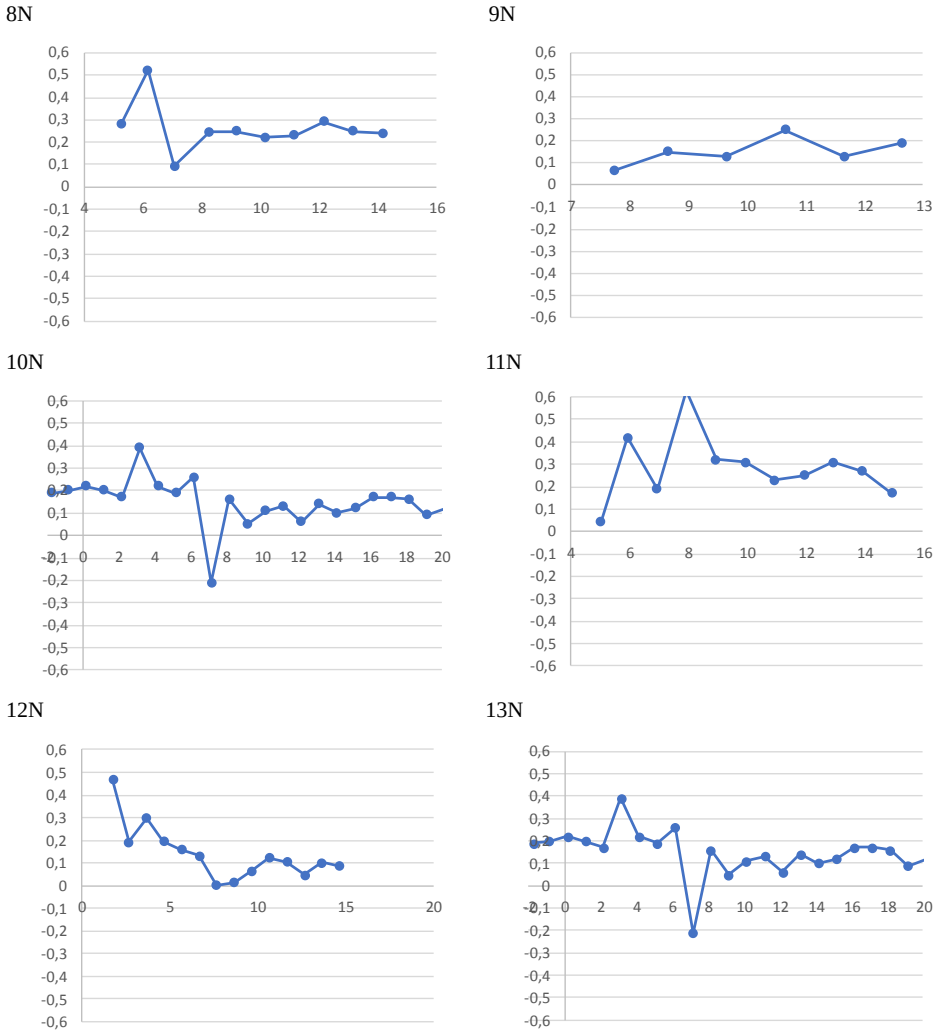

Figure 7.3 – **1st derivate of embryo total elongation curves for embryos cultivates in New culture;**

1st derivate of the total length per interval was calculated for each time point measured. The rate (y axis) in each interval (x axis) is represented in the graphs.

7.4 - HH5 and HH6 duration periods are not inversely proportional

Table 7.1- ***The duration periods of stage HH5 and HH6 are not inversely proportional;***

Duration periods of stage HH5 and HH6 were assessed using live-imaging. Only the embryos that had both stages present in the movie from the beginning to the end were included in the analysis. The sum of the time of duration of stage HH5 and HH6 are not similar among embryos. Therefore, the period calculated for stage HH5 and HH6 are not inversional proportional. This shows that the high standard deviations in stage HH6 and HH5 duration are not due to problems of detection of the transition from one stage to another. Each embryo corresponds to one video.

Embryos	HH5 (hours)	HH6 (hours)	Sum of the period in HH5 and HH6 (hours)
2N	5.1	1.85	6.95
3N	7.5	3.35	10.85
4N	7.25	1.9	9.15
6N	5.8	2.5	8.3

7.5 - Average total length of the embryos in the different conditions.

Table 7.2 - **Mean and standard deviation of the length of the total embryo, PSM region and segmented region;**

Embryos from the three conditions don't seem different in terms of total length (mm), however it seems that the H1+ embryos have smaller PSM and segmented regions when compared with the control and WT embryo groups. The average length was calculated considering all time points measured for all embryos.

	Total embryo (mm)	**PSM region (mm)**	**Segmented region (mm)**
WT	4.575 ±1.09	0.776 ±0.250	0.702 ±0.405
pCAT	4.983 ±0.90	0.964 ±0.278	0.690 ±0.370
pCAT-Hairy1	4.853 ±0.77	0.674 ±0.245	0.548 ±0.339

7.6 - Electroporated embryo movie

SupMovie3 - Live imaging of embryo cultured in Chapman culture and electroporated with empty vector. The movies comprise stages from stage HH6 to stage HH10. Embryo was staged according to Hamburger and Hamilton (Hamburger and Hamilton, 1951).

7.7 - Methods to assess cell division and migration

Table 7.3 – Methods to study cell division and/or cell migration

Methods that allow to study cell division migration that allow or not to perform live-imaging. All the methods were already used in biological models in the past years.

	Method	**Cell proliferation / cell migration**	**Live-imaging**	**Biological model (examples)**	**Reference (example)**
Immunolabelling	Phospho-histoneH3 labelling	Yes / No	No	Chicken	(Guy wiedermann et al., 2015)
	Anti-xMELK antibodies	Yes / No	No	Xenopus	(Guillaume Hatte et al., 2014)
Constructs and transgenic lines	eGFP-anilin fusion protein	Yes / No	Yes	Mouse	(Michael Hesse et al., 2012)
	PCNA	Yes / No	Yes	Mammal cells	(Alexis R. Barret. Et al., 2016)
	H2B::RFP/CAAX:GFP	Yes / Yes	Yes	Mouse	(Cayetana Vásquez-Diez et al., 2016)
	PGK1:H2B-chFP (transgenic quail	Yes / Yes	Yes	Quail	(Huss et al., 2015)
	Fucci system	Yes / No	Yes	Zebrafish	(Sugyiama et al., 2014)
	Bicistronic version of Fucci system	Yes / No	Yes	Mouse	(Anna Kicheva et al., 2014)
	GFP-tubulin and H2BmCherry	Yes / Yes	Yes	Mouse	Lucia Novakova et al., 2016)
Others	BRDU	Yes / No	No	Zebrafish	(Lixia Zhang et al., 2008)
Vital dyes	TOTO3-iodide	Yes / Yes	Yes	Drosophila	(M. Bettencourt-Dias et al., 2004)
	Syto dyes	Yes / Yes	Yes	-	-
	Draq5	Yes / Yes	Yes	-	-